University of Stavanger

FACULTY OF SCIENCE AND TECHNOLOGY

MASTER'S THESIS

Study programme/specialization: Petroleum Engineering/ Drilling Technology	Spring/Autumn semester, 2018 Open
Author: Afiya Akram	…….. (Signature of author)
Programme coordinator: Supervisor(s): Mesfin Belayneh. Muhammad Awais Ashfaq Alvi	
Title of master's thesis: MWCNT and SiO_2 Nanoparticle Enhanced Drilling Fluid Formulation and Characterization: Experimental and Simulation studies	
Credits: 30	
Keywords: Drilling fluid MWCNT nanoparticle Silica nanoparticle (SiO_2) Rheological properties Tribology Viscoelasticity	Number of pages: ……101…… + Supplemental material/other: 21…….. Stavanger, ……12-02-/2018…… Date/year

Dedication

This work is dedicated to the memory of my grandfather, M. Ellahi, who passed away during this thesis work. He was looking forward to read through this thesis.

Acknowledgements

First of all, I would thank God to give me the strength to complete this thesis.

I would like to express my sincere gratitude and appreciation to my supervisor Mesfin Belayneh for his knowledge, engagement and the endless support during this thesis work. I am so thankful to have you as a supervisor, you pushed me and motivated me when I needed it the most. Thank you for always having the door open at your office. You are a really caring person, and I wish you all the best in the future. I would also like to thank my supervisor Awais Muhammed. Your help through this thesis is highly appreciated. I wish you the best in future to come.

Furthermore, I would like to thank University of Stavanger for letting me use their facilities for my laboratory work and simulation studies.

Finally I would thank my husband, Hamad, who has supported me to fulfil my dream. I would also thank my mother and father. Sincerely thanks to my mother who took care of my beautiful daughters, Sarina and Raya, while I studied. Also thanks to Sarina and Raya for being patient while mummy studied.

Abstract

In recent years the application of nanotechnology has shown impressive results in improving the performance of drilling fluid, enhanced oil recovery and in cement. However, the research and development based on nanotechnology in the oil industry are at its early stage. This indicates a huge research and development potential of nanotechnology in this field as well as application of this advance systems in industry.

In this thesis the effects of single (MWCNT, SiO_2) and the composite (MWCNT-SiO_2) nanoparticles on Carboxymethyl cellulose (CMC) and Xanthan gum (XG) based reference drilling fluids were tested. Based on the considered laboratory drilling fluids and the nanoparticle concentration, the overall results summarized as:

- 0.38wt. % MWCNT nanoparticle reduced the friction coefficient of XG-base drilling fluid by 50%.
- 0.0095wt. % SiO_2 nanoparticle reduced the friction coefficient of XG-base drilling fluid by 25%.
- 0.37wt. % SiO_2 - 0.0095wt % MWCNT composite reduced the coefficient of friction of CMC base drilling fluid by 38%
- MWCNT and Silica nanoparticles increased the measured filtrate loss.
- Nanoparticle additives did not show a significant impact on plastic viscosity.
- The single MWCNT and Silica nanoparticles increased yield stress of base drilling fluid.
- Reduction of coefficient of friction reduced torque& drag.
- MWCNT nanoparticle treated drilling fluid showed improved hole-cleaning efficiency.

Table of content

1 Introduction

This thesis presents the formulation and characterization of nanoparticle-enhanced drilling fluids. Drilling fluid properties such as rheology, filtrate loss, lubricity and viscoelasticity were analyzed in this work. In addition, the performance of the drilling fluids was simulated with rheology models, torque and drag, hydraulics and hole-cleaning.

1.1 Background / Motivation

Drilling fluids are an essential part of the drilling operation. Drilling fluid is defined as a circulating fluid, used in rotary drilling operations to perform various functions [1]. The major functions of a drilling fluid are to transport cuttings to the surface, provide hydrostatic pressure, stabilizing the wellbore, and to cool and lubricate the drill bit [2]. A properly designed drilling fluid is very important to achieve success in the drilling operation [3]. One of the main consideration when designing a drilling fluid is to keep the well cost to a minimum [2]. Figure 1.1 shows a typical drilling and fluid circulation system [4].

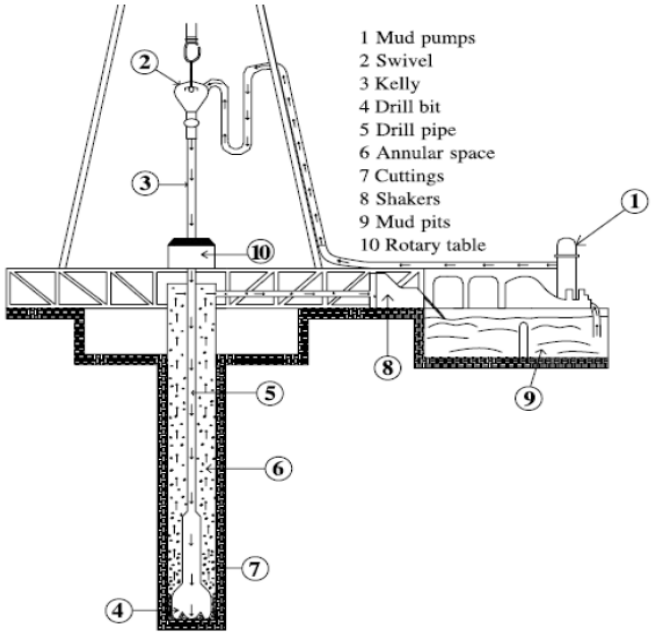

Figure 1.1: Drilling system [4]

The two commonly used drilling fluids in the oil industry are water based mud (WBM) and oil based mud (OBM). WBM is environmental friendly and cheaper. However, poorly designed WBM easily interact with clay minerals in shale which led to clay swelling. On the other hand, OBM gives good wellbore stability and lubricity properties as it minimizes the interaction with shale [5]. Moreover, OBM has a higher rate of penetration (ROP) and lower coefficient of friction compared to the WBM. However, OBM is very costly and has a negative impact on the environment due to spills and disposal [6].

The world's population is increasing, and so is the demand for energy, while the tendency of finding oil and gas easily is decreasing [7]. Hence, the oil industry is shifting towards higher risks and extremely challenging drilling environments such as extreme water depths, high pressure high temperature (HPHT) formations and complex geological formations. Drilling in these harsh environments requires new tools, equipment and technology, which have better technical performance than the conventional drilling methods.

The application of nanotechnology (1-100nm) is successfully proven in several industries such as electronic, material composites, medical and even consumer goods as well [8]. Recent research has shown an improved performance of nanotechnology in petroleum engineering, such as in drilling fluids, enhanced oil recovery (EOR) and cementing [9].

In this thesis the effect of single and composite nanoparticles in bentonite WBM will be investigated. Drilling fluids were designed both with and without nanoparticles to compare the nanoparticle drilling fluid with the conventional drilling fluid system. The drilling fluid systems were formulated with various concentrations of nanoparticles in order to check the effect of different concentrations of the particles on the properties of drilling fluid. The fluid rheology, pH, filtrate loss and friction coefficient were investigated, and the best system was selected to study the viscoelasticity of the fluids. At the end, a simulation study was performed to investigate the effect of nanoparticles further.

1.2 Problem formulation

The main issues to be addressed in this work are:

- Single effect of MWCNT and SiO_2 nanoparticles in the conventional drilling fluids
- Combined effect of MWCNT and SiO_2 nanoparticles in the conventional drilling fluids

1.3 Scope and Objective

The primary objectives of this thesis are to formulate and characterize nanoparticle-based drilling fluids. In addition, to perform simulation studies such as torque and drag, hydraulics and hole-cleaning.

1.4 Research methods

Figure 1.2 illustrates the summary of the thesis work. As shown, the thesis is divided into three main topics. Part 1 describes theories used for the evaluation of the drilling fluid, literature study deals with the review of the application of nanoparticles in drilling fluids and description of the drilling fluid ingredients. Part 2 contains experimental work, which deals with the drilling fluids formulation and characterization. Whereas, part 3 deals with the performance simulation studies.

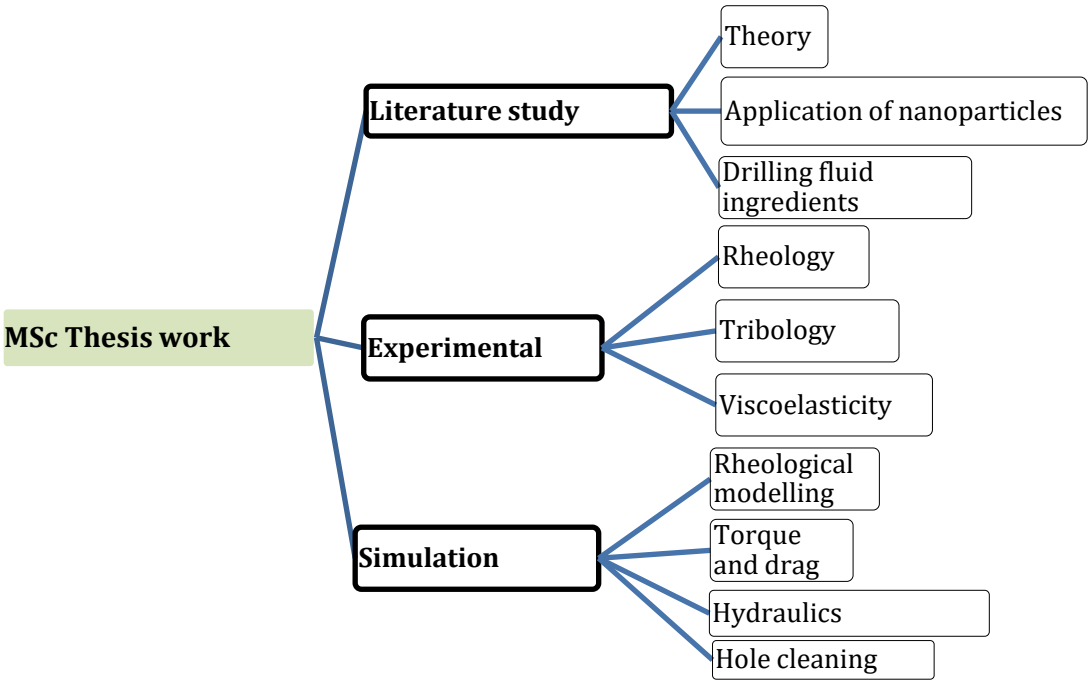

Figure 1.2: Research methods

2 Theory

This chapter reviews the relevant theories, which are being used for the analysis of experimental results obtained in chapter 4 as well as for the performance simulation studies in chapter 5. The theories are presented for the rheology, viscoelasticity, torque and drag and hydraulic.

2.1 Rheology

Rheology deals with the science of deformation and flow [10]. It is important to understand the rheological properties of the drilling fluid as the rheological properties directly affect the flow characterization and hydraulic calculations [11]. Drilling fluid has several functions, and the fluid rheology must be controlled in order to perform these functions in an optimal way [12].

The drilling fluid rheology also plays a key role during the drilling process. The rheology parameters are being used to describe the drilling fluid in different conditions, in order to design an optimum circulating system. The rheology of the drilling fluids are used in the following determinations [11]:

- To calculate the friction loss in the annulus and pipes
- To estimate ECD of the drilling fluid
- To determine the flow regime in the annulus
- To estimate the hole cleaning efficiency
- To evaluate the capacity of fluid suspension (surge and swab pressures)
- To calculate the settling velocity for cuttings

There are several basic concepts in rheology to describe the behaviour/properties of the fluids, the concepts are defined in the sections below.

Reynolds number and Flow regimes:

Reynolds number is a dimensionless number which is defined by the fluid`s inertial forces and the viscous forces.. The Reynolds numbers are used to indicate the flow regime of fluid. Figure 2.1 illustrates the three flow regimes, which are laminar, transitional and turbulent.

In laminar flow, the fluid is moving in parallel to the wall in straight and smooth lines. The fluid velocity increases from zero near the wall, to a maximum value in the middle of the pipe. The velocity profile has a parabolic profile. Generally, slowly moving fluids or viscous fluids are categorized to have laminar flow. The Reynolds number for laminar flow is lower than 2000.

The turbulent flow is recognised as when the flow pattern of the fluid is unsorted and chaotic. Turbulent flow occurs for higher velocities or for fluids with low viscosities. The Reynolds number for turbulent flow is greater than 4000.

Transition flow is a state between the laminar flow and turbulent flow. It is when the flow pattern changes from uniform to unsorted and chaotic movements. The Reynolds number for transition flow is between the range of 2000 and 4000.

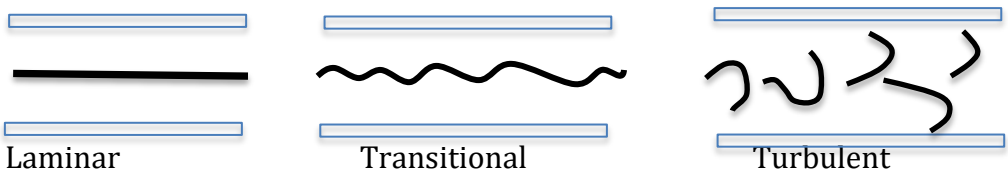

Figure 2.1: Illustration of fluid flow patterns

Viscosity:

Viscosity is a term which describes fluid`s flow resistance. Resistance to flow occurs due to the internal forces, like mechanical, friction and electrostatic forces between the molecules. Viscosity is defined as a relation between shear stress and shear rate. The shear stress of a fluid is the ratio of shear force and the shear area, while the shear rate is given by the ratio of velocity and the distance. The value of viscosity is not constant for most of the drilling fluids, the viscosity changes as the shear rate changes, therefore the shear stress is measured at different shear rates to fully understand the viscosity behaviour of the fluid. The viscosity is also dependent on the pressure, temperature and time.

Plastic Viscosity (PV):

The plastic viscosity describes the drilling fluid`s flow resistance which occurs due to the mechanical friction between the particle-particle, particles-fluid and fluid-fluid. The value of PV is dependent on the concentration, size and shape of the additives in the drilling fluid, as well on the viscosity of the fluid. The PV is determined by using 600RPM and 300RPM Fann viscometer and is given by [12]:

$$PV = Q_{600} - Q_{300} \quad (1)$$

Where:

- Q_{600}= Fann viscometer reading at 600 RPM shear rate
- Q_{300}=Fann viscometer reading at 300RPM shear rate

Yield Stress (YS):

The yield stress describes the drilling fluid´s flow resistance which occurs due to the electrostatic and chemical forces between the particles in the fluid. A higher YS indicates stronger internal molecular forces within the drilling fluid. To initiate flow, the pressure should exceed the shear yield stress. The YS can be calculated from Fann data as [12]:

$$YS = 2Q_{300} - Q_{600} \quad (2)$$

Gel-strength (gel):

Gel strength gives a measurement of the electrical attractive forces within the particles in the drilling fluids. Both gel strength and yield stress parameters are influenced by the internal forces between the particles.

2.2 Rheological Models

Several mathematical models have been developed to characterize the fluid flow by the rheological parameters. These models relate shear stress with the shear rate. By using the measured data and the models, it is possible to determine viscosity and gel strength of the drilling fluid. These two parameters are important in order to describe the performance of the drilling fluid, such as efficiency of cutting transport and pressure calculations.

Drilling fluids are very complex fluids. Selection of the best rheological model is based on the comparison between the measured and calculated shear stresses and shear rates. The rheological models can be categorized as Newtonian and non-Newtonian. For the Newtonian model, the viscosity remains constant with the change in shear rates. The viscosity for non-Newtonian models varies with the change in shear rates. Some of the rheological models are illustrated in figure 2.2.

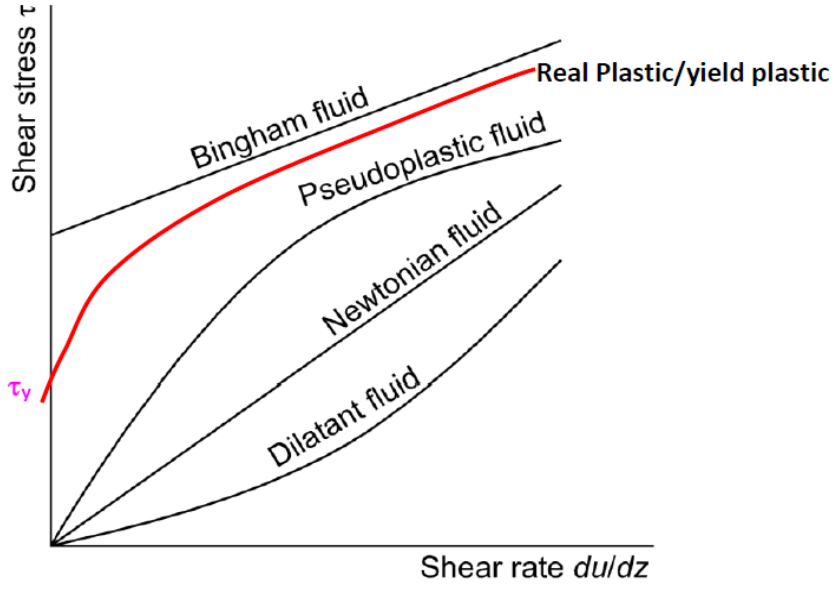

Figure 2.2: Illustration of shear stress-shear rate behavior of fluids [13]

In the following section, an example will be shown on how to transform data from the Fann viscometer into shear stresses and shear rates. A set of viscometer data from the experimental study and transformed data are presented in table 2.1.

To transform the RPM values and corresponding viscometer readings into shear stresses and shear rates following conversion factors has been applied [14]:

$\gamma = 1.703 * RPM$ (3)

$\tau = 1.063.Reading$ (4)

RPM	Reading
θ600	39
θ300	32
θ200	29
θ100	24
θ6	15
θ3	11

γ (s^{-1})	τ(lbf/100sqft)
1022	42
511	34
341	31
170	26
10	16
5	12

Table 2.1: Illustration of viscometer data and field unit transformed data

Figure 2.3: Photograph picture of Fann 35 viscometer

2.2.1 Newtonian Model

A fluid is characterized as Newtonian if the shear stress is directly proportional with the shear rate, with the viscosity as the proportionality constant. The graphical relation between the shear stress and the shear rate is a straight line, which passes through the origin. Water is an example of a Newtonian fluid, where the viscosity does not change as the shear rate change. The equation for the Newtonian model is given by [14]:

$$\tau = \mu\gamma \quad (5)$$

Where:

- τ=shear stress
- μ=viscosity
- γ=shear rate

Using measured data and equation 5, from the slope of the line, the viscosity can be estimated by using the following equation [14]:

$$\mu\ (cP) = 47880 * slope/100 \quad (6)$$

2.2.2 Non-Newtonian Models

For most of the drilling fluids, the Newtonian model does not apply to them. Most of the drilling fluids are non-Newtonian, the non-Newtonian models characterize the fluids by two or more parameters.

2.2.2.1 Bingham Plastic Model

The Bingham Plastic model is the most common rheological model used for the drilling fluids. It is a two parameters model. The shear stress and shear rate relation

are linear as in case of Newtonian model. The equation for Bingham plastic model is given by [14]:

$$\tau = YS + \mu_p \gamma \quad (7)$$

Where:

- YS =Yield stress
- μ_p (PV)=Plastic viscosity

Yield stress and plastic viscosity can be calculated using the Fann viscometer data and equations 1 and 2.

2.2.2.2 Power-law Model

As for Bingham plastic model, Power-law model also characterizes the fluid by using two parameters. The graphical relation for shear stress and shear rate is represented by a straight line in a log-log graph. The Power-law model is represented by the following equation [14]:

$$\tau = k\gamma^n \quad (8)$$

Where:

- k= Consistency index (lbf/100sqft)
- n= Flow behavior index []

The parameters *k* and *n* can be calculated by using the following equations [14]:

$$n = 3.32 \log\left(\frac{\theta_{600}}{\theta_{300}}\right) \quad (9)$$

$$k = \frac{\theta_{300}}{511^n} \quad (10)$$

Graphically, the value of n represents the slope of the straight line, and the value of k represents the intercept at γ=1.

The flow behavior index (n) represents the type of fluid, hence the Power-law model can be used to represent more than one type of fluid, when:

- n<1 it is a pseudoplastic fluid
- n=1 it is a Newtonian fluid
- n>1 it is a dilatant fluid

When the n-value is below one, the fluid is called a shear thinning fluid, which means that the viscosity decreases as the shear rate increases. Most of the drilling fluids show shear thinning behavior. When the n-value is greater than one, the fluid is dilatant. The viscosity of dilatant fluid increases as the shear rate increases. This behavior is not shown by drilling fluids.

2.2.2.3 Herschel Bulkley Model

Herschel Bulkley's model characterizes a fluid by three parameters. The model is given by [14]:

$$\tau = \tau_o + K\gamma^n \qquad 11$$

Where:

- τ_o =Yield point
- K= Consistency index
- n= Flow behavior index

The Herschel Bulkley model is a modified Power-law model. In this model, yield stress is included. This model describes the rheological behavior of drilling fluid.

The n-value and k-value can be found graphically. τ_o can be calculated by using the following equation [14]:

$$\tau_o = \frac{\tau^{*2} - \tau_{max}\tau_{min}}{\tau^* - \tau_{max} - \tau_{min}} \qquad 12$$

Where, τ_{max} and τ_{min} are the maximum and minimum measured shear stresses. The shear stress, τ^*, is determined by interpolation from the corresponding geometric mean of the shear rate $\gamma^* = \sqrt{\gamma_{max}\gamma_{min}} = 72.25s^{-1}$, which is between the Q_6 and Q_{100}.

2.2.2.4 Unified Model

The unified model is a simplified version of Herschel Bulkley model. This model involves the parameters k and n as in the case of Herschel Bulkley model, but instead of τ_o, a new parameter is introduced, that is τ_y, a lower shear yield point. The lower shear yield is derived from the Fann viscometer readings at 6 RPM and 3RPM. The Unified model is described by [14]:

$$\tau = \tau_y + K\gamma^n \quad (13)$$

Where:

- $\tau_y(lbf/100sqft) = 1.066*(2Q_3 - Q_6)$ (14)

2.2.2.5 Robertson and Stiff Model

The Robertson and Stiff model is shown to be superior to Bingham and Power-law model, but has not gained recognition in the drilling industry because of its complexity. The model can be represented by the following equation [14]:

$$\tau = A(\gamma + C)^B \quad (15)$$

Where:

A, B and C are the parameters of the Robertson and Stiff model. A and B parameters are similar to the parameters k and n of the Power-law model. The parameter C is the correction factor to the shear rate, and the term (γ+C) represents the effective shear rate. The parameter C is given by [14]:

$$C = \frac{\gamma_{max}\gamma_{min} - \gamma^{*2}}{2\gamma^* - \gamma_{max} - \gamma_{min}} \quad (16)$$

Where:

γ^* is calculated by interpolation of the corresponding geometrical shear stress, given as: $\tau^* = \sqrt{\tau_{max}\tau_{min}}$ (17)

2.2 Viscoelasticity

Viscoelastic behavior is shown by the materials having both fluids and solids. Drilling fluids exhibit viscoelastic behavior, which means that they can be characterized with respect to viscous and elastic behavior under deformation. Viscoelastic properties are time-dependent, where viscosity decreases or increases with a change in shear stress or shear rate. Viscosity increases with time when higher shear stress is applied, however higher shear stress can also lead to viscous heating, which can decrease the viscosity. Hence, viscosity can also be decreased with the increase in the shear rates. The elastic property of the drilling fluids stores energy when deformation is applied and has great effect on the behavior of flow and pressure drop. The viscoelastic properties play very important role in order to evaluate the structure and strength of gel, barite sag, hydraulic modelling and solid suspension [15]. Viscosity is not the only parameter which can define the behavior of the drilling fluids. Even though the viscous components are dominating factor in common operations. Even when infinitesimal deformation is applied on the drilling fluids, the response of the applied deformation provides viscoelastic response, as indicated by the gel structure. Gel structure formation is one of the many requirements which the drilling fluid has to fulfill. Gel structure formation is important in order to transport cuttings and to keep the cuttings floating while the circulation stops. The viscoelastic response of the drilling fluids can be determined by performing oscillatory tests with the rheometer shown in figure 2.4.

The basic principle behind the oscillatory tests can be explained by using Two-Plates-Model, illustrated in figure 2.5. The drilling fluid sample is placed between two plates, where the bottom plate is stationary and the upper plate has oscillatory movements. The movement of the upper plate induces shear in the fluid sample [10].

Figure 2.4:Photograph picture of Anton Paar MCR 302 rheometer

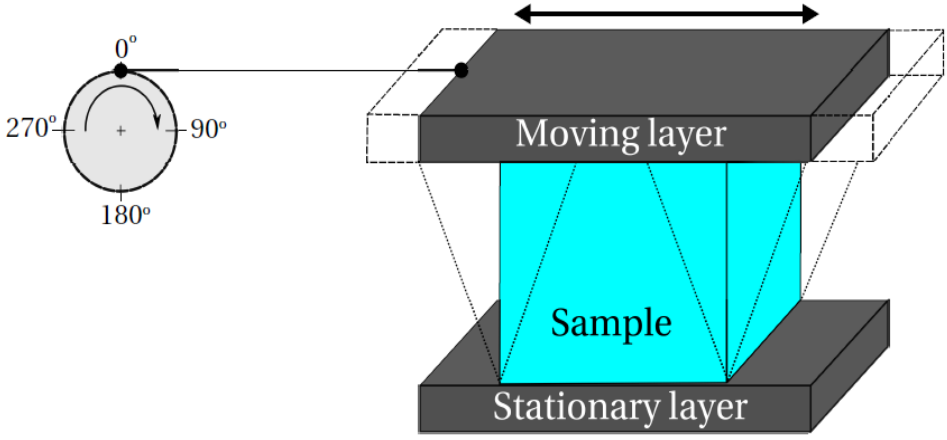

Figure 2.5: Illustration of the two-plate-model oscillatory test [16]

During the oscillatory tests, the fluid sample is exposed to varying sinusoidal deformation (strain) and the resulting stress is measured. Figure 2.6 shows the stress and strain response as a function of time, the phase angle and amplitude is also illustrated.

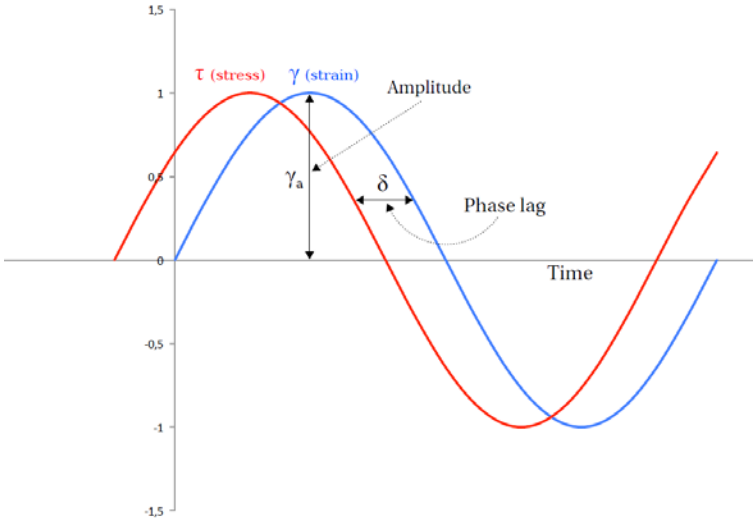

Figure 2.6: Stress strain response for an oscillatory measurement of a viscoelastic material [16]

The applied shear strain (γ) and the measured shear stress (τ) are defined as [15]:

$$\gamma(t) = \gamma_o \sin(\omega t) \quad (18)$$

$$\tau(t) = \tau_o \sin(\omega t + \delta) \quad (19)$$

$$\tau(t) = \tau_o[\sin(\omega t)\, cos\delta + \cos(\omega t)\, sin\delta] \quad (20)$$

$$\tau(t) = \gamma_0 \left[\left(\frac{\tau_o}{\gamma_0} cos\delta\right) \sin(\omega t) + \left(\frac{\tau_o}{\gamma_0} sin\delta\right) \cos(\omega t)\right] \quad (21)$$

$$\tau(t) = \gamma_0[G' \sin(\omega t) + G'' \cos(\omega t)] \quad (22)$$

The Storage Modulus and Loss modulus are defined by following equations [15]:

$$G' = \left(\frac{\tau_o}{\gamma_0} cos\delta\right) \quad (23)$$

$$G'' = \left(\frac{\tau_o}{\gamma_0} sin\delta\right) \quad (24)$$

The damping factor, also called loss factor, is the ratio of the lost and the stored energy, caused by the deformation, and is given as:

$$tan\delta = \left(\frac{G''}{G'}\right) \quad (25)$$

$$\delta = tan^{-1}\left(\frac{G''}{G'}\right) \quad (26)$$

Where δ is the phase angle, this parameter describes where the phase changes occur for the fluids. The phase angle is equal to 90^0 for an ideally viscous fluid, in

this case the Loss Modulus completely dominates the Storage Modulus. For the ideally elastic fluid the phase angle is equal to zero and for this case Storage Modulus dominates the Loss Modulus. When the phase angle is 45^{o}, the Storage Modulus is equal to the Loss Modulus, and the fluid then comprises of 50 percent viscous portion and 50 percent elastic portion and is at the transition point. This point is also called the flow point. The viscoelastic materials have phase angle values between 0 and 90. The viscoelastic parameters are presented schematically in table 2.2.

Phase angle	$0 < \delta < 45$	$\delta = 45$	$45 < \delta < 90$
Behaviour	Elastic dominated	Transitional	Viscous dominated
G' and G''	G' > G''	G' = G''	G' < G''

Table 2.2: Classification of materials from oscillatory tests [10]

2.2.1 Oscillatory Amplitude Sweep Test

An oscillatory sweep test is performed at a variable amplitude of oscillation, while the frequency is held constant. The measuring temperature of the sample fluid is also kept constant. When a small strain is applied to the fluid sample, the sample will undergo a deformation while the internal structure of the fluid remains unchanged. The Storage and Loss Modulus will have constant values at different levels, and are presented as a linear horizontal range on the graph, called linear viscoelastic range (LVER). LVER is obtained at low amplitude values. A higher strain is further applied on the fluid sample, until it reaches a critical value where the internal structure of the fluid sample is irreversibly deformed and LVER changes into a nonlinear viscoelastic range. The flow point and yield point can be determined from the curves that are based on the data from the amplitude sweep tests. The flow point is the point where the fluid starts to flow, and can be found by taking the value at which Storage Modulus curve and Loss Modulus curve meets, at this point the phase angle is 45^{0} and the system is equally balanced with respect to viscosity and elasticity. In the LVER the fluid sample exhibits gel-like character, after the flow point the fluid sample becomes more viscous. The yield point can be found at the limit of the LVER,

where the linearity of the Storage Modulus and Loss Modulus starts to deviate from horizontal plateau. The LVER, flow point and yield point are illustrated in figure 2.7.

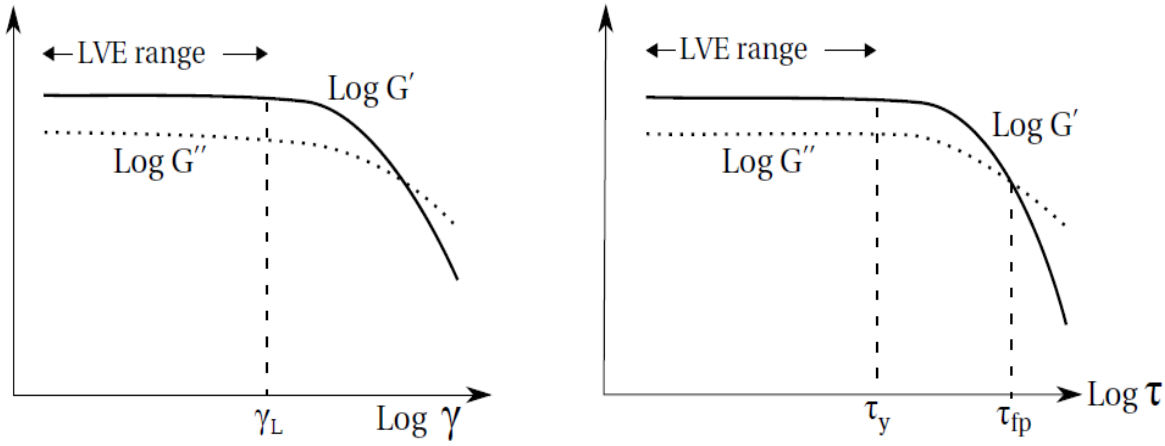

Figure 2.7: Right: Strain amplitude sweeps showing gel-like character. Left: Stress amplitude showing yield point and flow point [10]

2.4 Torque and Drag

Figure 2.8 shows a drill string which is divided into small segments. The axial load transfer in the drilling string during tripping is given as the vectors sum of loadings in the axial direction, which are static weight and friction-drag force. As illustrated in figure 2.8, the small element ds is loaded with axial loads and torque. The force at the top is computed by using (Johancsik et al. 1989) [17]:

$$F_{i+1} = F_i \pm \mu\left(\sqrt{(\beta w_s \sin\theta ds - F_e d\theta)^2 + (F_e \sin\theta d\varphi)^2}\right) + \beta w_s \cos\theta ds + dF_L \qquad 27$$

Where, μ is coefficient of friction, w is weight per unit length, θ and φ are well inclination and azimuth, respectively.

As shown in the equation 27, lower coefficient of friction provides better drag reduction, which allows to drill a longer offset. This can be done by improving the lubricity of drilling fluid. Therefore, this thesis work is designed for this purpose.

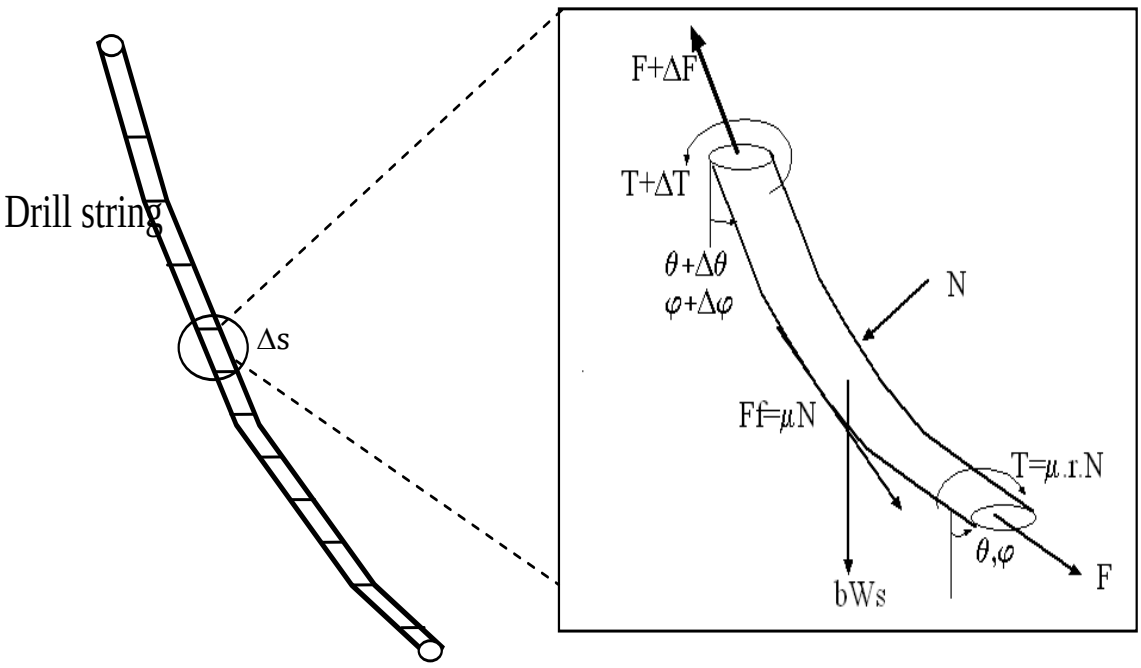

Figure 2.8: Segmented drill string and loads [13]

dF_L in equation 27 is the fluid flow effect on drill string, which is a function of flow rate.

Maidla and Wojtanowicz (1987) [18] also derived the effect of viscous pressure gradient on each pipe element. The hydrodynamic viscous drag force, which is combined with the drag equation, is given as dynamic viscous drag force, which is to be coupled with the drag equation, is given as:

$$F_{fl} = \frac{\pi}{4}\sum_{i=1}^{n}\left(\frac{\Delta P}{ds}\right)\Delta s_i d_i^2 \qquad 28$$

Where, the pressure loss term with fluid velocity and density in the annulus is given as:

$$\frac{\Delta P}{ds} = \frac{f\rho V_{av}^2}{D-d} \qquad 29$$

Where:

- D = well diameter and d = outer diameter of the drill string

The friction factor, *f*, calculated based on the flow regimes, as shown in the table 2.3.

For laminar	***For turbulent,***
$f = \frac{16}{N_{\mathrm{Re}}}$ 30	$f = \frac{0.0791}{N_{\mathrm{Re}}^{0.25}}$ 31
$N_{\mathrm{Re}} = 10.9x10^{4} \frac{\rho V_{an}^{2-n}}{k} \left(\frac{D-d}{48} x \frac{n}{2n+1} \right)^{n}$ 32	
For laminar flow: $N_{Re} \leq 3470 - 1370xn$ & For turbulent flow: $N_{Re} \geq 420 - 1370xn$	

Table 2.3: Friction factor for laminar and turbulent flow [18, 19]

Where:

- N_{Re} is the Reynolds number
- n is flow-behavior index
- k is consistency index *dyne.s/100 cm²*

2.2 Torque

Aadnøy et al. (2009) also derived a three-dimensional model in a curved section given as [19]:

$$T = \mu r N \quad 33$$

Where, μ is the coefficient of friction, r is the radius of the drill string, and N is contact force. Drilling fluid with higher lubricity reduces the torque, which is suitable for the drilling operation. This thesis will investigate the effect of nanoparticles on the lubricity of drilling fluid.

2.5 Hydraulics

Hydraulics deals with the determination of pressures when drilling fluid circulates. Drilling fluid is pumped through the circulation system by mud pump. During circulation process, as illustrated in figure 2.9, friction pressure losses occur in the different part of the circulation system. Pressure losses prediction is important for [2]:

- Drill bit hydraulic program design
- ECD during tripping in and tripping out operations
- ECD during drilling and well control operations

The Equivalent Circulating Density (ECD) describes the density of the drilling fluid when the friction loss while circulating is taken into account. ECD is given by [12]:

$$ECD = \rho_{st} + \frac{\Delta P_{annulus}}{g.TVD} \quad 34$$

Where:

- ρ_{st}= Static mud density
- ΔP= Pressure loss in annulus
- TVD= True vertical depth

During tripping out operation, well pressure in the annulus will decrease. This is called swab pressure and can lead to kick. Likewise, when tripping in operation, an increase in annular pressure (also called surge pressure) may cause formation fracture. Therefore, it is important to analyze hydraulics in the wellbore in order to determine accurate well pressure.

Figure 2.9 illustrates the different components of frictional losses in a circulating system. The pump pressure is given as the sum of pressure losses in circulation systems [14]:

$$PP = \Delta Ps + \Delta Pdp + \Delta Pdc + \Delta Padp + \Delta Padc + \Delta Pb \quad 35$$

Where,

- ΔPs = Pressure loss at surface equipment
- ΔPdp = Pressure loss inside of drill string
- ΔPdc = Pressure loss inside of drill collar
- $\Delta Padp$ = Pressure loss in annulus (drill pipe/well or casing)
- $\Delta Padc$ = Pressure loss in annulus (drill collar/well)
- ΔPb = Pressure loss across the drill bit

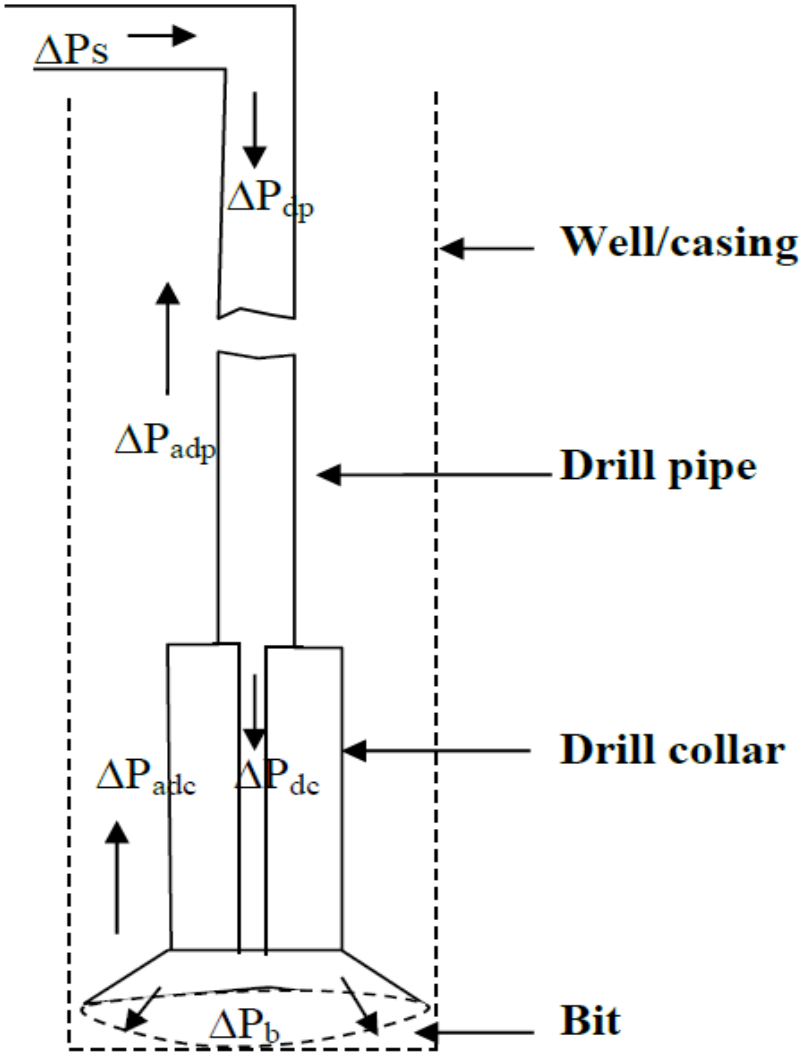

Figure 2.9: Friction pressure losses during circulation [14]

Several hydraulics models are available in the literature. Since the Unified hydraulics model [20] includes both Bingham plastic and Power-law parameter, in this thesis Unified hydraulic model was selected for the analysis of pump pressure and equivalent circulation density (ECD) of drilling fluids to be formulated in Chapter 4. *Sadigov* [21] has also analyzed the model with the field and experimental data and he as reported the good prediction of the model. A summary of Unified hydraulics model used in chapter 5 for hydraulic calculations is presented in table 2.4.

Pipe Flow	Annular Flow
$\mu_p[cP] = \theta_{600} - \theta_{300}$ $\tau_y = \theta_{300} - \mu_p$ $\tau_0 = 1.066(2\theta_{300} - \theta_{600})$	
$n_p = 3.32 \log\left(\frac{2\mu_p + \tau_y}{\mu_p + \tau_y}\right)$ $k_p = 1.066\left(\frac{\mu_p + \tau_y}{511}\right)$	$n_p = 3.32 \log\left(\frac{2\mu_p + \tau_y - \tau_y}{\mu_p + \tau_y - \tau_y}\right)$ $k_p = 1.066\left(\frac{\mu_p + \tau_y - \tau_o}{511}\right)$
$G = \left(\frac{(3-\alpha)n+1}{(4-\alpha)n}\right)\left(1 + \frac{\alpha}{2}\right)$ α= 1 for annular, α= 1 for pipe	
$v_p[\frac{ft}{min}] = \frac{24.51\, q}{D_P^2}$	$v_a[\frac{ft}{min}] = \frac{24.51\, q}{D_2^2 - D_1^2}$
γ_w [1/sec]= $\frac{1.6*G*v}{D_R}$ $\tau w = \left[\left(\frac{4-\alpha}{3-\alpha}\right)\right]\tau 0 + k\,\gamma wn$	
$N_{Re} = \frac{\rho\, v_p}{19.36\tau_w}$	$N_{Re} = \frac{\rho\, v_e}{19.36\tau_w}$
Laminar: $f_{laminar} = \frac{16}{N_{Re}}$ Transient: $f_{transient} = \frac{16\, N_{Re}}{(3470-1370n_p)}$ Turbulent: $a = \frac{\log n + 3.93}{50}$ } $f_{turbulent} = \frac{a}{N}$ $b = \frac{1.75 - \log n}{7}$ }	Laminar: $f_{laminar} = \frac{24}{N_{Re}}$ Transient: $f_{transient} = \frac{16\, N_{Re}}{(3470-1370n_p)}$ Turbulent: $a = \frac{\log n + 3.93}{50}$ } $f_{turbulent} = \frac{a}{N}$ $b = \frac{1.75 - \log n}{7}$ }
$f_{partial} = (f_{transient}^{-8} + f_{turbulent}^{-8})^{-1/8}$	
$f_p = (f_{partial}^{12} + f_{laminar}^{12})^{1/12}$	$f_a = (f_{partial}^{12} + f_{laminar}^{12})^{1/12}$
$\left(\frac{dp}{dL}\right)[\frac{psi}{ft}] = 1.076\frac{f_p v_p^2 \rho}{10^5 D_p}$ $\Delta p[psi] = \left(\frac{dp}{dL}\right)\Delta L$	$\left(\frac{dp}{dL}\right)\left[\frac{psi}{ft}\right] = 1.076\frac{f_a v_a^2 \rho}{10^5 (D_2 - D_1)}$ $\Delta p[psi] = \left(\frac{dp}{dL}\right)\Delta L$
$\Delta p_{Nozzles}[psi] = \frac{156\rho q^2}{\left({D_{N1}}^2 + {D_{N2}}^2 + {D_{N3}}^2\right)^2}$	

Table 2.4: Summary of the equations used in the Unified model [14]

3 Literature study

This chapter presents the review of nanoparticles application in the oil industry and the description of chemical ingredients used to formulate the drilling fluids this thesis work.

3.1 Application of nanoparticles in the oil industry

As mentioned initially, nanotechnology has been successfully applied to numerous fields such as electronics, medical, painting and coating industry, cosmetics, the oil industry and many more. In the oil industry nanotechnology has been applied to drilling fluids, cementing and EOR. In the following sections some of the results from nanotechnology application in the drilling fluids, cement and EOR will be presented.

3.1.1 Drilling fluids

Sharma M. M. et al. (2012) [22] presented a paper where they have tested water based drilling fluids containing silica nanoparticle with 20-nm diameter silica spheres, and evaluated its interaction with shales. The tests were conducted to get details about the rheology and stability of the nanoparticle-treated drilling fluids, and to quantify the extent of water invasion into shales. Transient-flow test, also called pressure penetration test, were performed on the samples, which determined the physical plugging on the shales. Permeability changes for the nanoparticle enhanced fluids were compared to the same shale sample, and were used as an indicator of physical plugging. The results showed that the WBM having silica nanoparticle reduced the invasion into the shale by 10 to 100 times, which indicates that a good wellbore stability is obtained by using silica nanoparticles in drilling fluids. Another test result showed that silica nanoparticle effectively plugged pores in shales without micro-cracks, but could not alone plug the micro-cracks, at least not with this nanoparticle particle size and concentration.

Sedaghatzadeh M. et al. (2012) [23] studied the thermal and rheological effects of bentonite WBM with MWCNT as an additive. The thermal effects of the sample

drilling fluids were measured by the transient hotwire (THW) method which determined the thermal conductivity of the materials. The thermal conductivity enhanced by 23.2% by adding 1 vol% of MWCNT at room temperature, by increasing the temperature to 50°C, the thermal conductivity was increased by 31.8%. In addition, the rheological properties also showed significant improvements.

Li G. et al. (2012) [24] studied the effect of nanoparticles enhanced drilling fluids on the sealing ability for shale with micro-cracks. In order to form an appropriate mud cake with very low filtration, there must be a match between pore throat size and the particle size. The rheology and filtration effects were determined. Further, cake strength tests, pressure transmission tests and sound wave propagation speed tests were performed to verify sealing properties of the mud cake and permeability effects of the nanoparticles. The conventional sized calcium carbonate particles were compared with nano-sized calcium carbonate. The results of the test showed that conventional sized calcium carbonates could not effectively plug the small pore throats. The pressure transmission test showed that pressure transmission of shale decreased and coefficient of shear strength had increased after nanoparticles were added, which indicates that adding nano-sized material into the drilling fluid seals the pores of the shale. The concentration of nanoparticle used for this evaluation was 3%.

3.1.2 Cement

Baig M.T. et al. (2017) [25] studied the effect of various concentrations of nano-zeolite mixed with API Class G cement. Compressive strength was measured by ultrasonic cement analyzer (UCA) under HPHT conditions, porosity and permeability were analyzed in an automated permeameter/porosimeter, and finally the structure was examined by use of SEM. The results showed that by adding nano-zeolite into the cement, the strength development process was accelerated. During well-cementing operations, there are three important parameters, 50-, 500- and 2000psi compressive strength, and it is important to determine how much time it

takes to achieve these strengths. By adding 2% nano-zeolite, the time to reach 2000psi strength was reduced by almost 30%, which means the wait-on-cement (WOC) time can be reduced by adding nanoparticle additives. The permeability and porosity also reduced significantly by the addition of 1% nano-zeolite, 98% and 17% respectively.

3.1.3 EOR

Moradi B. et al. (2015) [26] studied the effect of silica nanoparticle on EOR. Water alternating gas (WAG) is one of the methods used to improve oil recovery, in this study the improvement of the WAG method by adding silica nanoparticles (Nano-WAG) into the aqueous phase was investigated. Silica nanoparticles powder with nanoparticle size of 11.14 nm, medium crude oil sample and plugs from a mature oil field in the Middle East was used for the experiments. Core-flooding experiments, IFT measurements and wettability measurements were performed. IFT measurements measured the interfacial force between oil and water and oil and the nano-fluid, by using Du Nouy ring method. During all experiments, the temperature was held 122^{o} F and the initial pressure at 800psi. The rate of injection was 8cc/hr and 15cc/hr for water/nano-water and gas, respectively. The results showed more than 20% incremental in recovery factor by adding nanoparticles in the conventional WAG process. The study also showed that silica nanoparticle adsorption changed the wettability of the rock from oil-wet to strongly water-wet, a property which affects the recovery. IFT also reduced by adding silica nanoparticle.

3.2 Description of chemicals used in this thesis work

3.2.1 Bentonite

Clay is involved in two different scenarios during the drilling process, one during drilling in shale formations and one by using bentonite as an additive in the drilling fluids. The main component of WBM is clay, mostly bentonite [27]. Bentonite is added into the WBM as a viscosifier and to control filter loss. In this thesis the bentonite clay is used as an additive in the drilling fluids. The term bentonite was first used to describe the plastic clay found near the Fort Benton in Wyoming in the US [28]. Bentonite is defined as a clay, which may have volcanic or non-volcanic origin, consisting of smectite group minerals [29]. Smectite was earlier referred as montmorillonite, and the term is still being used in the oil industry [12]. Montmorillonite is the dominating mineral in the bentonite, bentonite can also contain other clay minerals, like illites and kaolinites. Non-clay minerals can comprise 10-30 percent of the total amount of bentonite [12]. The unique properties obtained by bentonite in the drilling fluids, like clay swelling and thixotropic qualities, are due to the montmorillonite minerals. The chemical composition of the commercial bentonites is presented in table 3.1.

Chemical composition in %			
	Wyoming "Volclay"	*Panther Creek Mississippi*	*Ponza, Italy*
Silica, SiO_2	64.32	64.00	67.42
Alumina, Al_2O_3	20.74	17.10	15.83
Ferric oxide, Fe_2O_3	3.03	} 4.70 {	0.88
Ferous oxide, FeO	0.46		-
Titanium dioxide, TiO_2	0.14	1.50	-
Lime, CaO	0.50	3.80	2.64
Magnesia, MgO	2.30	0.50	1.09
Potash, K_2O	0.39	0.20	}1.09
Soda, Na_2O	2.59	-	
Phosphoric anhydride, P_2O_5	0.01	-	-
Sulfuric anhydride, SO_3	0.35	0.20	0.01
Other minor constituents	0.01	8.00	-
Combined water	5.14	64.00	10.88

Table 3.1: Composition of commercial bentonite [28]

Bentonite can be classified into two categories, depending on the swelling abilities in the water. Sodium (Na+) bentonite exhibits higher swelling capability, called

osmotic swelling, this swelling is caused by the water that comes between the unit layers in the clay structure due to the higher concentration of cations between the unit layers than the cations in the surrounding water [1]. Whereas, bentonite with calcium (Ca++) ions exhibits a lower swelling ability, called surface hydration. This type of swelling occurs when the layer of water molecules holds to the oxygen atoms, and the water molecules are adsorbed on the crystal surfaces [1]. The sodium-saturated bentonite may cause a greater expansion than calcium-saturated bentonite, therefore it is important to obtain an appropriate ion exchange reaction in order to stabilize the clay.

As described earlier, smectite is the dominating component of bentonite, and the unique physical and chemical properties are depicted by bentonite due to this mineral. The smectite group minerals have similar structures, since majority of the clay minerals consists of

- Octahedral layer
- Tetrahedral layer

Various chemical compositions can be attained with different combinations of these two structures. The octahedral layer consists of two layers packed with oxygen atoms (O) or hydroxyl molecules (OH). An octahedral structure is built up of O-atoms or OH-molecules, and an aluminium atom (A) is placed within this structure, having the same distance to all O-atoms or OH-molecules, as shown in figure 3.1. The aluminium atom can be replaced by iron (Fe) or magnesium (Mg).

On the other hand, tetrahedral layer consists of a tetrahedral structure where O-atom or OH-molecule is placed in the four corners of the structure, and are surrounding by a silicon atom (Si) which is being placed in the gravitational center of the tetrahedral structure. Several of these structures can be tied together in a hexagonal pattern with an oxygen or hydroxyl corner, as can be seen in the figure3.1. The tetrahedral structure is placed in such a manner that the top of the structure points in the upward direction, while bases are on the same plan.

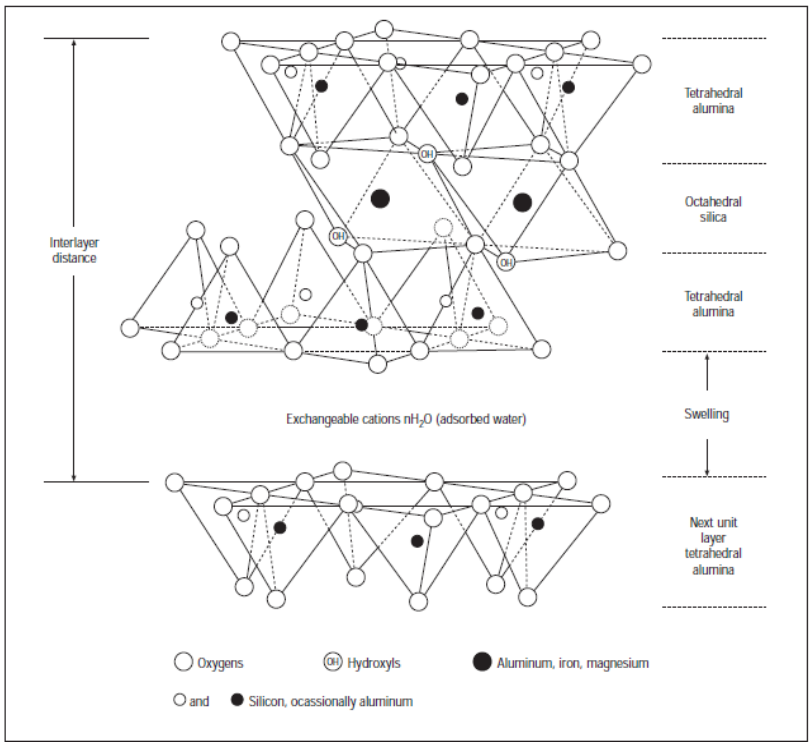

Figure 3.1: Structure of clay [12]

It is important to study the behaviour of the clay particles in drilling fluids as it affects important fluid properties such as viscosity, yield point and filter loss [30]. The property of the drilling fluid depends on the interaction between the clay crystals, which in turn are dependent on properties like pH and salt concentration of the solution [30]. In the following sections, four typical conditions for clay particles in the aqueous solution will be described, the conditions are also illustrated in figure 3.2.

Deflocculated system: Similar charges of the suspended particles in the solutions induce repulsive force between the particles and eventually the system becomes deflocculated [30]. The alkalinity of the solution increases this effect. As there are no ionic interactions between the particles in the deflocculated system, therefore the filter loss and yield point will be low.

Flocculated system: A fluid system is flocculated when the sum of repulsive forces and attracting forces between the particles are zero that is charge neutralization,

the particles make a bond, either connected edge-to-edge or edge-to-surface. This takes place when clay crystals have positive charges on the edges. In a flocculated bentonite system, viscosity will increase and the filter loss will also increase.

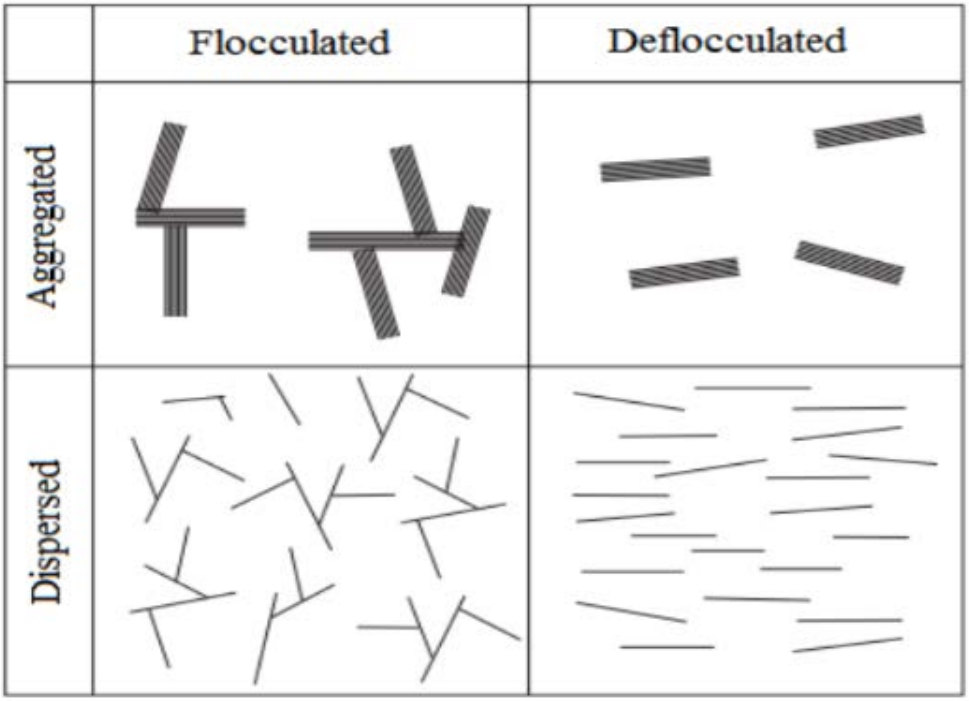

Figure 3.2: Typical conditions for clay particles in drilling fluids [12]

Aggregated system: As the name indicates, in this system particles are bound together in aggregates. The aggregated bentonite system does not contain individual crystals or small groups of crystals, but crystals are packed together in aggregates. The montmorillonite is packed together in bonded sheets, and when the montmorillonite is hydrated, the sheets will separate and there will be a significant increase in the viscosity.

Dispersed system: A dispersed system is described as when all the aggregates are splits up into individual crystals or small group of crystals. When the system is dispersed, the charges at the edges can either be positive or negative, it depends on the pH value of the solution. A dispersed system can be either flocculating or deflocculating.

3.2.2 Xanthan Gum-XG

Xanthan gum is polysaccharides and water soluble long chain anionic polymer. It is not usually compatible with cationic surfactants and polymers. Xanthan gum is used in drilling fluid for the control of viscosity and filtrate loss. As illustrated in figure 3.3, structurally, xanthan gum comprises of three-ring side chain and two-ring backbone, which consists of glucose that is identical to the ring structures in CMC. The functional groups such as carbonyl and hydroxyl are attached to the side of the chain. This branching structure gives xanthan gum thixotropic properties. The polymer branches are connected by weak hydrogen bonding. During shearing, the bond will break easily and the fluid becomes thin. As drilling fluid is under static condition, the chains will retain their interaction by hydrogen bonding, and as a results viscosity returns back to the initial state [31].

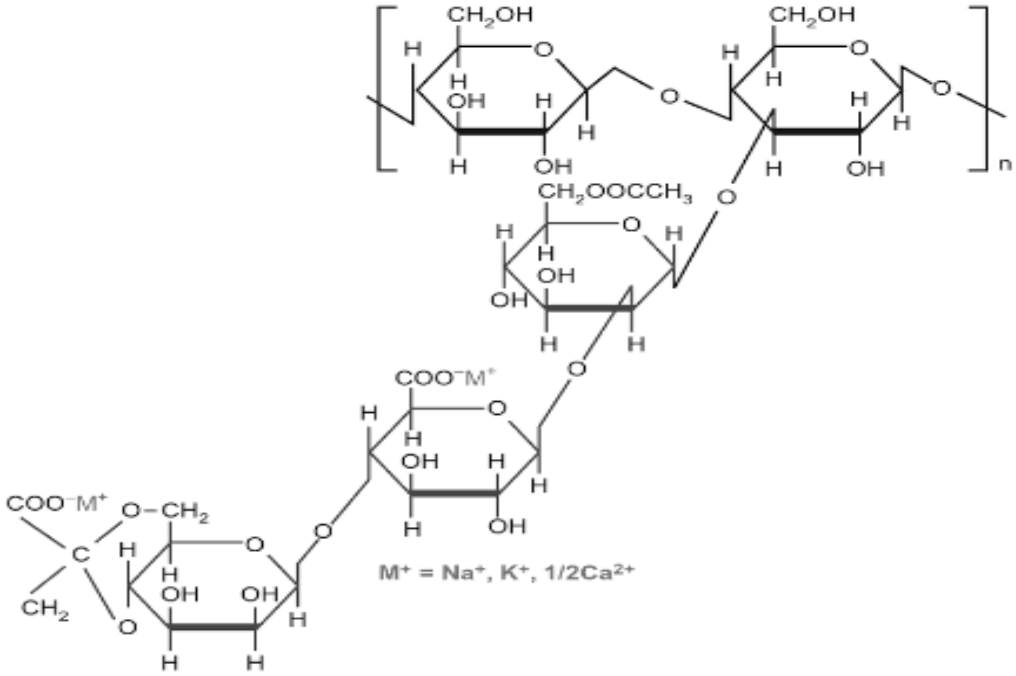

Figure 3.3: Structure of Xanthan gum [31]

3.2.3 CMC

Carboxymethyl cellulose (CMC) is derived from cellulose, where carboxymethyl groups (-CH_2-COOH) are bounded to the hydroxyl groups. As shown in figure 3.4, CMC has a linear structure and is a water soluble anionic polymer. In drilling fluids,

CMC is used as a viscosity modifier and to control the fluid loss [31]. Soluble CMC is also used in the development of biofilms, emulsions and nanoparticles for drug delivery [32].

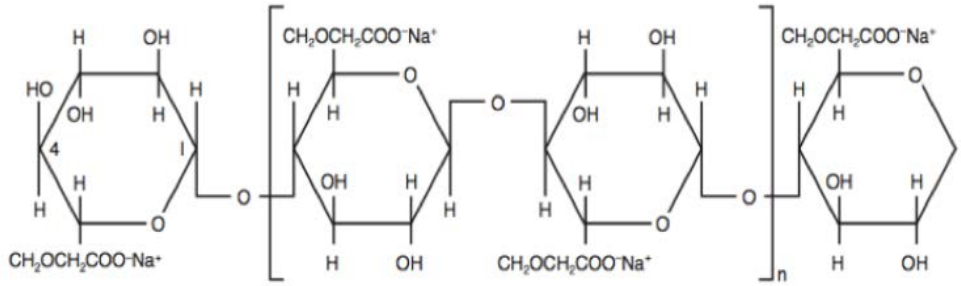

Figure 3.4: Structure of CMC [31]

3.2.4 KCl salt

Potassium chloride based drilling fluids are widely accepted for drilling water-sensitive shales. Since the K^+ ions are attracted towards the negative charge of the clay surface and size of the ions can fit into the plates of clay, it can provide stability to the shale against drilling fluids [33].

3.3 Nanoparticles

3.3.1 MWCNT nanoparticle description

Carbon nanotube (CNT) is a cylindrical molecule composed of carbon atoms. It has hexagonal patterns that repeats itself periodically in space. Each neighbouring atoms are bonded with strong covalent bond. CNT's are light materials and shows properties like electrical, mechanical, thermal conductivity and resistant to corrosion. The measured specific tensile strength of a single layer of a multi-walled carbon nanotubes can be as high as 100 times that of steel [34]. Figure 3.5 shows the SEM picture of 20-40nm and 2.1gm/cc MWCCNT. The particles were purchased from EPRUI Nanoparticles and Microspheres Co. Ltd [35].

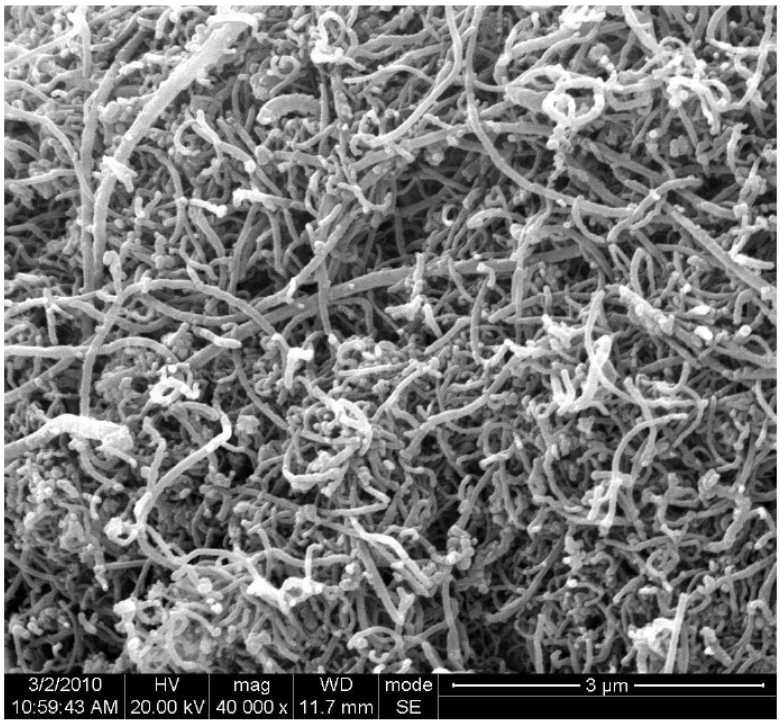

Figure 3.5: Morphology of MWCNT particles – SEM photograph

3.3.2 Silica dioxide nanoparticle description

Silicon dioxide nanoparticles (SiO_2) are chemically composed of silicon and oxygen. These particles are also known as silica nanoparticles or silica. They have low toxicity and can be functionalized with several types of polymers.

White powdered form of silicon dioxide nanoparticles was purchased from EPRUI Nanoparticles and Microspheres Co. Ltd [35]. In the literature, wide application of silica nanoparticles as an additive for rubber and plastics, and also to strengthen concrete is documented. In addition, due to their stable and non-toxic properties, silica nanoparticles are used in drug delivery.

In this thesis work, 15nm silica particles were tested in the drilling fluid [35]. The particles size and elements have also been characterized with the Scanning Electron Microscopy (SEM) (figure 3.6) and Elemental Dispersive Spectroscopy (EDS) (figure 3.7). As shown in EDS figure, there was a small amount of palladium. However, actually palladium was not present in these particles. It was just used for coating of the particles during SEM analysis. Therefore nanoparticles contains Si and O.

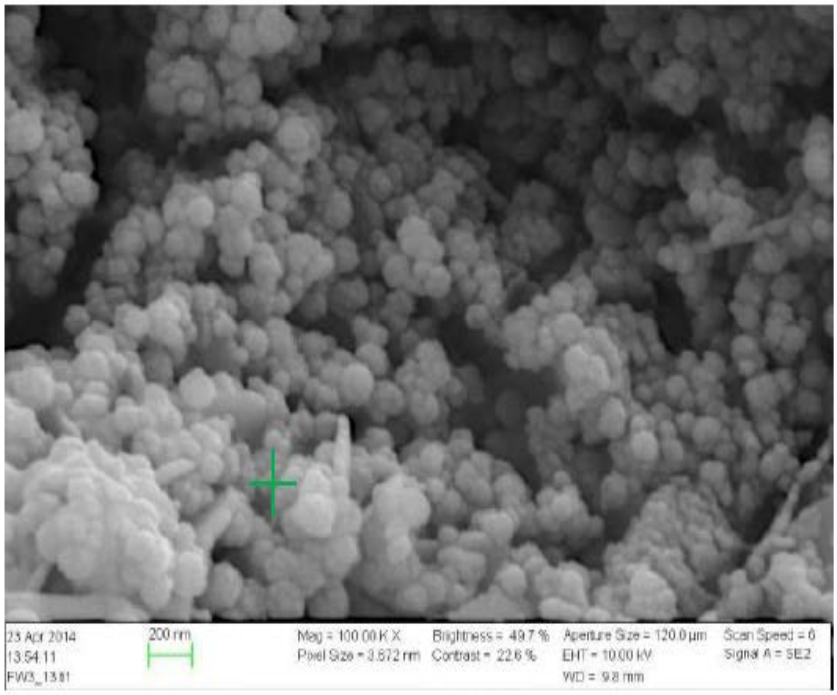

Figure 3.6: SEM picture of Nano-Silica

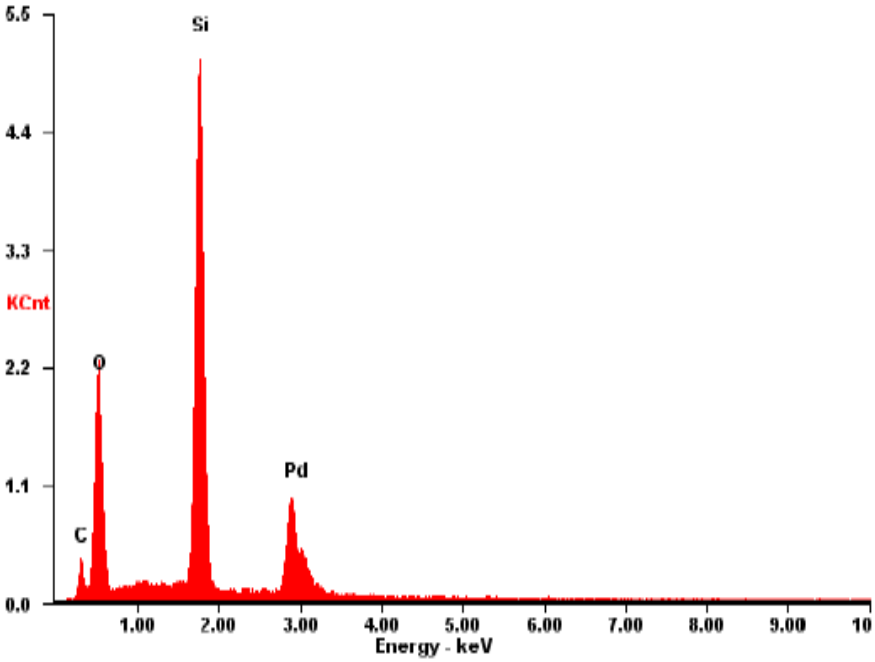

Figure 3.7: Element analysis of Nano-Silica

4 Experimental work

Several types of drilling fluid were formulated in order to investigate the effect of a single type as well as composites of nanoparticles in WBM. The additives used in the experimental work are reviewed in chapter 3. The different fluids are characterized by their rheological properties, filtrate loss, pH, friction coefficient and viscoelasticity.

4.1 Effect of MWCNT in XG

In this section the effect of the MWCNT nanoparticles in XG is investigated, most samples are formulated with lower concentrations of nanoparticles. However, to investigate the effect of high concentration one of the samples was made with the higher concentration.

4.1.1 Description and fluid formulation

As mentioned above, in this study MWCNT nanoparticles along with XG polymer was used. The fluid was designed to get the idea of how nanoparticles, salt and polymers affect each other, and which fluid system provides the best results. The salt was added to stabilize the system, the polymer was added for viscosity purpose, in addition to the filtrate loss control additive bentonite. The fluids were mixed in following order:

- Water
- Salt
- Polymer
- Nanoparticles
- Bentonite

For the reference drilling fluid no nanoparticles were added, and the other drilling fluids contained different concentrations of MWCNT, meanwhile the amount of water, polymer, salt and the bentonite were constant for all the fluids as shown in table 4.1. To formulate drilling fluid, first tap water was added in the container,

afterwards salt was added in the water. KCl salt was used for all the experiments. After mixing the salt in the water, polymer was added in the system and the system was mixed with the Hamilton beach mixer. It is important to add polymer in the system carefully to avoid the formation of lumps. After the mixing, the fluid was allowed to age for 48 hours in order to allow enough time for bentonite to swell properly, then the drilling fluid was further characterized.

Additives	Ref (XG)	Fluid 1 (0.05g MWCNT)	Fluid 2 (0.10g MWCNT)	Fluid 3 (0.15g MWCNT)	Fluid 4 (0.20g MWCNT)	Fluid 5 (2.0g MWCNT)
Water	500	500	500	500	500	500
XG, polymer	0,5	0,5	0,5	0,5	0,5	0,5
KCl	2,5	2,5	2,5	2,5	2,5	2,5
MWCNT	0	0,05	0,1	0,15	0,2	2
Bentonite	25	25	25	25	25	25

Table4.1 Fluid formulation test matrix for MWCNT drilling fluids in XG

4.1.2 Characterization of MWNCT fluids

There are some basic properties which characterize the drilling fluids. Next section will be focused on the characterization techniques which was used to characterize the drilling fluids.

4.1.2.1 Viscometer response and rheology parameters

Figure 4.1 shows the viscometer data for MWCNT drilling fluids, along with the reference drilling fluid. The viscometer data showed some changes to the nanoparticle-treated drilling fluids compared to the reference drilling fluid. The shear stress increased for all of the drilling fluid with MWCNT as an additive, maximum increase was achieved for the fluid with the highest amount of MWCNT as shown in the graph. From the viscometer readings the Bingham and Power-law parameters were calculated. The parameters are presented in figure 4.2 and figure 4.3.

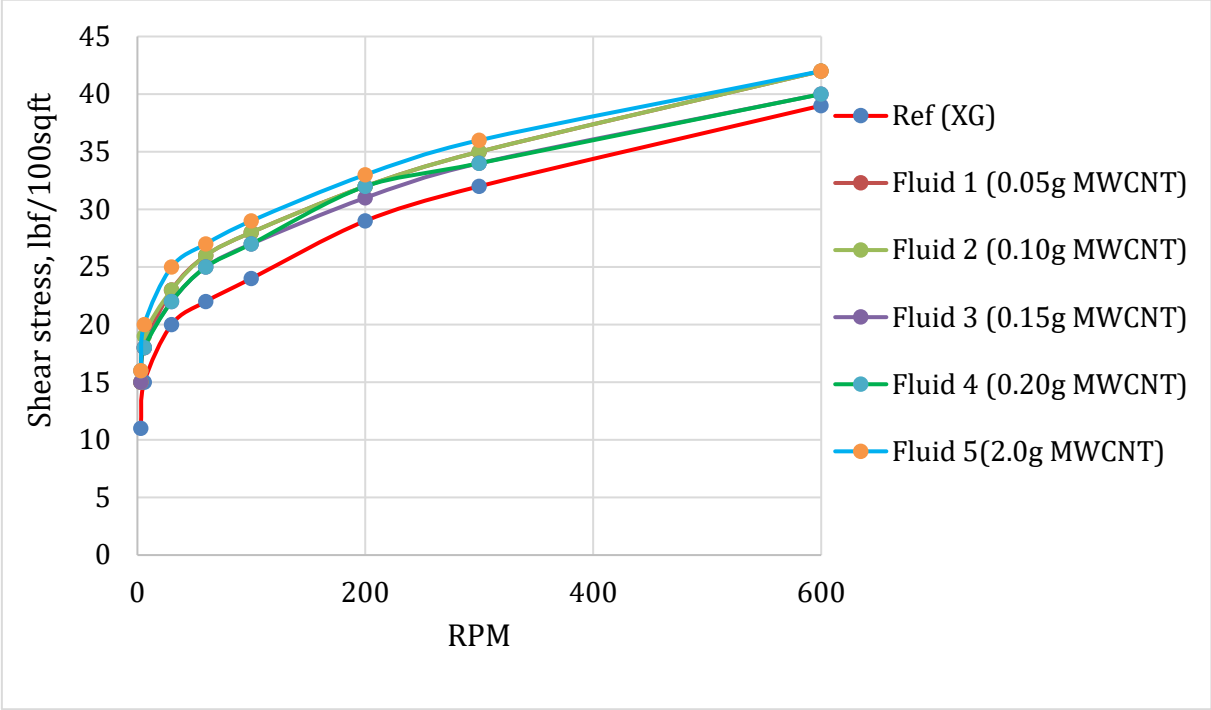

Figure 4.1: Viscometer responses of drilling fluids formulated in table 4.1

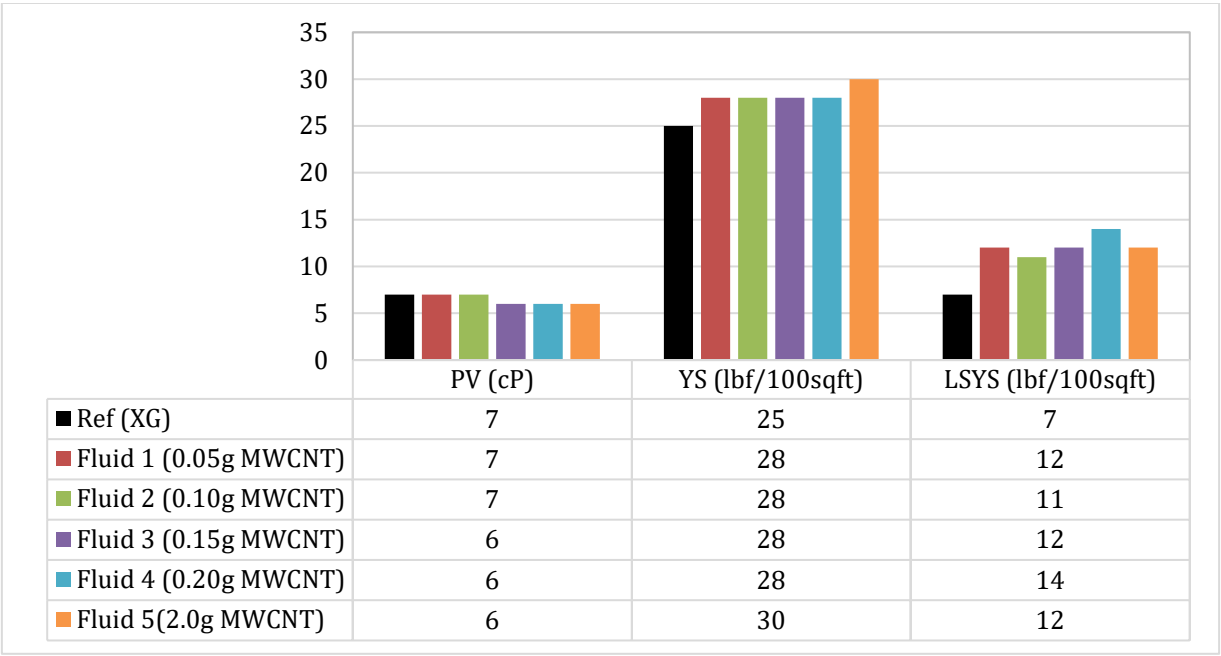

	PV (cP)	YS (lbf/100sqft)	LSYS (lbf/100sqft)
Ref (XG)	7	25	7
Fluid 1 (0.05g MWCNT)	7	28	12
Fluid 2 (0.10g MWCNT)	7	28	11
Fluid 3 (0.15g MWCNT)	6	28	12
Fluid 4 (0.20g MWCNT)	6	28	14
Fluid 5(2.0g MWCNT)	6	30	12

Figure 4.2: Bingham parameters for the drilling fluids formulated in table 4.1

The Bingham parameters shows that:

- The PV remained unchanged for Fluid 1(0.05g MWCNT) and Fluid 2(0.10g MWCNT), while for the rest of the fluids with the increase in nanoparticles concentration the PV decreased with 14%.

- The YS increased for the nanoparticle-treated fluid compared to the reference fluid, however concentration does not have much effect on the YS, and it was constant for all the nanoparticles concentrations, except for Fluid 5(2.0g MWCNT) which had the highest increase with 20%.

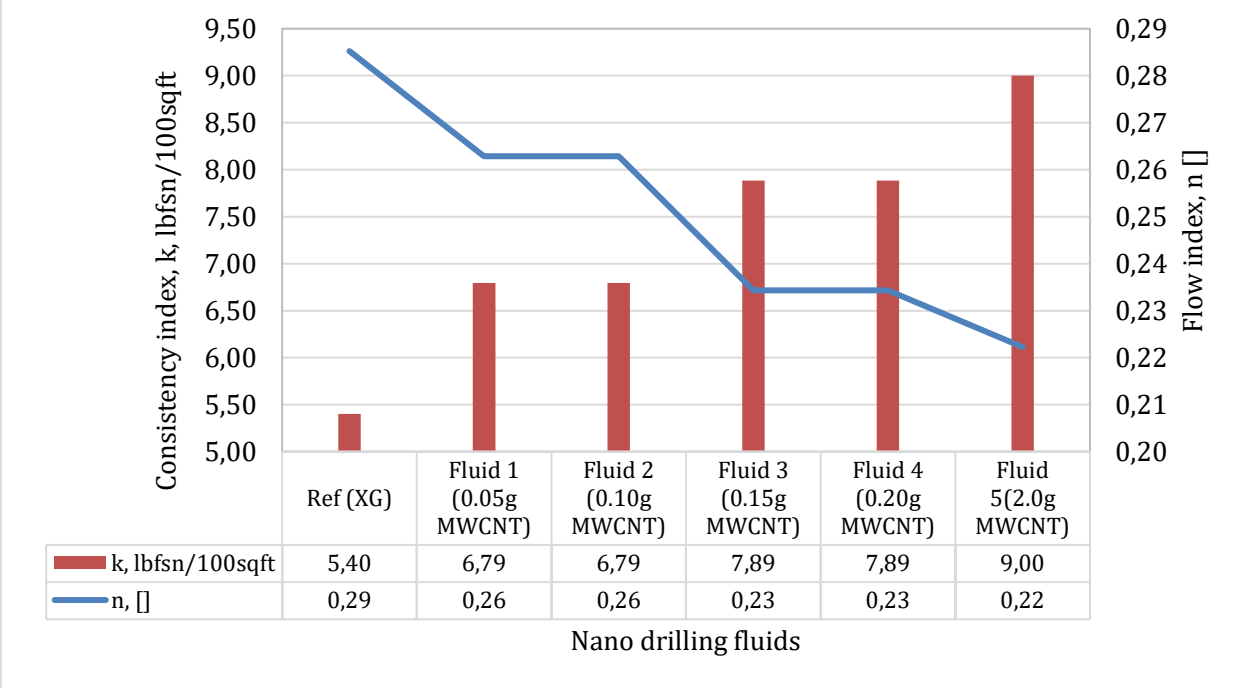

Figure 4.3 Power-law parameters for the drilling fluids formulated in table 4.1

The Power-law parameters shows that:

- The consistency index values increased for all the drilling fluids having nanoparticles compared to the Ref (XG), it increased the most for higher concentration that is Fluid5(2.0g MWCNT), with 67%.
- The flow index values decreased for all the drilling fluids which have nanoparticles compared to the Ref (XG), and it decreased the most for the Fluid5(2.0g MWCNT), with 24%. According to flow index values all the fluids has pseudo plastic behavior.
- Fluid 1(0.05g MWCNT) and Fluid 2(0.10g MWCNT) had the same consistency index values and flow index values, for instance it was the same case with Fluid 3(0.15g MWCNT) and Fluid 4(0.20g MWCNT), this indicates that small increase in the concentration does not have much effect.

4.1.2.2 pH and filtrate loss

To determine the pH values of the drilling fluids, a pH-meter was used for the measurements, shown in figure 4.4. Filter loss values can be used as an indicator to determine if the filter cake is thin or thick, for a drilling fluid it is desirable to develop a thin and low permeable filter cake. The filtrate loss tests were performed by using an API static filter press, shown in figure 4.5.

Figure 4.4: Picture of pH-meter

Figure 4.5: Photograph picture of API static filter press

Parameters	Ref (XG)	Fluid 1 (0.05g MWCNT)	Fluid 2 (0.10g MWCNT)	Fluid 3 (0.15g MWCNT)	Fluid 4 (0.20g MWCNT)	Fluid 5(2.0g MWCNT)
pH	8,89	8,89	8,91	8,9	8,95	8,29
Filtrate	7	7,5	7,75	7,75	7,5	7,5

Table 4.2: pH and filtrate changes for drilling fluids formulated in table 4.1

Table 4.2 shows pH and filtrate changes for the MWCNT drilling fluid. The additives didn't have any impact on the pH modification. The filtrate loss increased for all the MWCNT drilling fluid compared to the REF (XG). It increased most for Fluid 2(0.10g MWCNT) and Fluid 3 (0.15g MWCNT), with an increase of 11%.

4.1.2.3 Tribometry coefficient of friction measurement

To measure the lubricity of the nanoparticle enhanced drilling fluids, the coefficients of friction were measured for all the fluids, by using a CSM tribometer, shown in figure 4.6. The drilling fluids were tested by applying a constant normal force of 5N

to the tribometer arm. The temperature was held constant at 22 ^{o}C. Several tests were perfromed for each of the drilling fluids in order to get averaged value of the friction coefficient. A picture of the tribometer is shown in figure 4.6.

Figure 4.6: Photograph picture of CSM tribometer

Figure 4.7 presents coefficient of friction for the MWCNT nanoparticles based drilling fluids, along with the reference drilling fluid. Several tests were performed with the tribometer to investigate the lubricating effect of the nanoparticles treated drilling fluid, in the figure below the averaged values are presented. The lowest value of the coefficient of friction was obtained for Fluid 5(2.0g MWCNT). The coefficient of friction has nonlinear character.

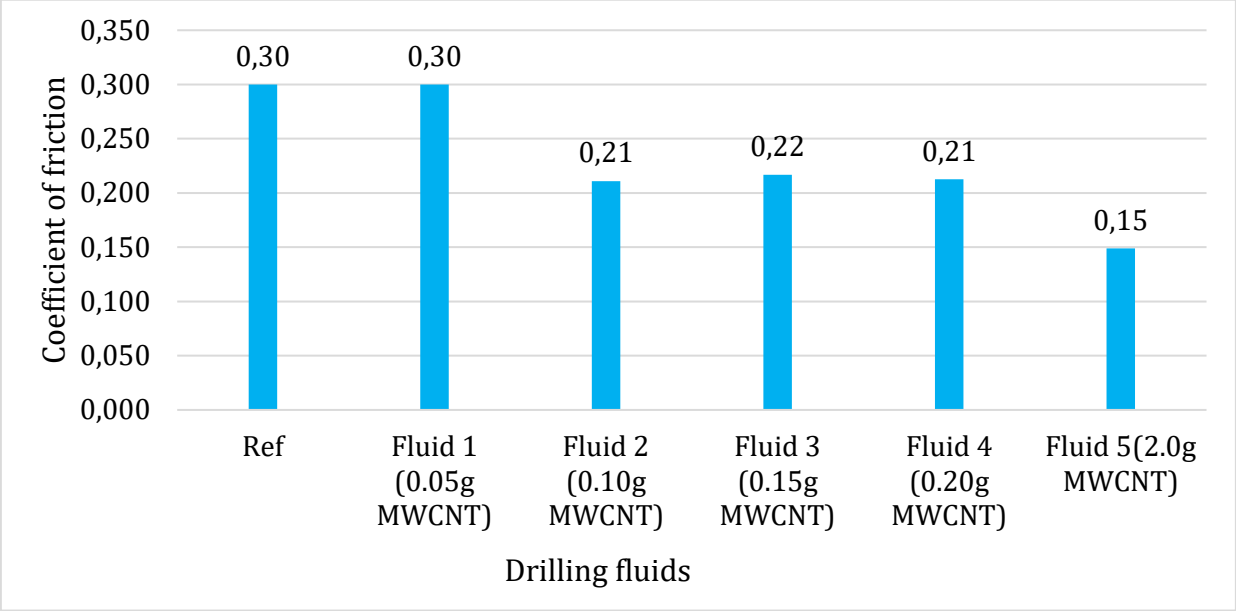

Figure 4.7: Coefficient of friction changes for drilling fluids formulated in table 4.1

Figure 4.8 presents the coefficient of friction changes in terms of percentage, for Fluid 5 (2.0g MWCNT) this value decreased with 50.3%. For Fluid 2(0.1g MWCNT), Fluid 3(0.15g MWCNT) and Fluid 4(0.20g MWCNT) the coefficient of friction in percent decreased by 29.7%, 27.8% and 29.2%, respectively.

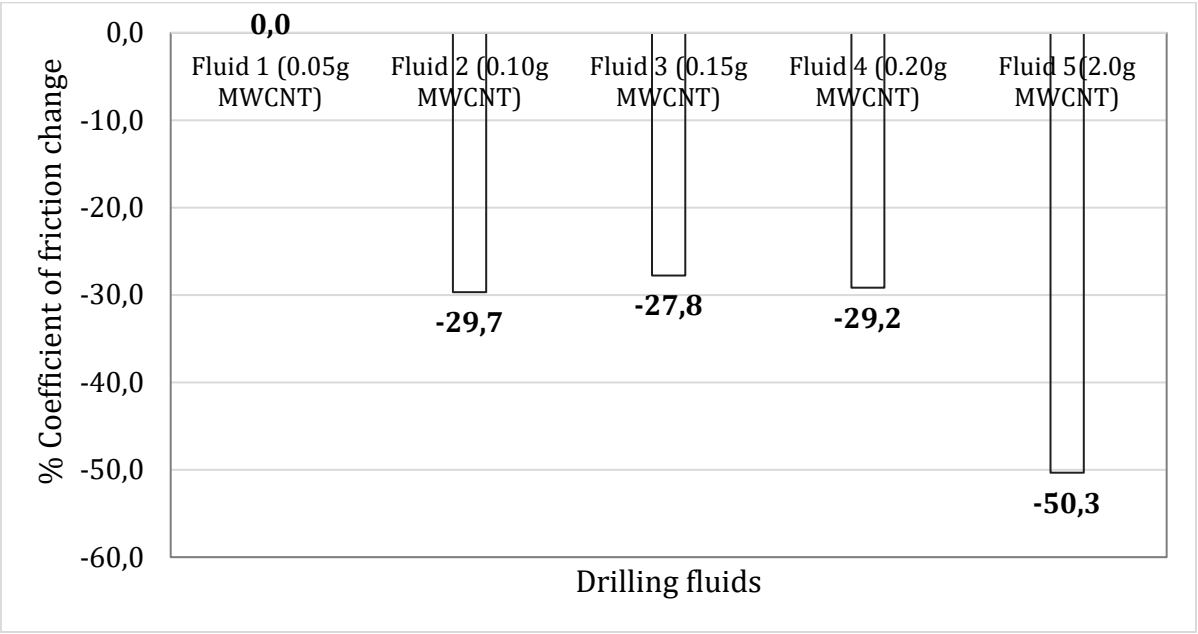

Figure 4.8: Coefficient of friction changes in percent for drilling fluids formulated in table 4.1

4.2 Effect of SiO2 in XG

In this section the effect of the SiO_2 nanoparticle in XG is investigated, mainly in low concentrations, but one of the drilling fluid samples was formulated with the higher concentration of SiO_2.

4.2.1 Description and fluid formulation

The nanoparticles chosen for this fluid system was SiO_2 and the polymer was XG. The procedure of mixing drilling fluid is described in section 3.1.1. The amount of water, polymer, salt and bentonite were constant for all the drilling fluids. Ref (XG) was prepared without nanoparticles, while the other drilling fluids had an increasing amount of SiO_2. Table 4.3 shows the composition of the fluid system.

Additives	Ref (XG)	Fluid 1- (0.05g SiO2)	Fluid 2 (0.10g SiO2)	Fluid 3 (0.15g SiO2)	Fluid 4 (0.20g SiO2)	Fluid 5 (2.0g SiO2)
Water	500	500	500	500	500	500
XG	0,5	0,5	0,5	0,5	0,5	0,5
KCl	2,5	2,5	2,5	2,5	2,5	2,5
SiO_2	0	0,05	0,1	0,15	0,2	2
Bentonite	25	25	25	25	25	25

Table 4.3: Fluid formulation test matrix for silica nanoparticle drilling fluids in XG

4.2.2 Characterization of SiO2 fluids

4.2.2.1 Viscometer response and rheology parameters

Figure 4.9 shows the viscometer data for SiO_2 drilling fluids, along with the reference drilling fluid.

The viscometer data shows the minor changes for all the nanoparticles treated fluids compared to the reference drilling fluid, except for the Fluid 5(2.0g SiO_2) which had an apparent decrease in the shear stress. The lower concentration of nanoparticles additives did not affect the shear stress significantly, only the drilling fluid with the higher concentration of silica nanoparticles have a considerable effect on shear stress. Based on the viscometer results Bingham parameters and Power-law parameters are calculated and presented in the figure 4.10 and figure 4.11.

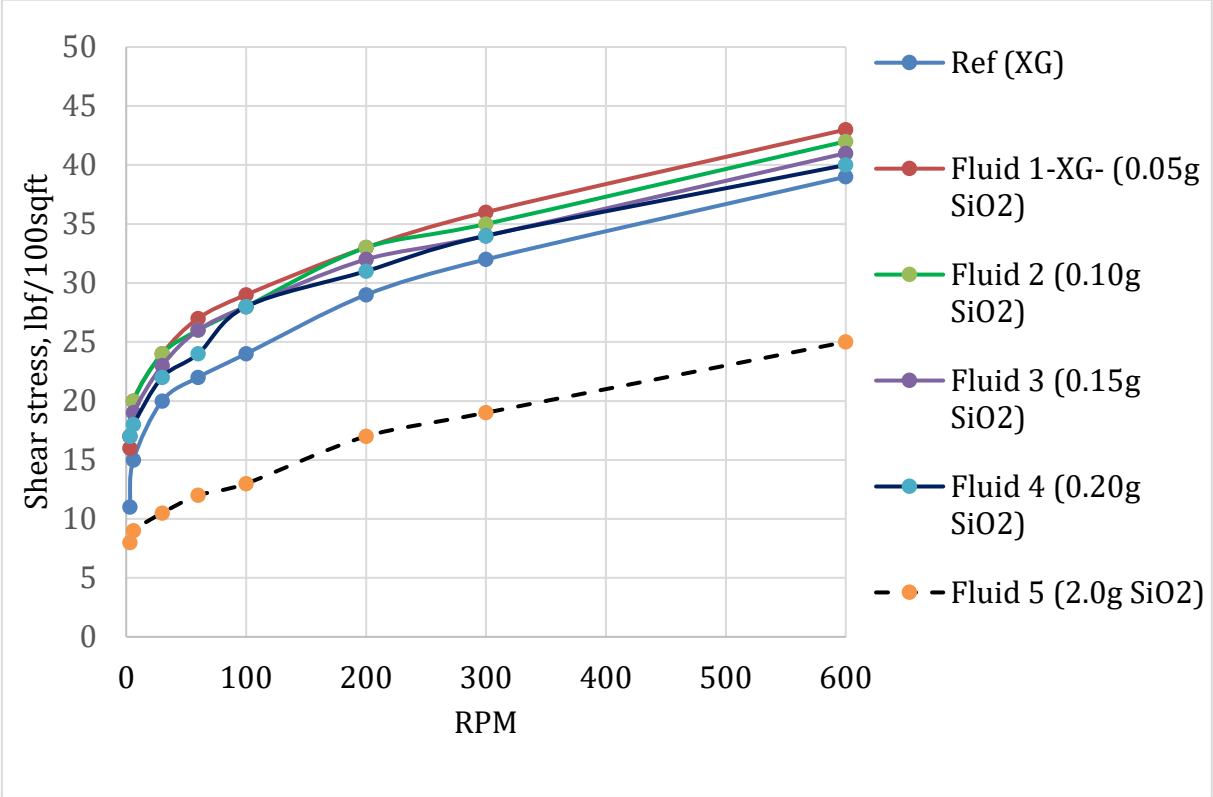

Figure 4.9: Viscometer responses of drilling fluids formulated in table 4.3

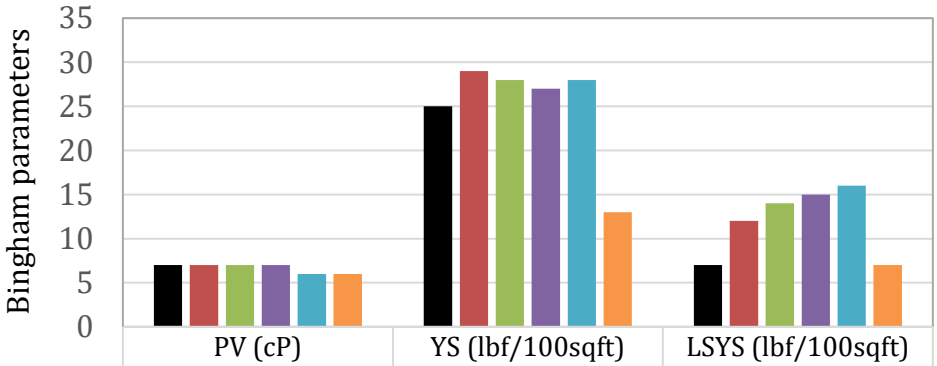

	PV (cP)	YS (lbf/100sqft)	LSYS (lbf/100sqft)
Ref (XG)	7	25	7
Fluid 1-XG- (0.05g SiO2)	7	29	12
Fluid 2 (0.10g SiO2)	7	28	14
Fluid 3 (0.15g SiO2)	7	27	15
Fluid 4 (0.20g SiO2)	6	28	16
Fluid 5 (2.0g SiO2)	6	13	7

Figure 4.10: Bingham parameters for the drilling fluids formulated in table 4.3

The Bingham parameters shows the following:

- The PV remained unchanged for Fluid 1(0.05g SiO_2), Fluid 2(0.10g SiO_2) and Fluid 3(0.15g SiO_2), whereas for the other two drilling fluids the PV decreased by 14%.
- The YS increased for all the systems with SiO_2 as an additive, except for the Fluid 5(2.0g SiO_2), where it decreased by 48% compared to the Ref (XG).
- The LSYS increased for all the fluids, except Fluid 5(2.0g SiO_2) where it has the same value as the reference drilling fluid. The greatest LSYS value was achieved by Fluid 4(0.20g SiO_2), with an increase of 129%.

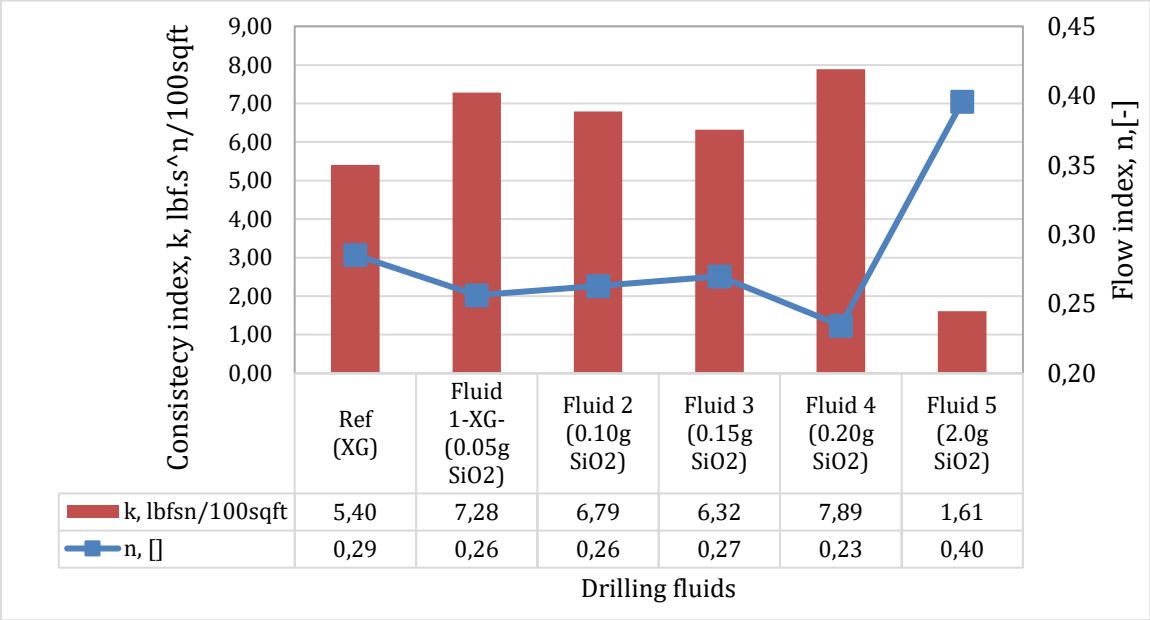

Figure 4.11: Power-law parameters for the drilling fluids formulated in table 4.3

The Power-law parameters shows that:

- The consistency index increases for all the fluids, except for Fluid 5(2.0g SiO_2), where it has a decrease of 70%. For all the fluids having low concentrations, the increase of the consistency index varies from 17% to 46% compared to the reference drilling fluid.
- The flow index decreases for all the low concentration drilling fluids, with the highest decrease for Fluid 4 (0.20g SiO_2) of 21%. For the high concentration

of nanoparticles in drilling fluid, Fluid 5(2.0g SiO_2), the flow index increased by 38%. For all the drilling fluids the n-value is below 1, hence the fluids are pseudo plastic fluids.

- The largest change in Power-law parameters was achieved by the Fluid 5(2.0g SiO_2).

4.2.2.2 pH and filtrate loss

Table 4.4 shows the pH and filtrate changes for the SiO_2 drilling fluid

Parameters	Ref (XG)	Fluid 1-XG-(0.05g SiO2)	Fluid 2 (0.10g SiO2)	Fluid 3 (0.15g SiO2)	Fluid 4 (0.20g SiO2)	Fluid 5 (2.0g SiO2)
pH	8,89	8,66	8,85	8,84	8,73	8,06
Filtrate	7	8,5	7	7,25	7,5	8
% Filtrate loss change		21	0	4	7	14

Table 4.4: pH and filtrate changes for drilling fluids formulated in table 4.3

SiO_2 nanoparticle additives in general decreased the pH of the drilling fluid as compared to nanoparticle free Ref (XG). For instance, Fluid 5(2.0g SiO_2) decreased the pH by 9.3%.

As shown, none of the considered SiO_2 nanoparticles improved the filtrate loss performance. The additives in the bentonite /XG system increased the filtrate loss in the range of 0-21%.

4.2.2.3 Tribometry coefficient of friction measurement

Figure 4.12 presents the averaged values of coefficient of friction for the nanoparticles based drilling fluids, along with the reference drilling fluid. The coefficient of friction decreases as the nanoparticles are added to the drilling fluid, the coefficient of friction has its lowest value for Fluid 1 (0.05g SiO_2), as the concentration of nanoparticles increases, the coefficient of friction increases. When a higher concentration of SiO_2 is added in the drilling fluid, the coefficient of friction value exceeds the Ref (XG) fluid's value.

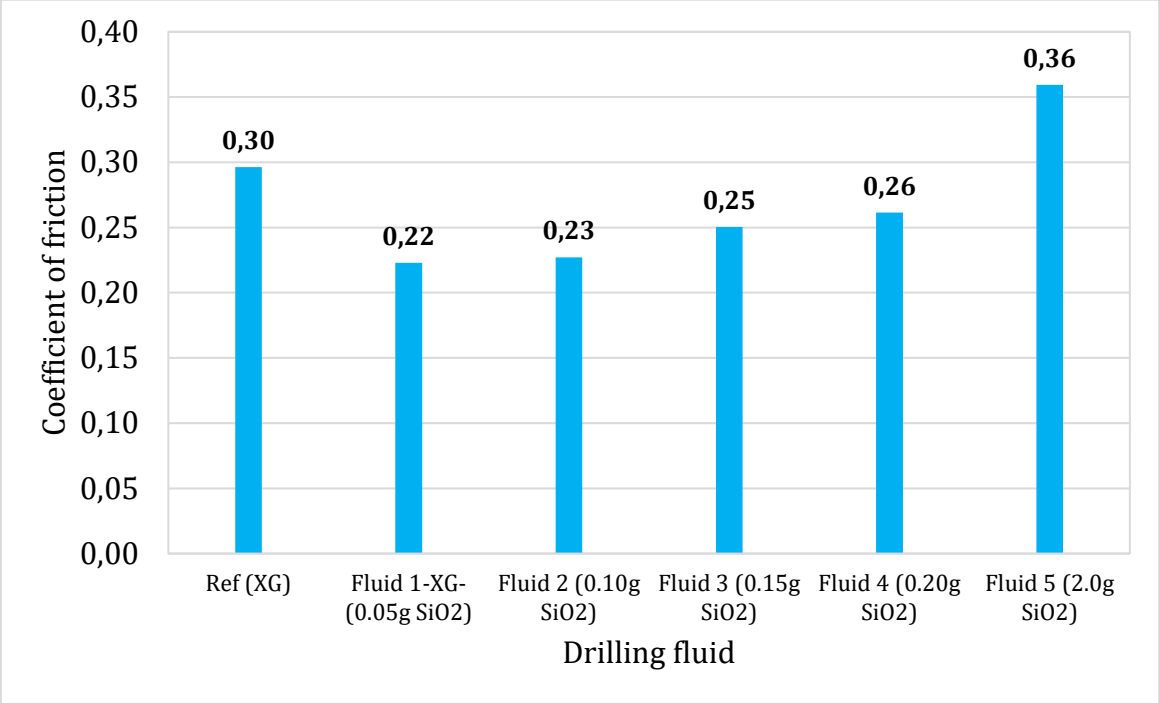

Figure 4.12: Coefficient of friction changes for drilling fluids formulated in table 4.3

Figure 4.13 presents the coefficient of friction change in percentage. For Fluid 1(0.05g SiO_2) the friction decreased by24.7%, and it increased to 21.3% for Fluid 5 (2.0g SiO_2). Higher concentration of silica nanoparticles increases the friction coefficient.

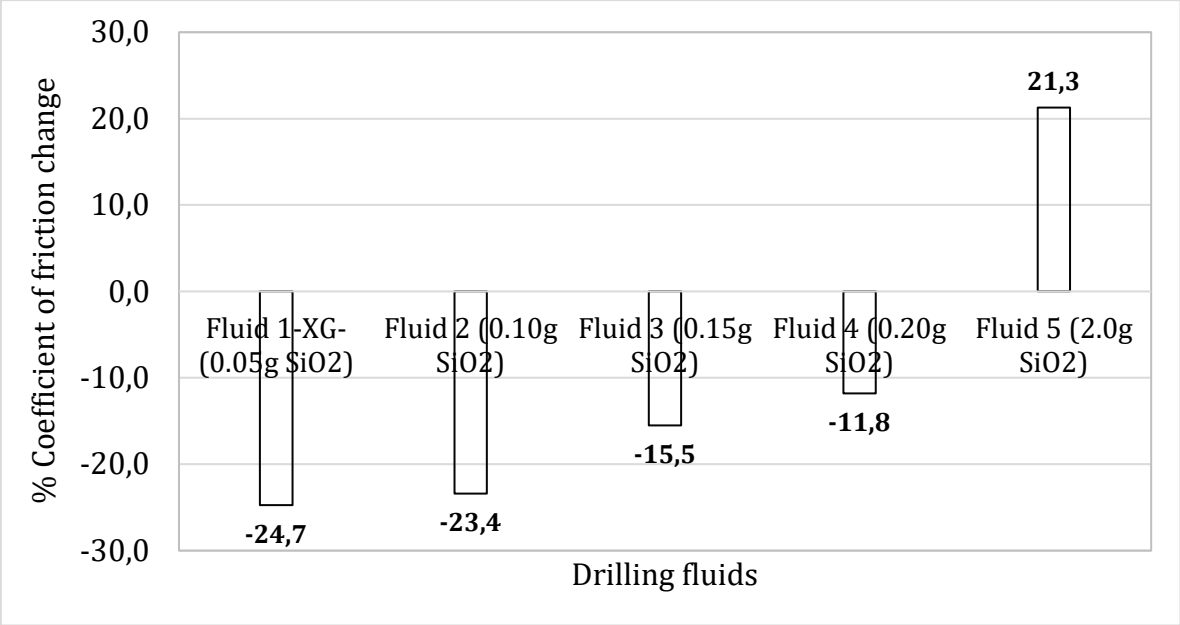

Figure 4.13: Coefficient of friction changes in percent for drilling fluids formulated in table 4.3

4.3 Effect of SiO_2-MWCNT composite effect in CMC

In this section the effect of the MWCNT and SiO_2 mixture in CMC is investigated along with a higher concentration of each of nanoparticles separately in CMC. The polymer CMC was chosen in place of XG on the basis of friction results. MWCNT and SiO_2 in high concentrations were investigated in both CMC and XG, for the MWCNT the friction coefficients were not significantly changed, but for the SiO_2 the friction coefficient was lower in CMC than XG. Therefore the polymer CMC was used because it provided better performance in both nanoparticles on the basis of friction.

4.3.1 Description and fluid formulation

The nanoparticles chosen for this fluid system were MWCNT and SiO_2, and the polymer was CMC. The procedure of mixing drilling fluid is described in the section 3.1.1. The amount of water, polymer, salt and bentonite were constant for all the drilling fluids, Ref (CMC) was prepared without nanoparticles, Fluid 1, Fluid 2 and Fluid 3 had an equal amount of MWCNT and SiO_2, while Fluid 4 had a higher amount of SiO_2 and a smaller amount of MWCNT. Fluid 5 was formulated with a high concentration of SiO_2 only, and Fluid 6 was formulated with just high concentration of MWCNT. Table 4.5 shows the drilling fluids formulation.

Additives	Ref (CMC)	Fluid 1 (0.075g SiO_2+ 0.075g MWCNT)	Fluid 2 (0.1g SiO_2+ 0.1g MWCNT)	Fluid 3 (1.0g SiO_2+ 1.0g MWCNT)	Fluid 4 (1.95g SiO_2+ 0.05g MWCNT)	Fluid 5 (2g SiO_2+ 0.0g MWCNT)	Fluid 6 (0.0g SiO_2+ 2g MWCNT)
Water	500	500	500	500	500	500	500
CMC	0,5	0,5	0,5	0,5	0,5	0,5	0,5
KCl	2,5	2,5	2,5	2,5	2,5	2,5	2,5
SiO_2	0	0,075	0,1	1	1,95	2	0
MWCNT	0	0,075	0,1	1	0,05	0	2
Bentonite	25	25	25	25	25	25	25

Table 4.5: Fluid formulation test matrix for silica nanoparticle and MWCNT mixture drilling fluids in CMC

4.3.2 Characterization of SiO_2-MWNCT fluids

4.3.2.1 Viscometer response and rheology parameters

Figure 4.14 shows the viscometer data for the mixture of MWCNT and SiO_2 in drilling fluids and for the drilling fluid 5 and 6, along with the reference drilling fluid.

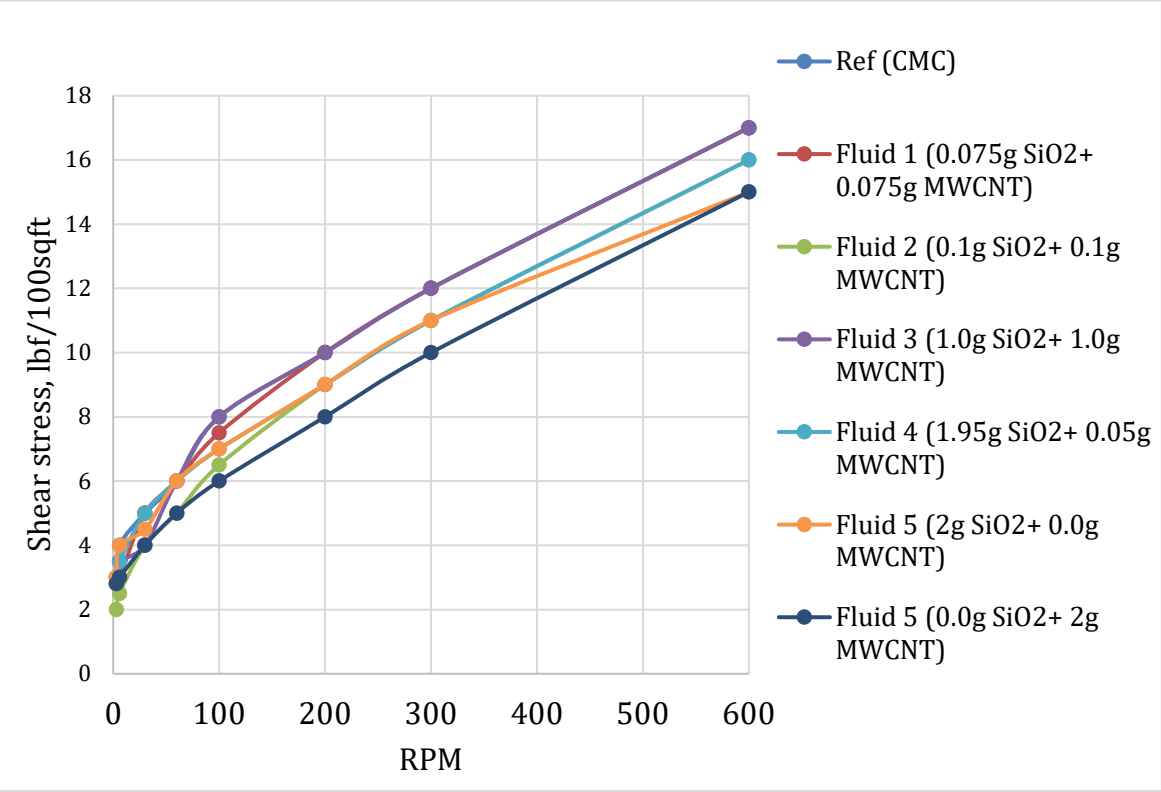

Figure 4.14: Viscometer responses of drilling fluids formulated in table 4.5

The viscometer data shows that the shear stress decreased for Fluid 6(0g SiO2+ 2.0g MWCNT), and increased for Fluid 1(0.075g SiO2+0.075g MWCNT) and for Fluid 3(1.0g SiO2+1.0g MWCNT). Fluid 2(0.1g SiO2+0.1g MWCNT) and Fluid 5(2.0gSiO2+0g MWCNT) shows almost similar values. After an increase in the mixing speed to 400RPM, the shear stress decreased for the Fluid 5. Bingham parameters and Power-law parameters based on the viscometer results are calculated and presented in the figure 4.15 and figure 4.16.

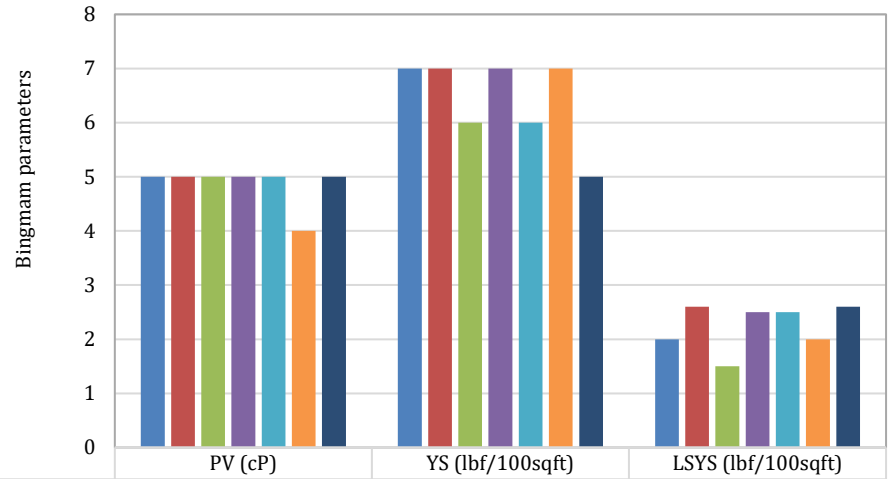

	PV (cP)	YS (lbf/100sqft)	LSYS (lbf/100sqft)
Ref (CMC)	5	7	2
Fluid 1 (0.075g SiO2+ 0.075g MWCNT)	5	7	2,6
Fluid 2 (0.1g SiO2+ 0.1g MWCNT)	5	6	1,5
Fluid 3 (1.0g SiO2+ 1.0g MWCNT)	5	7	2,5
Fluid 4 (1.95g SiO2+ 0.05g MWCNT)	5	6	2,5
Fluid 5 (2g SiO2+ 0.0g MWCNT)	4	7	2
Fluid 5 (0.0g SiO2+ 2g MWCNT)	5	5	2,6

Figure 4.15: Bingham parameters for the drilling fluids formulated in table 4.5

The Bingham parameters shows the following:

- The PV remains unchanged for all the drilling fluids, except for Fluid 5, where the PV has a decrease of 20%. The MWCNT and SiO_2 nanoparticles combined does not affect PV.
- As shown in figure 4.15, the YS remains the same as Ref (CMC) the three nanoparticle treated drilling fluids. The YS decreases 14.3% for Fluid 2 and Fluid 4, and it decreases 28.6% for Fluid 5.
- The LSYS varies between 25% decrease and 30% increase on the basis of concentration compared to Ref (CMC).

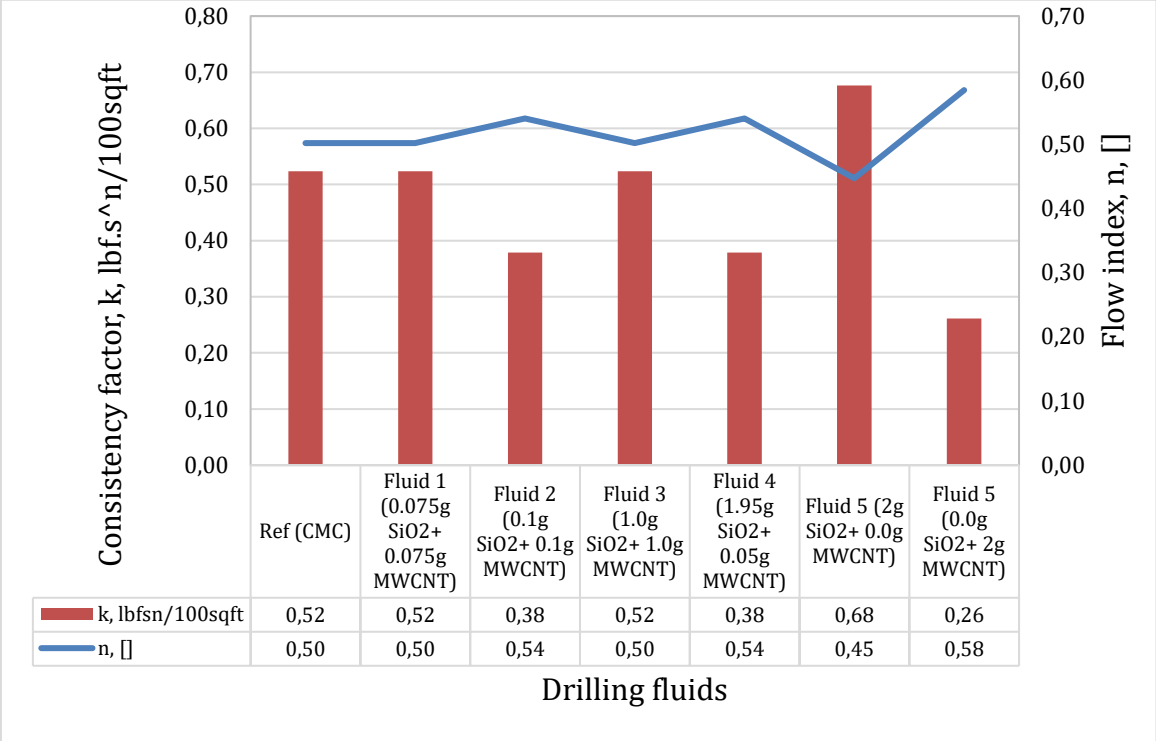

Figure 4.16: Power-law parameters for the drilling fluids formulated in table 4.5

The Power-law parameters shows the following:

- The consistency index increased the most for Fluid 5(2.0gSiO_2+0g MWCNT).
- The flow index remained the same as the Ref (CMC) for Fluid 1(0.075g SiO_2+ 0.075g MWCNT) and for Fluid 3(1.0g SiO_2+ 1.0g MWCNT). The highest increase was of 16%, obtained by Fluid 6(0gSiO_2+2.0g MWCNT). The drilling fluids formulated in CMC obtained the highest values for the flow index compared to the drilling fluids in XG. The flow index values are still under 1, hence the fluids exhibit pseudo plastic behavior, which is common for drilling fluids.

4.3.2.1 pH and filtrate loss

Table 4.6 shows pH and filtrate changes for the SiO_2 and MWCNT mixture drilling fluid. The pH decreased for all the drilling fluids with the addition of nanoparticles as an additive, it decreased the most for Fluid 4(1.96g SiO_2+ 0.05g MWCNT). The decrease was of 6.5% compared to the reference drilling fluid.

Parameters	Ref (CMC)	Fluid 1 (0.075g SiO2+ 0.075g MWCNT)	Fluid 2 (0.1g SiO_2+ 0.1g MWCNT)	Fluid 3 (1.0g SiO_2+ 1.0g MWCNT)	Fluid 4 (1.95g SiO_2+ 0.05g MWCNT)	Fluid 5 (2g SiO2+ 0.0g MWCNT)	Fluid 6(0.0g SiO_2+ 2g MWCNT)
pH	8,62	8,33	8,36	8,26	8,06	8,39	8,56
Filtrate	7	6,75	6,8	8,5	8,5	7,5	7,5
% Filtrate reduction		-3,6	-2,9	21,4	21,4	7,1	7,1

Table 4.6: pH and filtrate changes for drilling fluids formulated in table 4.5

When the same amount of nanoparticles SiO_2 and MWCNT were added in the lower concentration, filtrate loss was reduced compared to the reference drilling fluid. The reduction of 3.6% was achieved for Fluid 1(0.075g SiO_2+ 0.075g MWCNT) and 2.9% in case of Fluid 2 (0.1g SiO_2+ 0.1g MWCNT). For the other two composite drilling fluids, the filtrate loss increased by 21.4%. However, when higher concentrations of nanoparticles based on single nanoparticles system (either MWCNT or SiO_2) were used in drilling fluids, the filtrate increased by 7.1% for both SiO_2 and MWCNT.

4.3.2.2 Tribometry coefficient of friction measurement

Figure 4.17 presents the averaged values for friction coefficient for the composite of SiO_2 and MWCNT in drilling fluids, as well as single nanoparticles system having a higher concentration in drilling fluids, along with the reference drilling fluid. The value of friction coefficient is unchanged for Fluid 2(0.1g SiO_2+ 0.1g MWCNT) compared to Ref (CMC). For the other two drilling fluids with same concentrations of both nanoparticles, the friction coefficient is reduced, but not a significant change in the friction coefficient values. The lowest value is attained by the Fluid 4(1.95g SiO_2+ 0.05g MWCNT) when the combined effect is investigated.

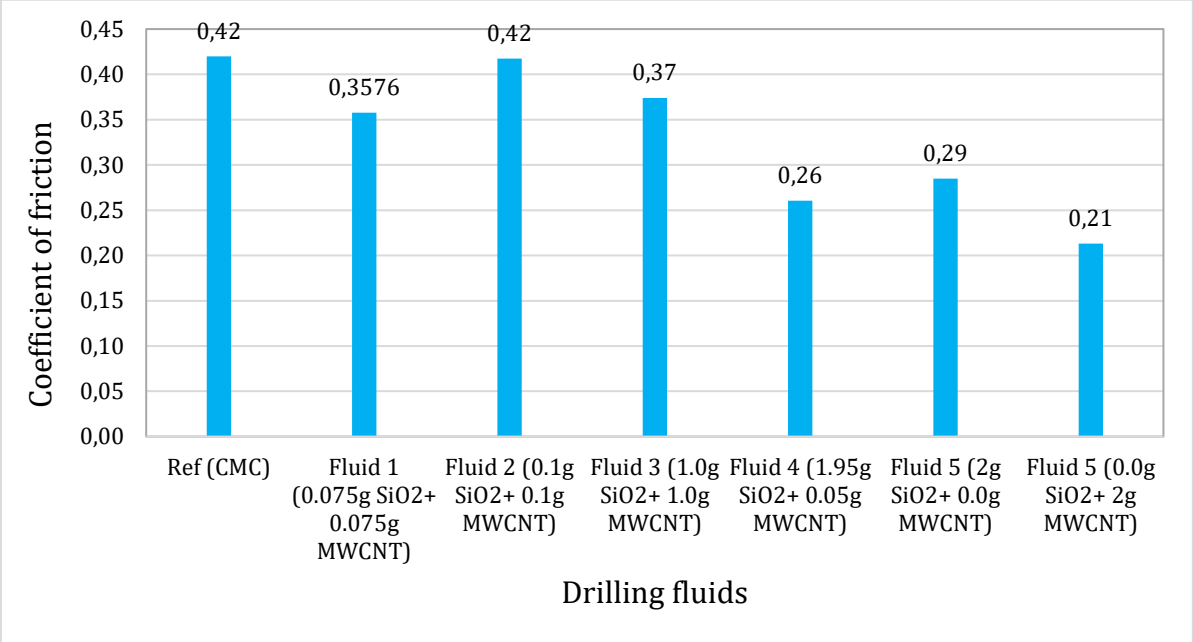

Figure 4.17: Coefficient of friction changes for drilling fluids formulated in table 4.5

Figure 4.18 presents the coefficient of friction change in percentage. Fluid 6 (0g SiO_2 + 2.0g MWCNT) provides the highest reduction with 49.3% reduction. When the SiO_2 nanoparticles and MWCNT are mixed together, the friction coefficient remains the same as the reference drilling fluid, as with Fluid 2(0.1g SiO_2+ 0.1g MWCNT).

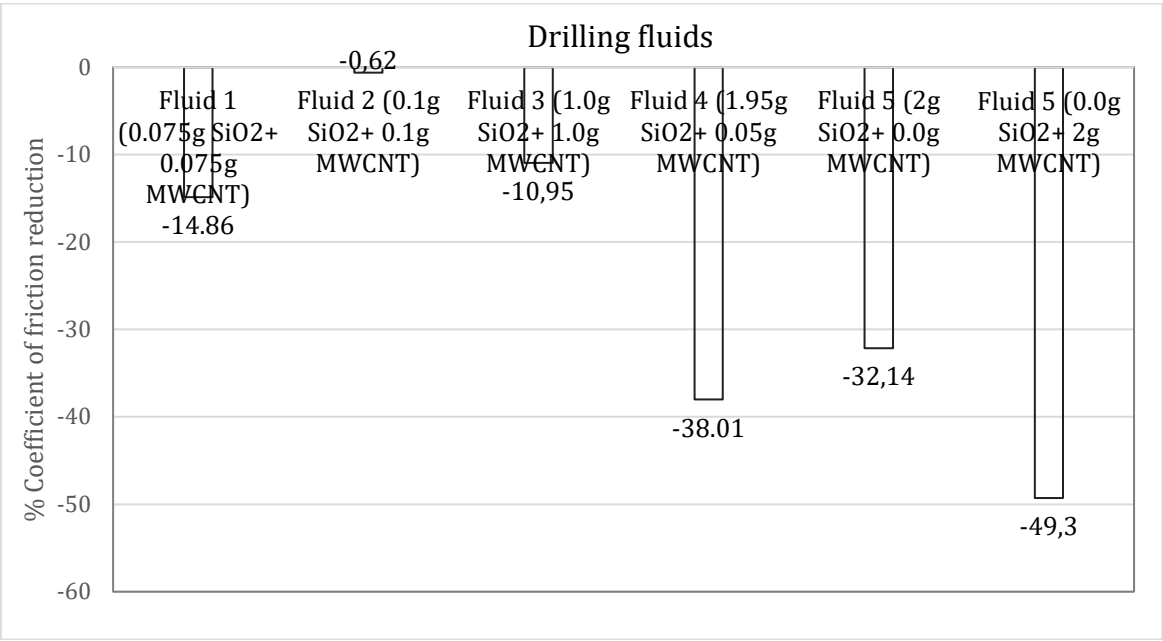

Figure 4.18: Coefficient of friction changes in percent for drilling fluids formulated in table 4.5

4.4 Viscoelasticity

Based on the best friction results, a total of five nanoparticles treated drilling fluids have been selected for further characterization. The reference systems with both XG and CMC are also further investigated in order to compare the results. This section evaluates the effect of nanoparticles on the viscoelastic behavior of the drilling fluids. The drilling fluids that were used for viscoelastic testing are formulated in the table 4.7 The equipment used for this experiment was an Anton Paar rheometer MCR 302, as illustrated in figure 2.4.

Additives	Ref(XG)	Ref(CMC)	Ref(XG) +0.15g MWCNT	Ref(XG) +2.0g MWCNT	Ref(XG) +0.05g SiO_2	Ref(CMC)+0,075 g SIO_2+0,075g MWCNT	Ref(CMC)+1.95 g SIO_2+0.05g MWCNT
Water	500	500	500	500	500	500	500
XG	0,5	0	0,5	0,5	0,5	0	0
CMC	0	0,5	0	0	0	0,5	0,5
SiO_2	0	0	0		0,05	0,075	1,95
WMCNT	0	0	0,15	2	0	0,075	0,05
KCl	2,5	2,5	2,5	2,5	2,5	2,5	2,5
Bentonite	25	25	25	25	25	25	25

Table 4.7: Fluid formulation of nanoparticle enhanced drilling fluids with the best frictional results (called the best system)

4.4.1 Amplitude sweep measurement

The oscillatory amplitude sweep test measurements are presented for the Ref (CMC) and Ref (CMC)+1.95gSiO_2+0.05g MWCNT. The test results obtained from the rest of the drilling fluids are presented in appendix C (except for Ref(XG)+2.0gMWCNT). Before the tests were performed, the drilling fluids were mixed in a Hamilton beach mixer to get a homogeneous mixture. The amplitude sweep tests were performed at 22^{o}C in parallel plate, the frequency was kept constant at 10rad/s, while the strain varied between 0.0005% and 100%. The results from the test were further used to plot shear stress, Storage modulus, Loss modulus and damping factor against the strain, for the different fluids. From the graph it is possible to determine the flow point and shear yield point. The graph can also give information about linear viscoelastic range (LVER), which is the point where the storage modulus and loss modulus are constant. Figure 4.19 shows that the values of storage modules values are greater than the corresponding loss

modules values, which means that Ref (CMC) is showing a gel-like behavior, like a viscoelastic solid [10]. The flow point is obtained where the storage modulus curve crosses the loss modulus curve, hence the shear stress value of the flow point is 2Pa. The flow point is the point where the fluid starts to flow. At this point the viscous behavior starts to dominate the elastic behavior. The damping factor values are relatively small and constant, but reach a peak after the flow point.

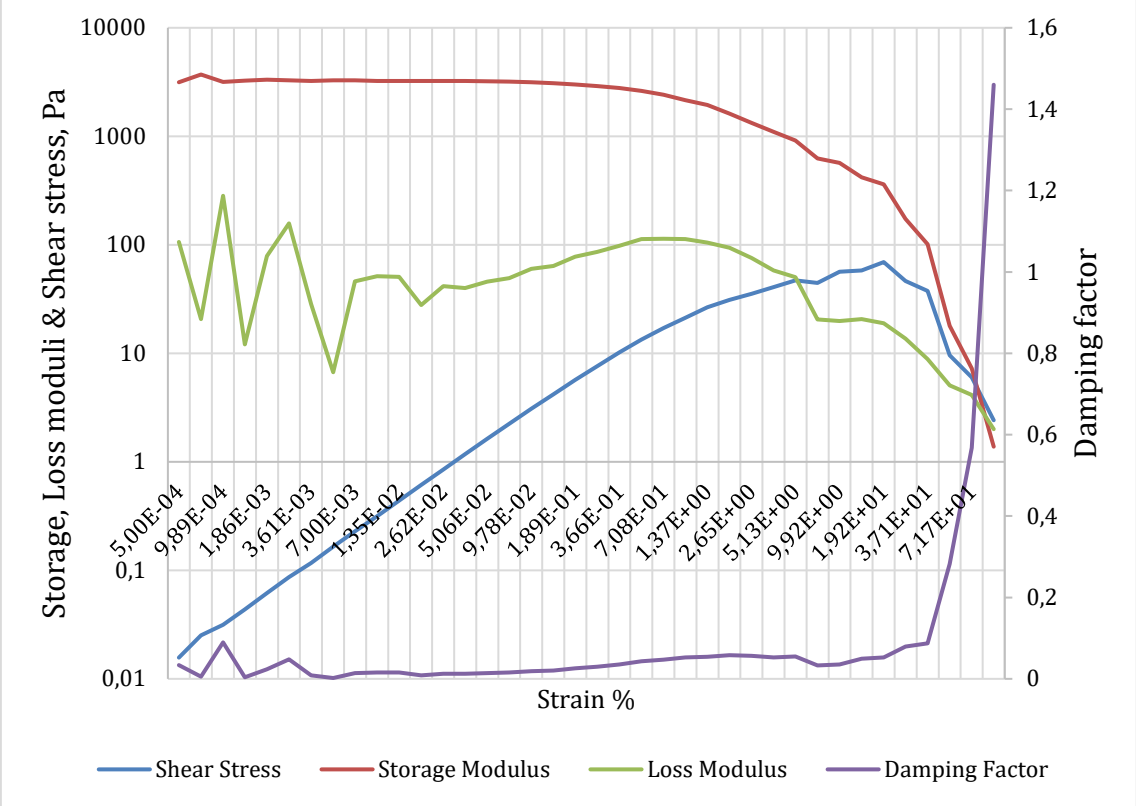

Figure 4.19: Plots of amplitude sweep measurements for Ref (CMC)

The oscillatory amplitude sweep test measurements are presented for Ref (CMC) +1.95gSiO_2+0.05gMWCNT in figure 4.20. As for Ref (CMC), the values of storage modules values are greater than the corresponding loss modules values for Ref (CMC)+1.95gSiO_2+0.05gMWCNT, which indicates that this fluid also has a gel-like behavior, before reaching the flow point. The flow point is reached when the shear stress is 3Pa. After the flow point is reached the fluid starts to flow and moves more and more towards viscous behavior. The damping factor values for nanoparticles additive fluid has some small peaks before it increases significantly right before the flow point and reaches its maximum value right after the flow point.

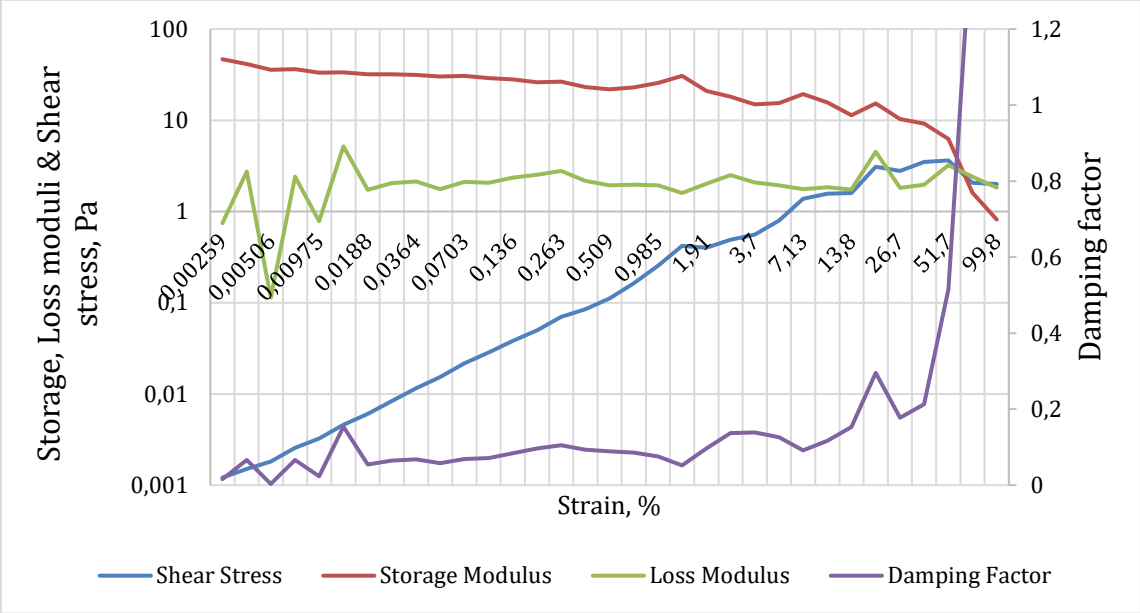

Figure 4.20: Plots of amplitude sweep measurements for Ref (CMC) +1.95g SiO_2+0.05g MWCNT

4.4.2 Flow point shear stresses comparisons

Figure 4.21 shows the comparison between the flow points of drilling fluids. The highest value of flow point shear stress is obtained by Ref (XG)+0.15gMWCNT, which is an increase of 162.5% compared to the Ref (XG). Comparing with the nanoparticle free CMC based reference drilling fluid, the addition of 0.075gSiO_2+0.075gMWCNT increased the flow point shear stress by 200%.

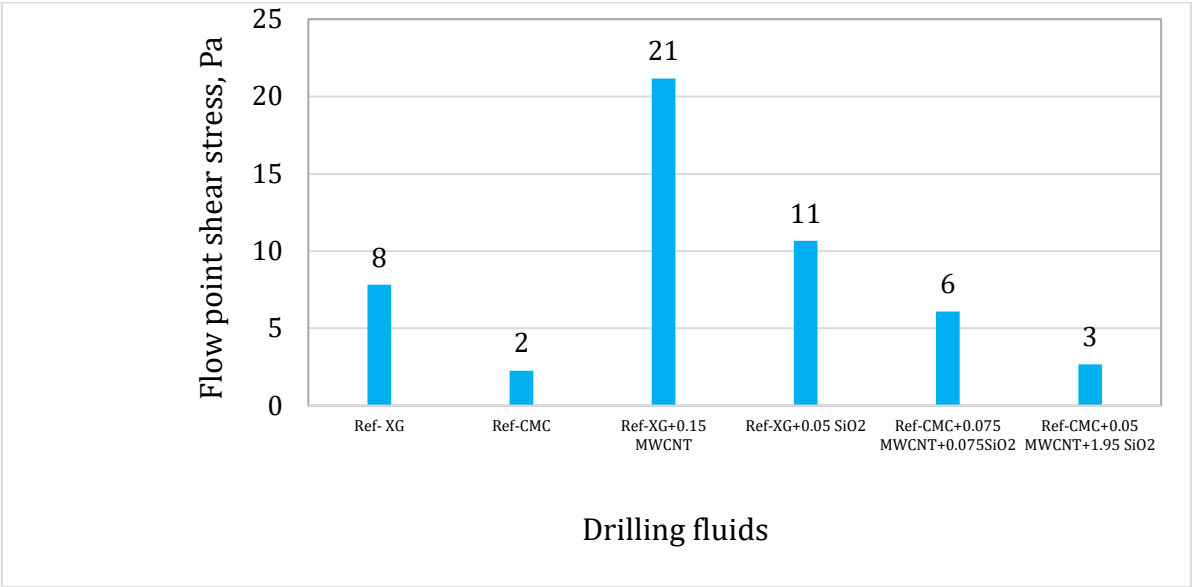

Figure 4.21: Flow point shear stresses for selected fluids from the best system (table 4.7)

5 Performance simulation

The optimized nanoparticles additive system was further analysed with a simulation study. The best system was chosen based on the friction results. This study is about rheological modelling, torque, drag, hydraulic and hole-cleaning simulation.

5.1 Rheological Modelling

The results of rheological modelling will be presented in this section. The RPM values from the Fann Viscometer was used to calculate the parameters of different rheology models, to investigate how good the drilling fluids correlated with the models. The purpose was to find the model that best describes the drilling fluids. The following rheological models were used:

- Herschel Bulkley
- Unified
- Robertson Stiff
- Power law
- Bingham plastic
- Newtonian

During modelling, the percent deviation between the model and the viscometer Fann data are computed. The rheological modelling has been performed on the selective drilling fluids from table 4.7, fluids are Ref (XG), Ref (XG)+ 0.15g MWCNT and Ref (XG)+ 0.05g SiO_2. The comparisons of model and measurement were done for all the drilling fluids with XG as a polymer, from table 4.7, while the effect of the rheology parameters was studied for all the drilling fluids from the best system.

5.1.1 Reference (XG) system

The trend-lines for the different rheology models for Ref (XG) are plot ed and presented in the Figure5.1. The corresponding equations and parameters for Ref (XG) are presented in table 5.1.

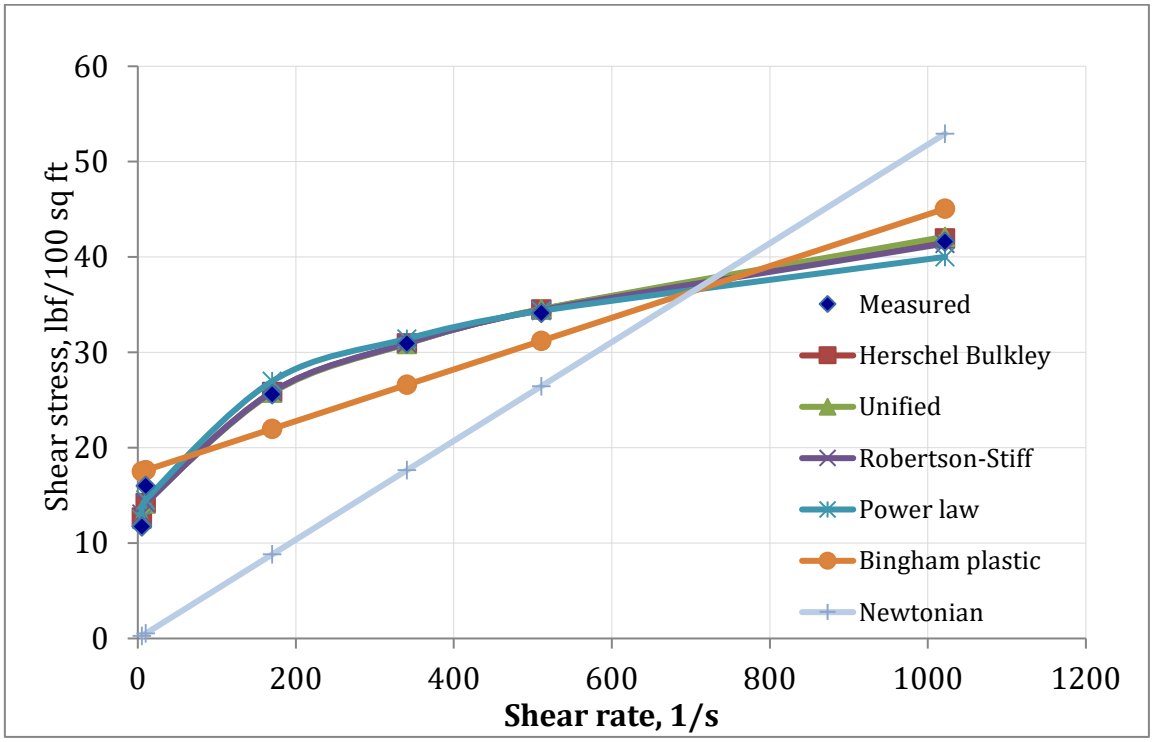

Figure 5.1: Modelled trend-lines for the different rheological models, with Ref(XG)

Model	Equation	Parameters					
		τo,τy, A	k, C	n, B	μp, μ	Sum of % Deviation	cP
Herschel Bulkley	7.144 + 3.1599* γ^0.3462	7,144	3,1599	0,34620		3,72	
Unified	7.469+2.9289* γ ^0,3566	7,469	2,9289	0,3566		3,81	
Power Law	8.7243*γ^0.2198		8,7243	0,2198		4,49	
Bingham	0.0271* γ +17.37	17,370			0,0271	17,41	12,975
Newtonian	0.0518* γ				0,0518	58,78	24,802
Robertson and Stiff	6.393*(9.0678+C)^0.2693	6,3932	9,0678	0,2693		4,17	

Table 5.1: Rheological modelled equations for Ref(XG)

The figure 5.1 shows that the trend-line for Bingham model differs considerably from the other non-Newtonian rheological models. The Newtonian model doesn't describe the drilling fluids behaviour. In table 5.1 the deviation in percentage is presented. As seen from the table 5.1, the Newtonian model shows a deviation of 58.78% and Bingham model shows about 17.41% deviation. All the other models have a deviation between 3.72% and 4.49%. Herschel Bulkley model has the lowest percentage deviation, which makes this model the most suitable for Ref (XG).

5.1.2 Reference (XG) + 0.15g MWCNT

The trend-lines for the different rheology models for Ref (XG)+0.15g MWCNT are plotted and presented in figure 5.2. The corresponding equations and parameters for Ref (XG)+0.15g MWCNT are presented in table 5.2.

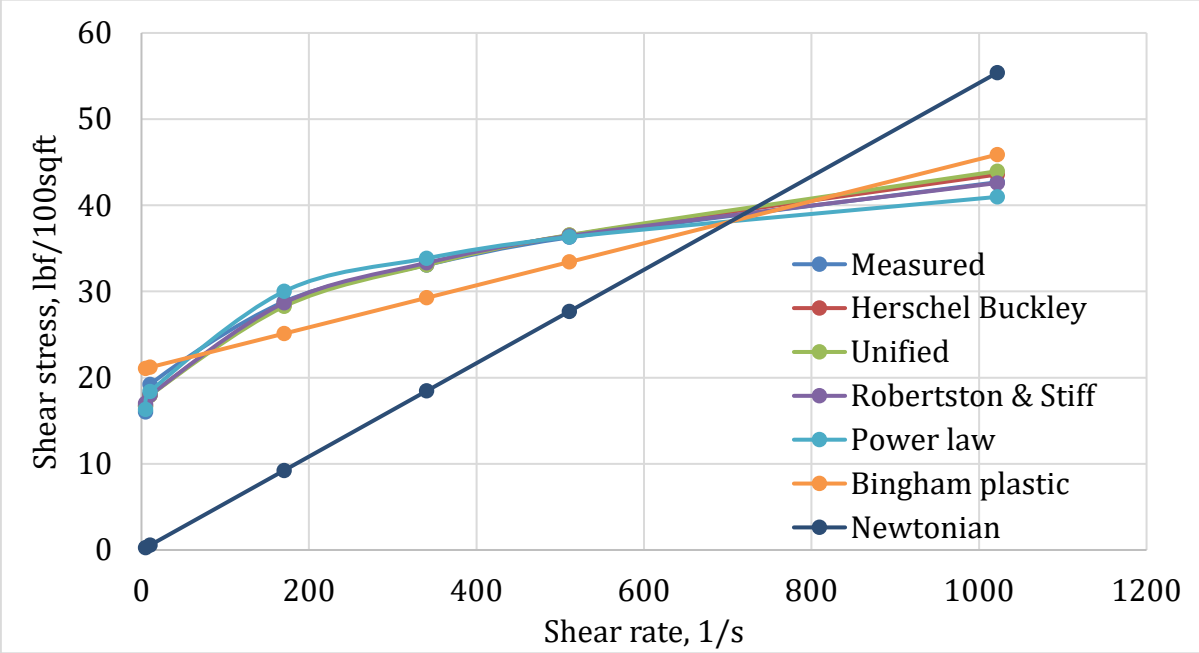

Figure 5.2: Modelled trend-lines for the different rheological models, with Ref(XG)+0.15gMWCNT

Model	Equation	Parameters					
		τ_o, τ_y, A	k, C	n, B	μ_p, μ	Sum of % Deviation	cP
Herschel Bulkley	12,270+2.4307* γ ^0,3688	12,270	2,4307	0,36880		2,48	
Unified	12,804+2,0684* γ ^0.3914	12,804	2,0684	0,3914		2,79	
Power Law	12,28* γ ^0.1739		12,28	0,1739		2,79	
Bingham	0,0244* γ +20,954	20,954			0,0244	13,64	11,683
Newtonian	0.0542* γ				0,0542	60,16	25,951
Robertson and Stiff	8,7034*(13,6579+C)^0,2287	8,7034	13,6579	0,2287		2,43	

Table 5.2: Rheological modelled equations for Ref(XG)+0.15gMWCNT

The same trend is seen in case of rheological modelling for the nanoparticles based drilling fluid treated with 0.15g MWCNT added as for Ref (XG). The Unified and

Power-law model has the same percent of deviation that is 2.79%. The lowest percent deviation is obtained by Robertson and Stiff model, which is 2.43%. Therefore, the model which describes Ref (XG)+0.15g MWCNT in the best way is Robertson and Stiff Model.

5.1.3 Reference (XG) + 0.05g SiO_2

The trend-lines for the different rheology models for Ref (XG)+0.05g SiO_2 are plotted and presented in figure 5.3. The corresponding equations and parameters for Ref (XG)+0.05g SiO_2 are presented in table 5.3.

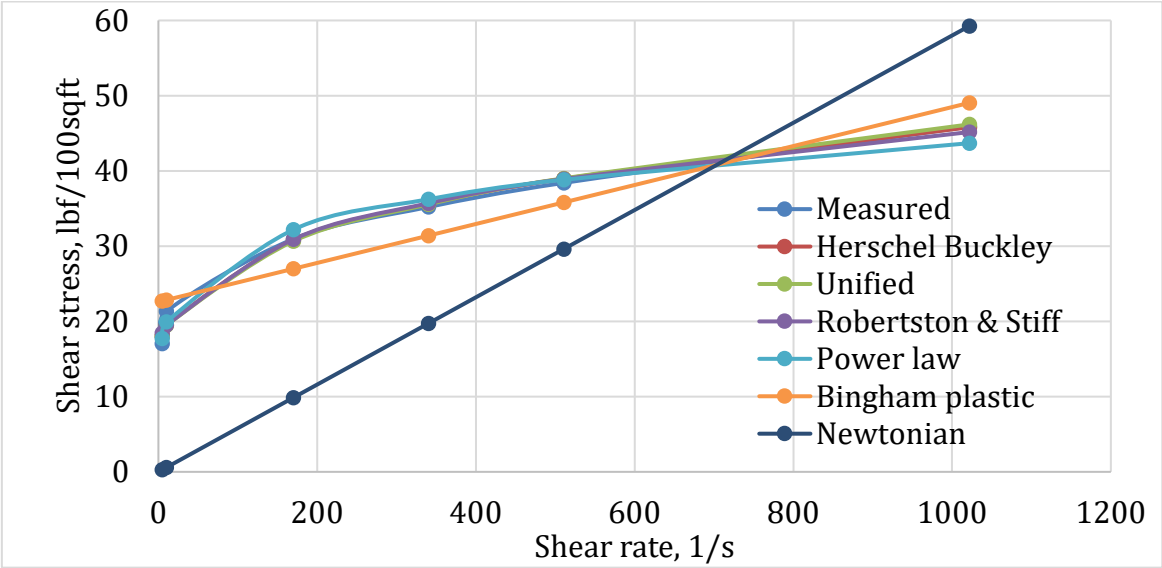

Figure 5.3: Modelled trend-lines for the different rheological models, with Ref(XG)+0.05gSiO2

Model	Equation	Parameters					
		τ_o, τ_y, A	k, C	n, B	μ_p, μ	Sum of % Deviation	cP
Herschel Bulkley	12,097+3,4924* γ ^0.3272	12,097	3,4924	0,32720		2,85	
Unified	12,804+2,9794* γ ^0.1702	12,804	2,9794	0,3487		3,09	
Power Law	0.9594* γ ^0.5227		13,433	0,1702		3,87	
Bingham	22,587+0,0259* γ	22,587			0,0259	12,90	12,401
Newtonian	0.058* γ				0,058	59,91	27,770
Robertson and Stiff	9,9192*(12,011+C)^0.2184	9,9192	12,0110	0,2184		3,48	

Table 5.3: Rheological modelled equations for Ref(XG)+0.05gSiO_2

In the drilling fluids with SiO_2 as an additive, the modified Power-law models describe the drilling fluid very well with % deviation between 2.85% and 3.87%. The Herschel Bulkley model has the lowest percent deviation which makes it the most suitable model for the Ref (XG)+ 0.05g SiO_2 system. This was also the case for Ref (XG). The value for PV increased 123.9% for Newtonian model compared to Bingham model.

5.1.4 Comparisons of model and measurement

The percentage deviation of the rheological models for all the drilling fluids with XG as a polymer, are presented in figure 5.4. As discussed earlier and can be seen in the chart, the Newtonian model has the highest deviation compared to the measurements, for all the drilling fluids. As shown in the table, Newtonian and Bingham model prediction record a higher percent deviation. On the other hand, Roberson & Stiff, Herschel-Bulkley and Unified models describe the rheology of the drilling fluids best, showing the lowest percentage deviation.

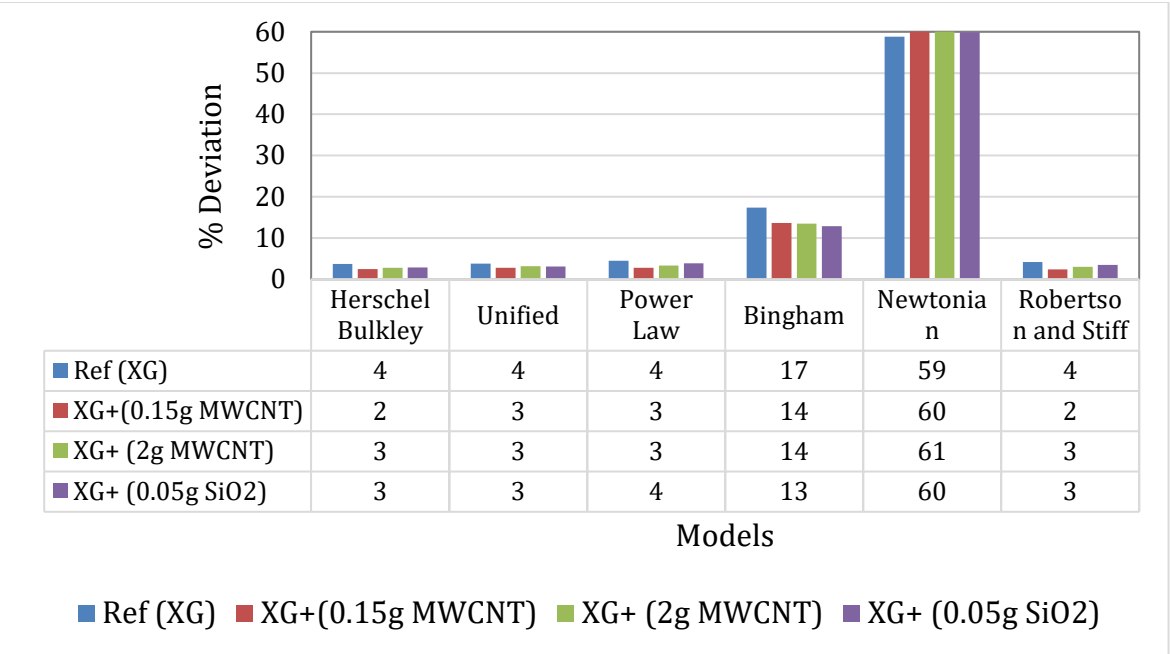

Figure 5.4: The percent deviation for all the rheological models for nanoparticle enhanced drilling fluids with XG as polymer

5.1.5 Effect of MWCNT and SiO2 on rheology parameters in XG system

In table 5.4 all the parameters for all the rheological models are presented alongside with % deviation of the parameters compared to the reference system, Ref (XG).

Model	Parameters	Ref (XG)	XG+(0.15g MWCNT)	XG+ (2g MWCNT)	XG+ (0.05g SiO2)
Herschel Bulkley	τo	7,14	12,27	11,65	12,10
	% deviation		71,75	63,01	69,33
	k	3,16	2,43	3,86	3,49
	% deviation		-23,08	22,12	10,52
	n	0,35	0,37	0,31	0,33
	% deviation		6,53	-9,82	-5,49
Unified	τy	7,47	12,80	12,80	12,80
	% deviation		71,43	71,43	71,43
	k	2,93	2,07	3,01	2,98
	% deviation		-29,38	2,64	1,72
	n	0,36	0,39	0,35	0,35
	% deviation		9,76	-3,08	-2,22
Power Law	k	8,72	12,28	13,52	13,43
	% deviation		40,76	54,97	53,97
	n	0,22	0,17	0,17	0,17
	% deviation		-20,88	-23,61	-22,57
Bingham	YS	17,37	20,95	22,74	22,59
	% deviation		20,63	30,93	30,03
	PV	12,98	11,68	11,92	12,40
	% deviation		-9,96	-8,12	-4,43
Robertson and Stiff	A	6,39	8,70	10,40	9,92
	% deviation		36,14	62,69	55,15
	B	0,27	0,23	0,21	0,22
	% deviation		-15,08	-22,13	-18,90
	C	9,07	13,66	10,22	12,01
	% deviation		50,62	12,75	32,46

Table 5.4: Summary of the parameters from rheological modelled equations for drilling fluids with XG as a polymer

Observations from table 5.4:

Herschel Bulkley model: The yield stress (τ_0) increased significantly for all the nanoparticles treated drilling fluids compared to the reference drilling fluid, the increase in yield stress varies from 63.01% to 71.75%. For the drilling fluids with MWCNT as an additive the increase of yield stress was higher in case of low concentration of the nanoparticles than the higher concentration. This indicates that

as the more MWCNT added to the drilling fluid, the less shear stress is needed to initiate the flow. The k-value decreased for Ref (XG)+0.15g MWCNT, while it increased for the other two drilling fluids (i.e. XG+ (2.0g MWCNT) and XG+ (0.05g SiO_2))provided in table 5.4. The n-value increased for Ref (XG)+ 0.15g MWCNT, while it decreased for the other two drilling fluids. The n-values for all the drilling fluids shows pseudo plastic behavior.

The Unified model: The low shear yield stress (τ_y) increased equally for all the nanoparticles treated drilling fluids, the increase was around 71.43%. The k-value decreased with 29.38% for Ref (XG)+0.15g MWCNT, while it increased for the other two drilling fluids. The n-value increased for Ref (XG)+0.15g MWCNT by 9.76%, and decreased to 3.1% for the other two drilling fluids.

Power-law model: The k-value increased for all the nanoparticles treated drilling fluids compared to the reference drilling fluid. The increase was between 40.76% and 54.97%, it increased the most for Ref (XG)+2.0g MWCNT. For the Herschel Bulkley model and the Unified model the k-value decreased for Ref (XG)+0.15g MWCNT, while it increased for the other two drilling fluids. Although, the highest k-values was achieved by Power-law model. The n-values decreased for all the drilling fluids, the average decrease of the n-values was 22.35%. This means that the nano drilling fluids are moving more towards a pseudo plastic behavior.

Bingham model: The yield stress (YS) had an average increase of 27.20% for all the nanoparticles treated drilling fluids according to this model. The YS increased for the MWCNT drilling fluids as more amount of nanoparticles were added, this result is opposite with comparison with the yield stress of Herschel Bulkley model. The PV decreased for all the fluids, the highest decrease was obtained by Ref (XG)+ 0.15g MWCNT with 9.96% decrease.

Robertson and Stiff model: The A parameter increased the most for Ref (XG)+2.0g MWCNT, with 62.69% increase. For Ref (XG)+0.15g MWCNT and Ref (XG)+ 0.05g SiO_2 the A parameter had an increase of 36.14% and 55.15%, respectively. The B parameter decreased for all the drilling fluid with nanoparticle additives, the

average decrease was of 18.70%. The highest deviation for parameter C was achieved by Ref (XG)+ 0.15g MWCNT, with 50.62% increase. In the Robertson and Stiff model the A parameter corresponds to k-value, for comparison with the other rheological models. The parameter B corresponds to the n-value, while the parameter C is a correction factor for the shear rate.

5.1.6 Effect of MWCNT and SiO_2 mixture in CMC system

In table 5.5 all the parameters for all rheological models are presented alongside with % deviation of the parameters compared to the reference system, Ref (CMC).

In this rheological analysis of the different parameters for all the fluids, Ref(CMC)+(0.075g SiO_2+0.075g MWCNT) is called Fluid 1, while Ref (CMC)+ (1.95g SiO2+ 0.05g MWCNT) is called Fluid 2.

Model	Parameters	Ref (CMC)	Ref (CMC) + (0.075g SiO2+ 0.075gMWCNT)	Ref (CMC) +(1.95g SiO2+0.05g MWCNT)
Herschel Bulkley	τo	2,42	2,60	2,81
	% deviation		7,24	15,85
	k	0,42	0,12	0,17
	% deviation		-70,88	-59,87
	n	0,52	0,71	0,64
	% deviation		37,15	23,29
Unified	τy	2,13	2,77	2,67
	% deviation		30,00	25,00
	k	0,58	0,06	0,23
	% deviation		-89,31	-60,35
	n	0,47	0,82	0,59
	% deviation		74,12	25,68
Power Law	k	1,98	1,56	1,86
	% deviation		-21,24	-5,78
	n	0,30	0,34	0,30
	% deviation		11,95	-1,92
Bingham	YS	4,78	4,24	4,23
	% deviation		-11,34	-11,54
	PV	6,75	7,09	6,37
	% deviation		4,96	-5,67
Robertson and Stiff	A	0,95	0,56	0,58
	% deviation		-41,25	-38,76
	B	0,42	0,50	0,48
	% deviation		19,63	14,66
	C	17,56	23,26	32,72
	% deviation		32,47	86,35

Table 5.5: Summary of the parameters from rheological modelled equations for drilling fluids with CMC as a polymer

Observations from the table 5.5:

Herschel Bulkley model: The yield stress (τ_0) increased with 7.24% for the Fluid 1, and it increased more than double for the Fluid 2, with 15.85%. Fluid 2 therefore needs more than double pressure to initiate flow, than Fluid 1. The k-value decreased significantly for both of the nanoparticles treated drilling fluids, the decrease was 70.88% for Fluid 1, while the decrease was 59.86% for Fluid 2. The n-value had an average increase of 30.22% for both the drilling fluids.

The Unified model: The low shear yield stress (τ_y) increased for both fluids, 30% for Fluid 1, and 25% for the Fluid 2. The k-value had a great decrease for both fluids, the decrease was of 89.31% for Fluid 1. The n-value increased for both of the fluids, the highest increase was obtained by Fluid 1, with an increase of 74.12%, indicating that the fluid is moving more and more away from pseudo plastic behavior.

Power-law model: The k-value decreased for both Fluid 1 and Fluid 2, with a decrease of 21.24% and 5.78%, respectively. The n-value increased for Fluid 1, while it decreased for the Fluid 2, still both fluids are in pseudo plastic state. Bingham model: The yield stress (YS) decreases for the drilling fluids with nanoparticles as an additive, which means that when nanoparticles are added to the conventional drilling fluid, less pressure is needed to initiate flow, according to Bingham model. The average decrease of the YS was 11.44%. The PV increased for Fluid 1, while it decreased for Fluid 2. The graphical result of PV for Fluid 1 is a steeper curve than the reference fluid, while for Fluid 2 the curve is less steep compared to the reference fluid.

Robertson and Stiff model: The A parameter, corresponding to k-value, decreased for both of the fluids, with an average decrease of 40%. The B parameter, corresponding to n-value, increased for both of the nanoparticles based drilling fluids, with an average increase of 17.15%, both in pseudo plastic state. The shear rate correction factor increased significant for Fluid 2, with an increase of 86.35%. While for the Fluid 1, it increased to 32.47%.

5.2 Torque and drag simulation

The theory part of the torque and drag models are reviewed in section 2.4. High torque and drag limits the extended reach drilling, and are critical for inclined wells. One of the methods to reduce torque and drag is to reduce the coefficient of friction, as the torque is determined by the normal force times the friction coefficient. The OBM`s has a lower coefficient of friction than WBM`s, but the experimental study showed that the coefficient of friction decreased when nanoparticles were added to the conventional WBM.

This section presents a torque and drag simulation that shows if it is possible to achieve elongated drilling length by using nanoparticle drilling fluid. The simulation was performed with the nanoparticle fluids with the lowest friction coefficient, shown in table 5.6.

Fluid	Friction Coefficient
Ref (XG)	0.30
Ref (XG)+0.1g MWCNT	0.21
Ref (XG)+ 2g MWCNT	0.15
Ref (XG)+0.05g SiO_2	0.22
Ref (CMC)	0.42
Ref (CMC)+2g MWCNT	0.21
Ref (CMC)+1.95g SiO_2+0,05g MWCNT	0.26

Table 5.6: Drilling fluids with lowest friction presented with friction coefficients, used for torque and drag simulations

5.2.1Simulation setup

The torque and drag simulation was performed in WellPlan™, a part of a Landmark software created by Halliburton. A deviated well with measured depth (MD) of 11000 ft was configured, to investigate the effects of the torque and drag. The well had a vertical cased section of 4012.5 ft, with 13 3/8 casing, and a deviated open hole-section, with 12.615 in diameter. An E-75 grade and 5'' drill string was used for drilling. An illustration of the well is presented in figure 5.5. The tripping in and tripping out speed was 60ft/min, and the RPM was set to 30. The pump flow rate

was 500gpm, and the density was set to 9.2ppg. The casing, drill string and survey data of the simulation well are provided in Appendix A and B.

The Fann 35 viscometer readings for the XG and CMC drilling fluids are presented in table 5.7 and table 5.8, respectively. The friction coefficients are presented in table 5.6.

RPM	Ref (XG)	Ref (XG)+0.1gMWCNT	Ref (XG)+2.0gMWCNT	Ref (XG)+0.05gSiO_2
600	39	42	42	43
300	32	35	36	36
200	29	32	33	33
100	24	28	29	29
6	15	19	20	20
3	11	15	16	16

Table 5.7: RPM readings for nanoparticle enhanced drilling fluids with XG as a polymer

RPM	Ref (CMC)	Ref (CMC)+ 2.0gMWCNT	Ref (CMC)+ 1.95gSiO_2+0.05gMWCNT
600	17	15	16
300	12	10	11
200	10	8	9
100	8	6	7
6	4	3	3.5
3	3	2.8	3

Table 5.8: RPM readings for nanoparticle enhanced drilling fluids with CMC as a polymer

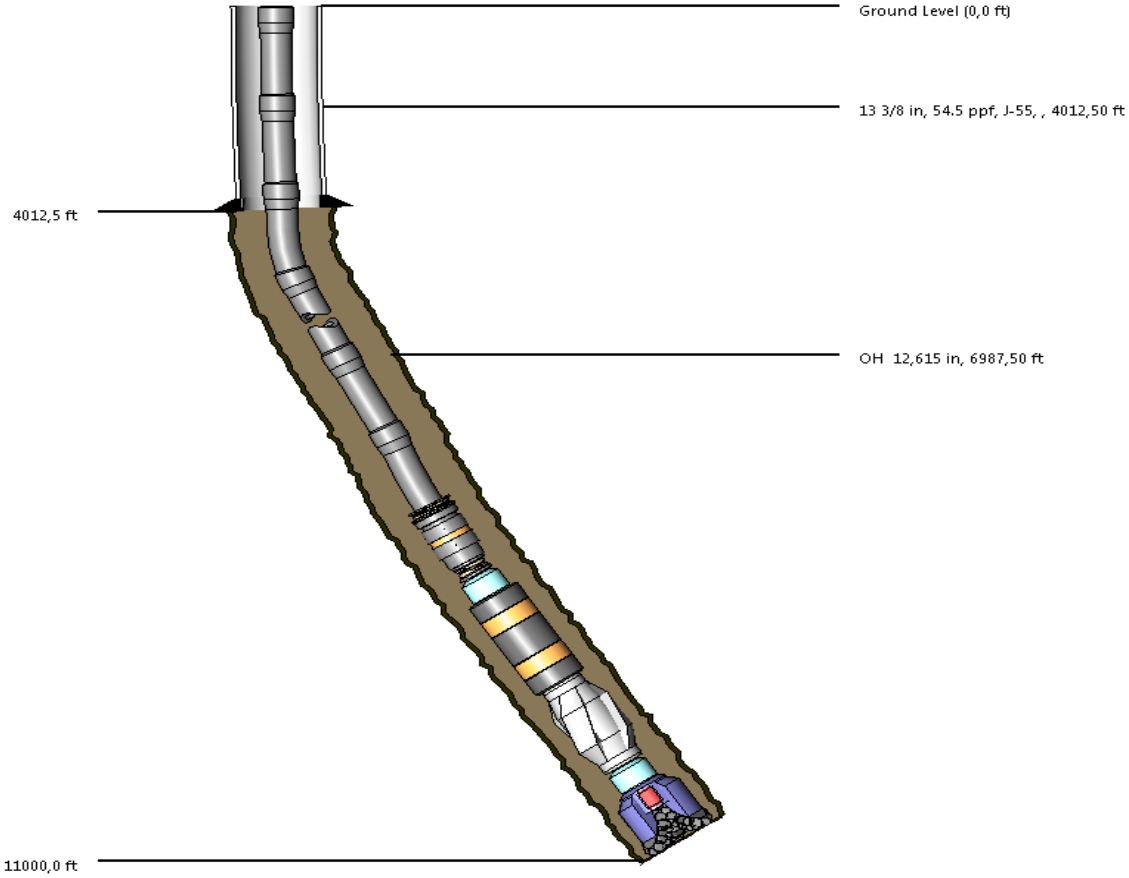

Figure 5.5: Torque and drag performance simulation setup

5.2.2 Simulation result

The torque and drag graphs for Ref (CMC) and Ref (CMC) + 2.0g MWCNT are presented in this section.

Ref (CMC)

As observed from the figure 5.6, tripping in and tripping out values does not exceed the tensile limit, which means that the operations will be safe at 11300ft MD, with the given speed and RPM. It will not be possible to drill deeper than 11300ft as the tripping out curve is very close to the tensile limit, any further drilling will cause yield to the drill pipe. The tripping in and tripping out graphs does not exceed the torque values as well, which can be observed from the figure 5.7. According to the

tensile limit and torque limit, the tripping in and tripping out operations are safe within the given measured depth (MD).

The stress graph for tripping in operations shows that it is a very good margin between Von-Mises stress and the stress limit for Ref (CMC), as seen in figure 5.8. The stress graph for tripping out operations shows that the Von-Mises stress does not exceed the stress limit, as seen in figure 5.9, hence it is safe to trip in and trip out to 11300ft MD regarding to the stress limits.

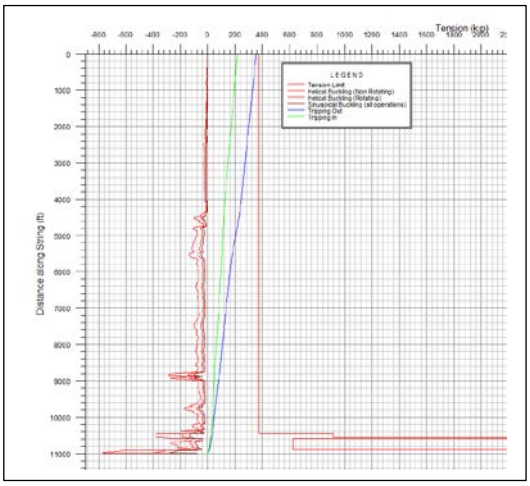

Figure 5.6: Drill string drag forces for Ref(CMC)

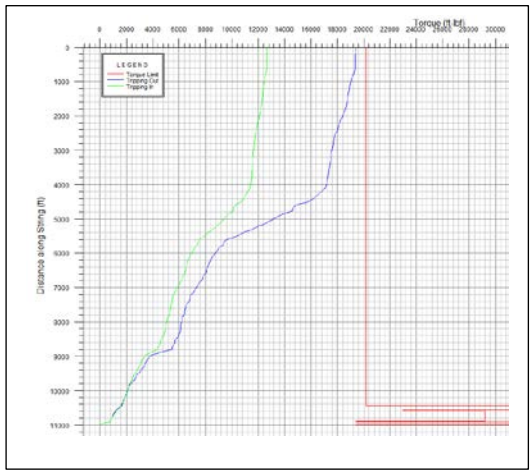

Figure 5.7: Drill string torque loads for Ref(CMC)

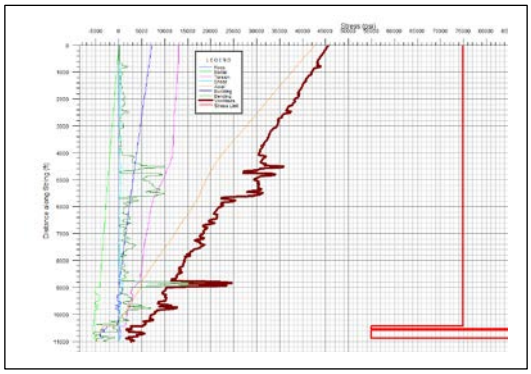

Figure 5.8: Von-Misses stress tripping in for Ref(CMC)

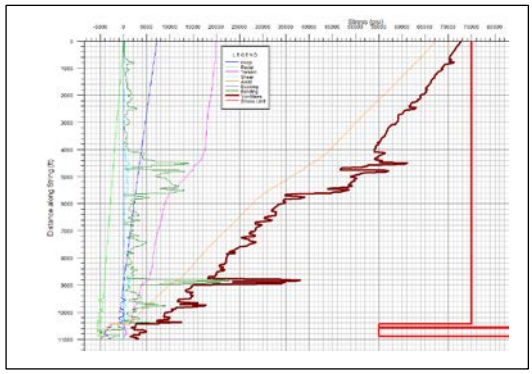

Figure 5.9: Von-Misses stress tripping out for Ref(CMC)

Ref (CMC)+2.0gMWCNT

Figure 5.10 illustrates that tripping in and tripping out values does not exceed the tensile limit for Ref (CMC)+2.0g MWCNT with given friction coefficient, the tripping out curve is very close to the tensile limit, which means 13000ft MD is the maximum drill length without yielding the drill pipe material. The tripping in and tripping out values have a very good margin according to the torque, as seen in figure 5.11, if only torque was considered, the drilling length could have been extended additionally. The stress graphs for tripping in and tripping out also shows that the operations are safe at 11300ft MD. The Von-Mises stresses do not exceed the stress limits as shown in the figure 5.12 and figure 5.13.

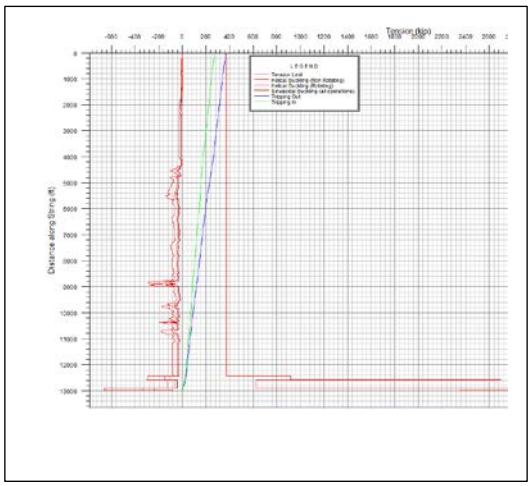

Figure 5.10: Drill string drag forces for Ref(CMC)+2.0gMWCNT

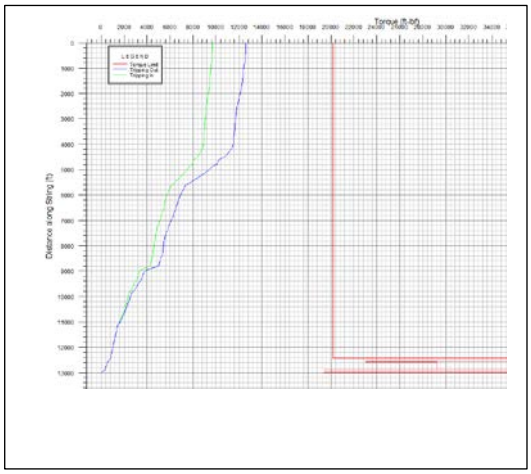

Figure 5.11: Drill string torque loads for Ref(CMC)+2.0gMWCNT

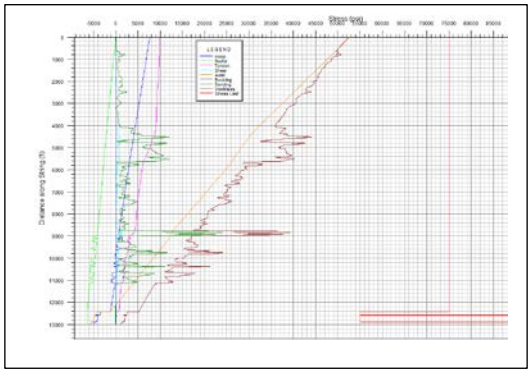

Figure 5.12: Von-Misses stress tripping in for Ref(CMC)+2.0gMWCNT

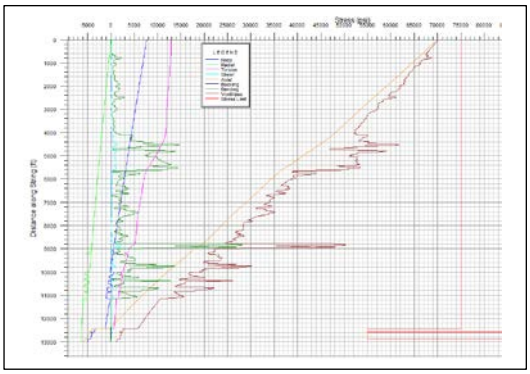

Figure 5.13: Von-Misses stress tripping out for Ref(CMC)+2.0gMWCNT

5.3.3 Summary of simulation

Table 5.9 gives a summary of different drilling lengths that can be achieved by adding nanoparticles to a conventional drilling fluid with CMC as a polymer. In the case of Ref (CMC), the maximum achievable drilling length was 11300ft MD, by adding MWCNT the drilling length increased to 13000ft MD. By adding MWCNT the friction reduced by 52%, and the drilling length increased up to 15%. For the SiO_2-MWCNT composite drilling fluid, the percent increase in drilling length was 10.6% when the percent friction coefficient reduced by 39%.

	Ref (CMC)	Ref (CMC)+2.0g MWCNT	Ref (CMC)+1.95gm SiO_2+0,05gm MWCNT
Friction	0,44	0,21	0,27
% Friction reduction		-52	-39
Drilling length,ft	11300	13000	12500
% increase		15	10.6

Table 5.9: Summary of extended reach with nanoparticle enhanced drilling fluids with CMC as a polymer

Table 5.10 shows the percent drilling length increase for drilling fluids with XG as a polymer. The highest increase in drilling length was obtained by the drilling fluid having the lowest friction namely Ref (XG)+2.0g MWCNT. Where 50% reduction in friction gave a 12% increase in drilling length for Ref (XG)+2.0g MWCNT. For Ref (XG)+0.1g MWCNT and Ref (XG)+0.05g SiO_2 the increase of drilling length was 1000ft, which is 8.3% increase compared to Ref (XG). The enhancement of drilling length for these two drilling fluids was same, although the amount of nanoparticle used was double in the case of MWCNT as compared with SiO_2.

	Ref (XG)	Ref (XG)+0,1g MWCNT	Ref (XG)+ 2.0g MWCNT	Ref (XG)+0,05g SiO_2
Friction	0,3	0,21	0,15	0,22
% Friction reduction		-30	-50	-27
Drilling length,ft	12000	13000	13500	13000
% increase		8.3	11.25	8.3

Table 5.10: Summary of extended reach with nanoparticle enhanced drilling fluids with XG as a polymer

5.3 Hydraulics Simulation

The theory part of the hydraulics simulation (i.e ECD and pump pressure) is reviewed in the section §2.5. This section will present hydraulic performance of the nanoparticle enhanced drilling fluids with best frictional results, presented in table 4.7. This study will show what kind of effect MWCNT and silica nanoparticle has on the ECD and total pressure loss in the well compared to the conventional nanoparticles free drilling fluid. The ECD values are the sum of the hydrostatic pressure and the pressure loss due to friction while circulation stop. It is important to determine these properties in order to design an optimized drilling fluid system. These parameters are determined by hydraulic models, where the Unified model among the rheological models was selected for calculations.

5.3.1 Simulation Setup

The hydraulics performance the drilling fluids have been simulated in a vertical well as illustrated in Figure 5.14. The true vertical depth of the well is 10000ft, and was cased with 8.5" casing. The drill pipe OD and ID was 5" and 4.8", respectively. The drill bit consists of three nozzles. The surface pressure was set to be zero. The flowrate was increased stepwise from 100 to 600gpm during the simulation, and the mud density was assumed to be equal for all the drilling fluids and was set to 8.539ppg (1.025sg).

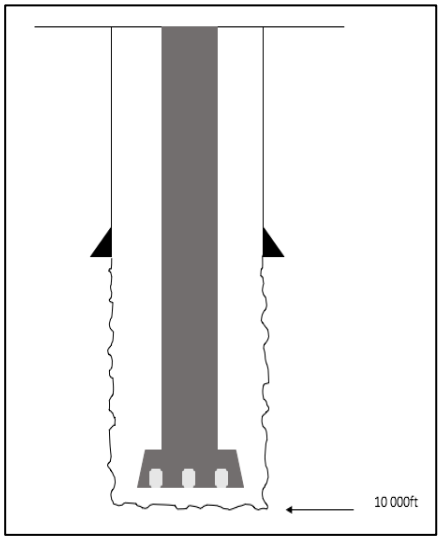

Figure 5.14: Hydraulic performance simulation setup

5.3.2 Simulation Result for XG Drilling Fluids

The simulation results for nanoparticle treated drilling fluid with XG as a polymer are presented in this section. Figure 5.15 shows the ECD results of the simulation. The ECD values are increasing with increasing flow rates. The increasing in ECD values are caused by pressure loss due to friction. The ECD values are, more or less, increasing with the same rate for all the drilling fluids. The drilling fluids with

nanoparticles as an additive exhibit higher ECD for all flow rates, compared to the nanoparticle free drilling fluid. The obtained simulation results for ECD shows that Ref (XG)+ 0.15g MWCNT achieved the lowest ECD when nanoparticle-based drilling fluids are considered, while Ref (XG)+ 2.0g MWCNT achieved the highest ECD results, which means that this fluid would not be an inappropriate option for wells with narrow operational window.

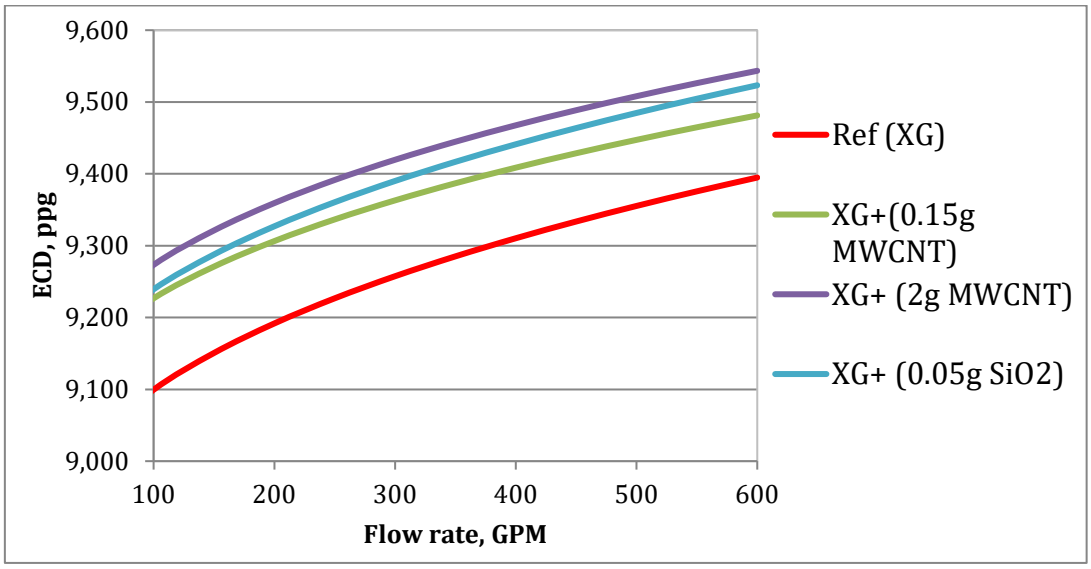

Figure 5.15: Comparison of ECD with increasing flowrates for nanoparticle enhanced drilling fluids with XG as a polymer

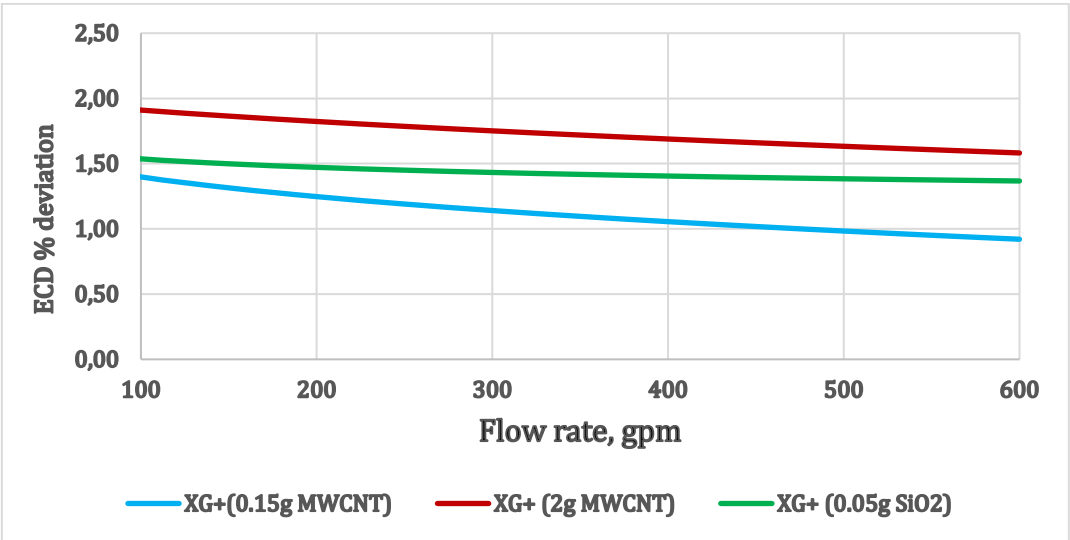

Figure 5.16: ECD percent deviation of nanoparticle treated drilling fluid with XG based reference drilling fluid

Figure 5.16 shows the percent deviation in ECD compared to the reference drilling fluid. As seen on the graph, the lowest percent deviation in ECD is achieved by Ref (XG)+0.15g MWCNT. The deviation gradually decreases and reaches its lowest point at the highest flow rate, 600gpm. Then the deviation is under one percent. The percent deviation in ECD compared to the reference drilling fluid also decreases for the other two nanoparticle drilling fluids as the flow rate increases.

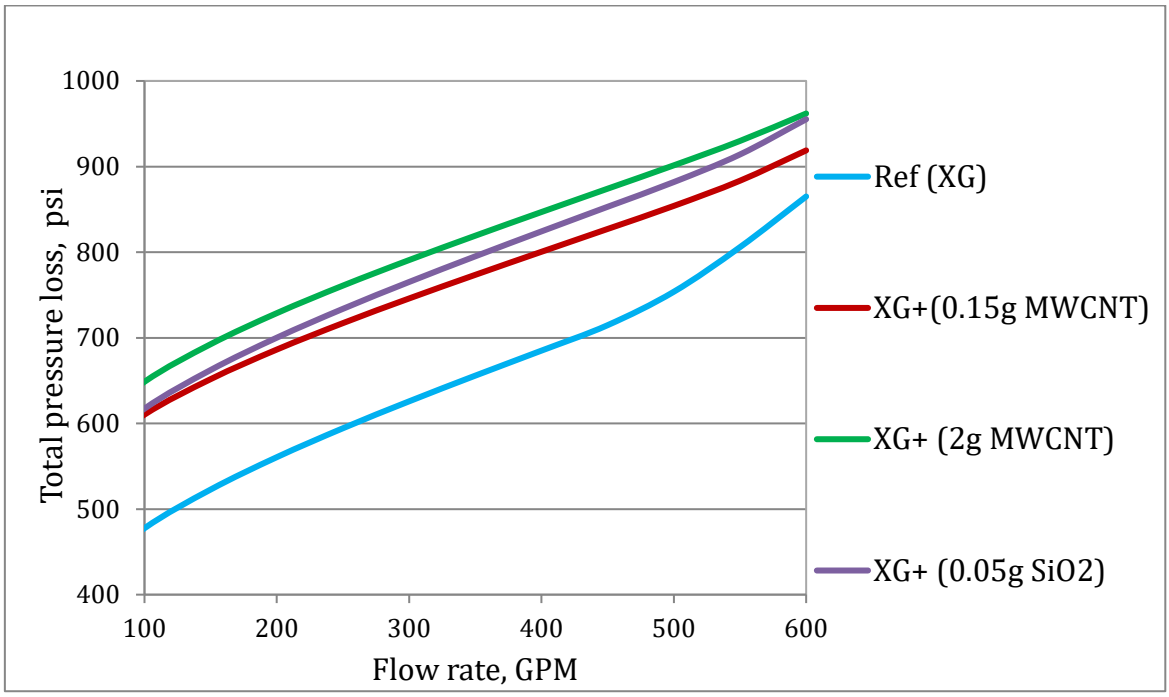

Figure 5.17: Comparison of total pressure loss at increasing flowrates for nanoparticle enhanced drilling fluids with XG as a polymer

The total pressure loss is increasing for all the drilling fluids as the flow rate increases. The drilling fluid with nanoparticles exhibited higher pressure loss than the reference drilling fluid, as seen in figure 5.17. The ECD and the total pressure loss are closely related, as ECD is a function of the friction loss, hence they exhibit similar behaviour. The highest total pressure loss is obtained Ref(XG)+2.0gMWCNT for all the flow rates, this fluid also obtained highest ECD values for all flow rates. Ref(XG)+0.15gMWCNT and Ref(XG)+0.05gSiO_2 are more adequate as drilling fluids as the total pressure loss in the annulus is lower, and a lower pump pressure is required to circulate the drilling fluid up to the surface.

5.3.3 Simulation Result for CMC Drilling Fluids

The simulation results for nanoparticle treated drilling fluid with CMC as a polymer are presented in this section and the results are displayed in the figure 5.18
Unlike the XG treated drilling fluid, the ECD of CMC drilling fluids shows transition flow behaviour after 400gpm.

As expected, the ECD behaviours of all the drilling fluids show nearly the same, which is due to the insignificant effect of nanoparticle additives on the rheological properties. Figure 5.19 presents the percent deviation of ECD compared to the reference drilling fluid. For the considered flow rate, the percent deviation of Ref (CMC)+0.075gSiO2+0.075gMWCNT from references is in the range of 0.07% - 0.16%. Similarly, the % deviation for Ref (CMC)+1.95gSiO2+0.05gMWCNT from reference is in the range of -0.18% to 0.24%. This shows that the additives do not have any significant impact on the ECD.

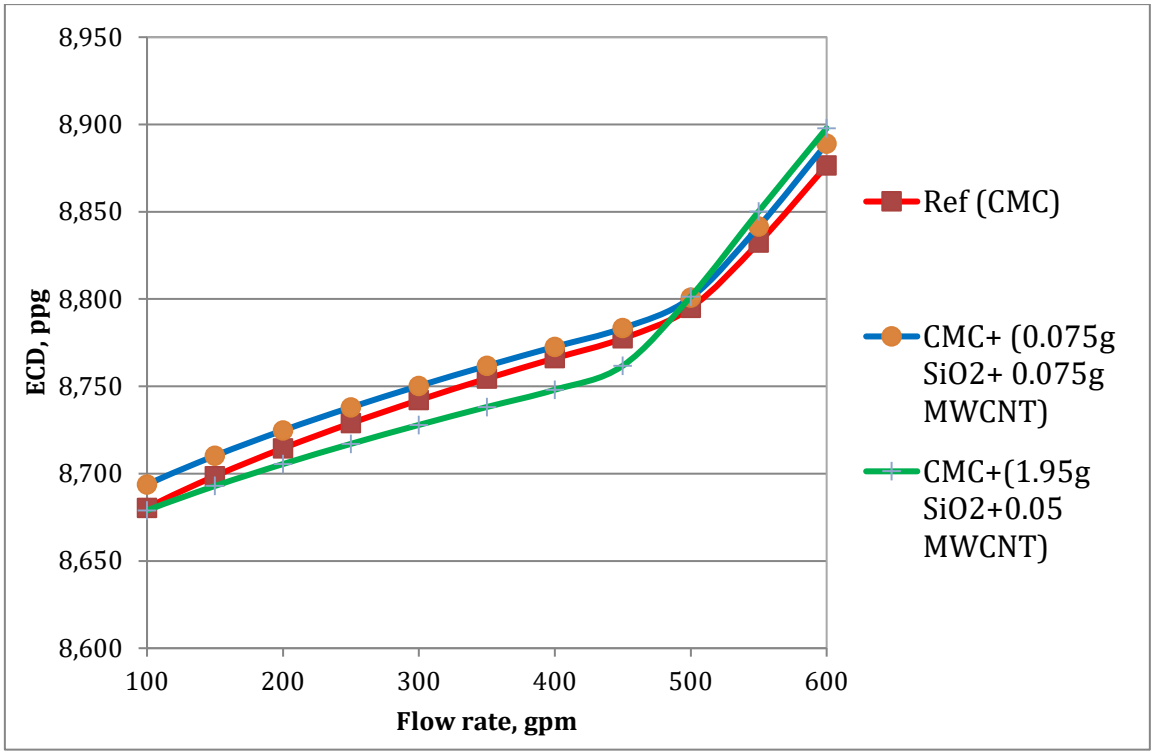

Figure 5.18: Comparison of ECD with increasing flowrates for nanoparticle enhanced drilling fluids with CMC as a polymer

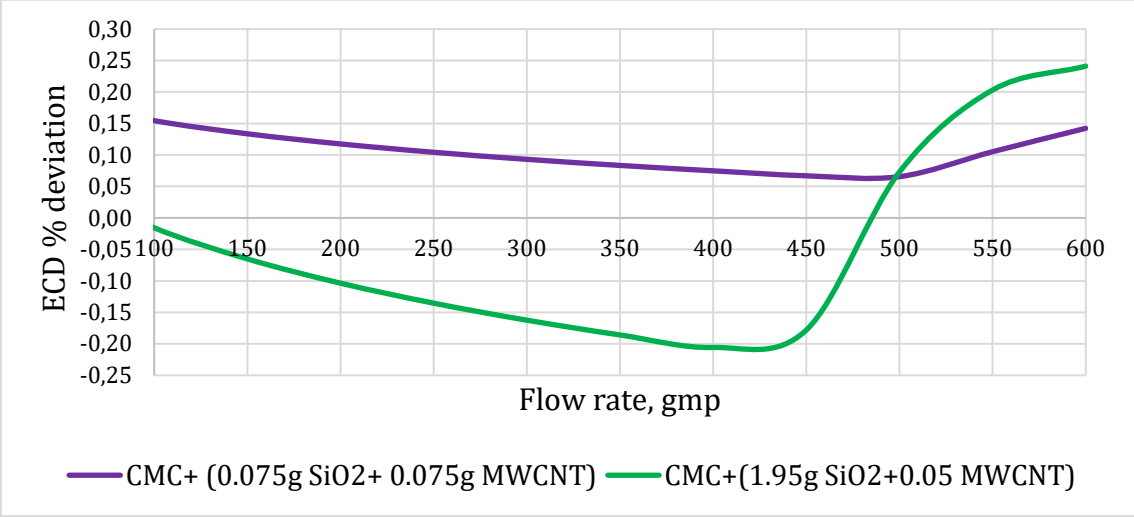

Figure 5.19: ECD percent deviation of nanoparticle treated drilling fluid with CMC based reference drilling fluid

Pump pressure is also another hydraulics issue to be evaluated. Figure 5.20 shows the total pressure loss at different flow rates for drilling fluids with CMC as a polymer. The figure shows that the curve for nanoparticle enhanced drilling fluids overlaps the reference drilling fluid for most of the flow rates. Additionally, where the curves do not overlap, the differences are minimal. As there are not considerable differences on the total pressure losses when silica nanoparticle is added into drilling fluid, this means that higher pump pressure is not required to transport the drilling fluids from annulus to the surface.

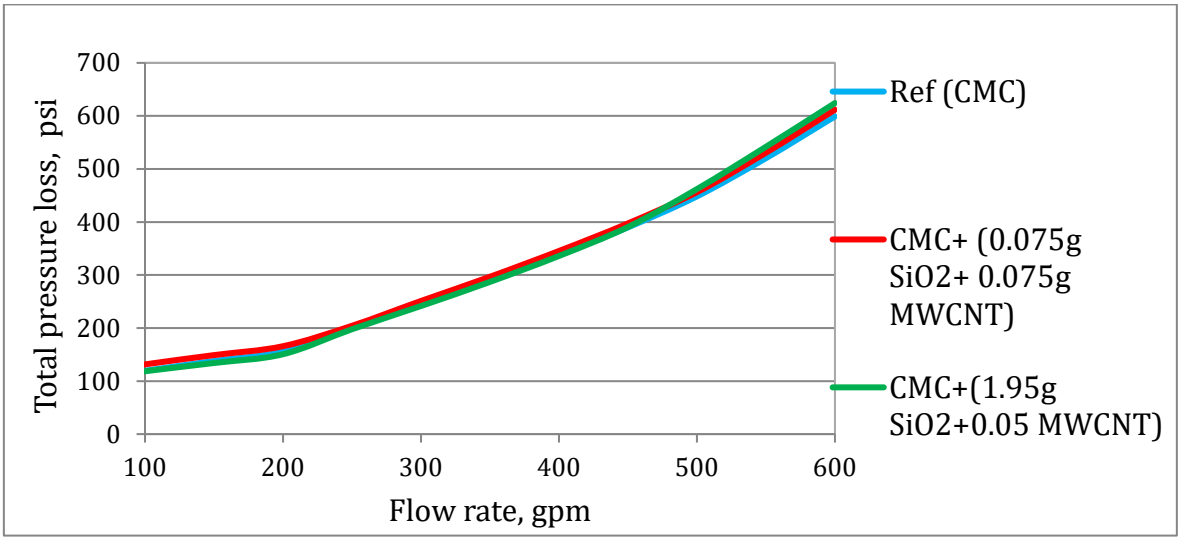

Figure 5.20: Comparison of total pressure loss at increasing flowrates for nanoparticle enhanced drilling fluids with CMC as a polymer

5.4 Hole-cleaning simulation

One of the main function of drilling fluids is to bring cuttings to the surface. Several parameters controls the cutting lifting efficiency of drilling fluids such as its density and rheology. To evaluate the combined impact of nanoparticles on the rheology of the drilling fluid, one way is to evaluate the drilling fluid cutting lifting and bed formation phenomenon.

5.4.1 Simulation setup

This was simulated in the experimental well used for torque and drag simulation. The well has 12000 ft measured depth and the well path, inclination and azimuth are shown in Appendix B.

The size of the well was 8.5 inch and 5'' OD drilling string rotating at a speed of 90 RPM is used along with its BHA elements to drill at a speed of 60 ft/hr. Cutting density and size to be circulated out were 2.5 g/cc and 0.125 inch. While the drilling fluids were circulated at a rate of 450 gpm. Table 5.11 is the simulation input parameters.

Parameter	Value
Cutting size	0.125''
Cutting density	2.5g/cc
ROP	60ft/hr
RPM	90RPM
Flow rate	450gpm

Table 5.11. Cutting and drilling parameters

5.4.2 Simulation results

Figure 5.21 shows well inclination and figure 5.22 shows the cutting bed height in the well as the nanoparticle free Ref (XG) and MWCNT nanoparticle-treated drilling fluids circulated in the well. The results clearly show an enhanced cutting transport in the nanoparticle treated drilling fluids. Moreover, one can observe that cutting deposition is a function of the well inclination. Evaluation of bed thickness in the

deviated part of the drilling well shows that the 0.1 g and 2.0 g MWCNT drilling fluids reduced the cutting bed height by an average of 53 %.

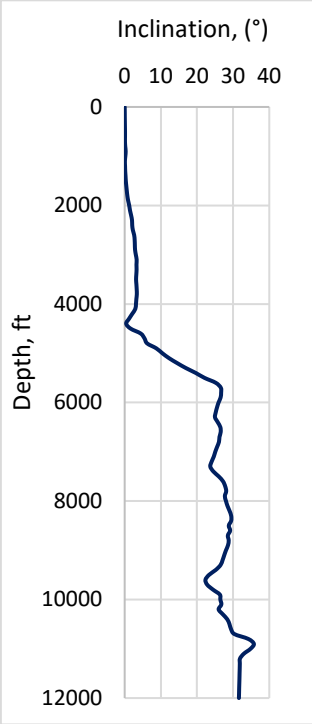

Figure 5.21: Well inclination

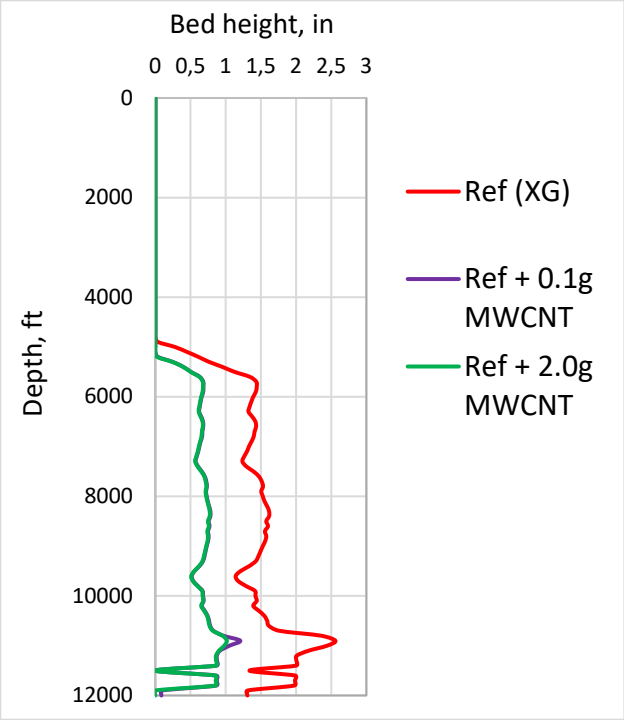

Figure 5.22: Cutting bed height

6 Result Discussion and Summary

This chapter will present the discussion and the summary for the work done in this thesis. The intention of the experimental part was to investigate the effect of nanoparticles on WBM system and to formulate a drilling mud which obtained the desirable mud properties. The fluids with the lowest friction were chosen for further investigation. Viscoelastic tests were performed on the set of drilling fluids having best frictional results. In the simulation part, rheological modelling, torque and drag, hydraulics and hole cleaning performance were executed. For the rheological modelling and hydraulic performance the same set of drilling fluids was used which was used on viscoelasticity tests. For the torque and drag simulation a new set of drilling fluid was chosen. The hole cleaning performance was performed on two MWCNT enhanced drilling fluids.

6.1 Rheological Effects of Nano-treated Drilling Fluids

Section §6.1.1, 6.1.2 and § 6.1.3 present the summary of the effect of MWCNT, silica and their mixture on the rheological properties of laboratory drilling fluids.

6.1.1 Rheological Effects of MWCNT in XG

In general, the addition of MWCNT increased the viscometer responses of the nanoparticles free drilling fluid. However, it is observed that nanoparticle concentration have a nonlinear effect on the rheological properties. For instance, the MWCNT nanoparticles showed significant impact on the Bingham yield stress and lower shear yield stress. On the other hand, the particles have shown less impact on plastic viscosity. Similarly, the considered nanoparticle concentrations have shown an increase in consistency index as concentration increases and decreases the shear thinning behaviour. The additives have shown an increasing filtrate loss, which might have dispersed the bentonite system significantly.

6.1.2 Rheological Effects of Nano-silica in XG

Unlike in MWCNT, as SiO_2 nanoparticles concentration decreases, the viscometer responses of the drilling fluid increases in linear manner. All viscometer data are higher than the referenced drilling fluid except 2g SiO_2 concentration. For instance, the additives didn't show a significant effect on the Bingham plastic viscosity. On the other hand, the additives have shown a very significant effect on the yield stress. Here again the additives increased filtrate loss.

6.1.3 Rheological effects of Nano-silica-MWCNT Composite in CMC

To investigate the effect of the silica-MWCNT nanocomposite, reference drilling fluid has been formulated with Bentonite/CMC/KCl additives. The viscometer results shows nonlinear and less impact as concentration and particle combination varies as compared with the reference drilling fluid. For instance, except for one drilling fluid, the additive didn't show any impact on plastic viscosity. Moreover, the lower shear yield stress value was considerably reduced as compared in CMC-fluids than XG-fluids. The Power-law parameters are also not influenced in the composite system. However, it should be remembered that the results could be different if the composites had been tested in XG polymer.

Unlike in XG system, the .075gSiO_2+0.075gMWCNT and 0.1gSiO_2+0.1gMWCNT composite reduced the filtrate loss by 3.6% and 2.9%, respectively. However, increasing other concentration increase the filtrate loss. The results illustrate the performance of nanoparticle varies from polymer to polymer and also there exist an optimum concentration that shows good drilling fluid performances.

6.2 Frictional Effects of Nano-treated Drilling Fluids

In this thesis, the reference –nanoparticle free drilling fluids have been formulated in CMC and XG polymers. The measured coefficient of friction showed that lubricity of CMC base drilling fluid is 40% higher than the lubricity of XG base drilling fluid. This result may indicate that the choice of polymer can affect the friction values.

In XG based drilling fluid, in general it is observed that higher addition of MWCNT decreed the coefficient of friction of the laboratory drilling fluid. On the other hand, the lower concentration of silica shows higher lubricity, and decrease the lubricity as the concentration increases.

The SiO2-MWCNT composite's effect in CMC based drilling fluids showed a significant decrease for the fluid with 1.95g SiO_2 and 0.05g MWCNT. Higher concentration of both MWCNT and SiO_2 in CMC drilling fluids had a great impact on friction.

6.3 Viscoelastic Effects of Nano-treated Drilling Fluids

The viscoelastic test results were unstable so it was difficult to find the LVER for the nanoparticle fluids, the Loss Modulus and the Storage Modules were non-linear, and hence YS could not be found either. The flow point was determined for selected fluids. For instance, Ref(XG)+0.15gMWCNT obtained the highest flow point shear stress, which had an increase of 162.5% compared to the reference system.

For all the nanoparticle-treated drilling fluids, the Storage Modulus was greater than Loss Modulus before the flow point, which means that before the flow is activated, the drilling fluid is elastic dominated. In the elastic dominated zone the fluid is characterized by gel structure.

6.4 Rheological Modelling of Nano-treated Drilling Fluids

Rheological simulation studies have shown that all the formulated drilling fluids behave like modified Power-law model. Among the non-Newtonian models the Herschel Bulkley, Unified and Robertson and Stiff model are the best rheological models to describe drilling fluids. The comparisons between the models and the measured viscometer data showed the sum average of about 3% deviation.

6.5 Torque and Drag Effects of Nano-treated Drilling Fluids

The friction coefficient is a limiting factor for drilling a longer offset since it has a huge impact on torque and drag. The tribometry results showed that nanoparticles increased the lubricity of the conventional nanoparticle free drilling fluid. The torque and drag simulation results have shown the nanoparticle enhanced drilling fluids allowed to drill about 8.3-15% more as compared with the reference drilling fluids.

6.6 Hydraulic Performance Effects of Nano-treated Drilling Fluids

ECD management is an important issue especially when drilling in extended reach well. ECD is controlled by several parameters such as rheological, density and flow rate among others. Hydraulic simulation results have shown that ECD of all of the XG nano drilling fluids increased due to the higher impact on the rheological properties, which can be managed during formulation. However, on the other hand these MWCNT based drilling fluids had shown lower friction coefficient. For instance, the simulation results have also shown that 0.05g SiO_2 nanoparticle exhibits higher ECD than 0.15g MWCNT additives. This indicates that impact of nanoparticles on rheological parameters depends on nanoparticle types and concentrations.

6.7 Hole Cleaning Effects of Nano-treated Drilling Fluids

Even though higher ECD was experienced as discussed in section §6.6, the hole cleaning performance of the MWCNT treated drilling fluid showed good cutting transport efficiency. Comparing with the reference drilling fluid, at a given flowrate, the nanoparticle-based drilling fluid reduced the bed height by an average of 53%.

6.8 Summary Matrix

Table 6.1 summarizes some of the results from the experimental and simulation study performed on the best nanoparticle enhanced drilling fluid system.

Fluids	Filtrate	Friction	Torque& Drag	Hole cleaning
Ref(XG)+0.10gMWCNT	Increase	Decrease	Increased drilling length	Improved
Ref(XG)+0.15gMWCNT	Increase	Decrease	X	X
Ref(XG)+2.0gMWCNT	Increase	Decrease	Increased drilling length	Improved
Ref(XG)+0.05gSiO_2	Increase	Decrease	Increased drilling length	X
Ref(CMC)+0.075gSiO_2+0.075gMWCNT	Decrease	Decrease	X	X
Ref(CMC)+1.95gSiO_2+0.05gMWCNT	Increase	Decrease	Increased drilling length	X
Ref(CMC)+2.0gMWCNT	Increase	Decrease	Increased drilling length	X

Table 6.1: Summary matrix for the drilling fluids from the best system. X= Not tested.

7 Conclusion

The main goal for this thesis was to investigate the effect of nanoparticles in laboratory water based drilling fluid, which was formulated with bentonite, KCl and CMC/XG polymers. The effect of the single nanoparticles (MWCNT & SiO_2 and their mixtures were studied. The performance of best drilling fluids was evaluated through simulation studies such as hydraulics, hole-cleaning, and torque and drag. Based on the experimental and simulation studies, the main observations will be summarized.

MWCNT in XG system shows that:

- All the additives showed a positive impact on the Bingham and Power-law parameters (except PV) nonlinearly as concentration increases.
- All the additives increase the filtrate loss of the base reference fluid.
- Addition of 0.10g MWCNT and 2.0g MWCNT reduced the friction coefficient by 30% and 50%, respectively.
- Torque and drag simulation results showed that the 0.1g MWCNT and 2.0g MWCNT increases the drilling depth by 8.3% and 11.25%, respectively.
- MWCNT as an additive in drilling fluids reduces the cutting bed height composition.

SiO2 in XG system shows that:

- PV values remained unchanged for low concentration of silica nanoparticles added into the base reference fluid. The decrease in PV was experienced after 0.20g of SiO_2 was added.
- All the additives increase the filtrate loss of the base reference fluid, except when 0.10g MWCNT was added, then no change in filtrate was experienced.
- Low concentrations of SiO_2 is more sufficient in regards to friction reduction properties, as the friction coefficient increases with higher concentrations of silica nanoparticle. This is an opposite result compared to MWCNT fluids.
- Low concentration of silica (0.05g) improved the torque and drag performance.

MWCNT – SiO_2 composite in CMC system shows that:

- 0.37wt. % SiO_2 - 0.0095wt % MWCNT composite reduced coefficient of friction of CMC base drilling fluid by 38%
- Except 0.013wt% MWCNT – 0.019wt% SiO_2 nanoparticles, all other composites increased filtrate loss.

The objective of this thesis was to improve the conventional WBM system by use of nanoparticle additives. By this thesis work, it can be concluded that the performance of nanoparticles has shown both positive and negative results. The negative results, which was increased filter loss, can be improved by using filtrate-reducing agents, as for example sodium metasilicate, polanionic cellulose (PAC) or starch products [1]. The greatest positive results obtained was in terms of friction reduction abilities. This great lubricity also led to positive results in torque and drag performance. In terms of cost and lubricity effect, silica nanoparticles can be a better choice as it gives the highest friction reduction for low concentrations, while the friction decreases more with a higher concentration of MWCNT.

8 References

1. Fink J. (2011)// **Petroleum Engineer`s Guide to Oil Field Chemicals and Fluids**// Gulf Professional Publishing. (ISBN:978-0-12-383844-5)
2. Azar J.J and Samuel G. R. (2007)//**Drilling Engineering**// PennWell Corporation. (ISBN-13: 978-1-59370-072-0)
3. Lummus J. L. and Azar J.J (1986)// **Drilling Fluids Optimization- A Practical Field Approach**//PennWell Publishing Company. (ISBN: 0-87814-306-8)
4. H.H. Rodriguez, J.B Ramirez, D.C. Vela'zquez, A.N Conejo and J.A Martinez//**Annular flow analysis by tracers in drilling operations //** Journal of Petroleum Science and Engineering, Volume 41, Issue 4, February 2004, Pages 287–296.
5. Jung C.M., Rui Z., Chenvert M. and Sharma M. (2013)// **High- Performance Water- Based Mud Using Nanoparticles for Shale Reservoirs**// SPE 168799/ URTeC 1581549 prepared for presentation at the Unconventional Resources Technology Conference held in Denver, Colorado, USA, 12-14 August 2013.
6. Falope F.D and Orodu O. D (2014)// **Improved Drilling Efficiency via Enhanced Water Based Mud in The Niger Delta**// SPE-172406-MS prepared for presentation at the SPE Nigeria Annual International Conference and Exhibition held in Lagos, Nigeria, 05-07 August 2014.
7. Amanullah M. and Ramasamy J. (2014)// **Nanotechnology Can Overcome the Critical Issues of Extremely Challenging drilling and Production Environments**// SPE-171693-MS prepared for presentation at the Abu Dhabi International Petroleum Exhibition and Conference held in Abu Dhabi, UAE, 10-13 November 2014.
8. Hoelscher K. P., Young S., Friedheim J. and Stefano G.D. (2013) // **Nanotechnology Application in Drilling Fluids**// Paper presented at the 11th Offshore Mediterranean Conference and Exhibition in Ravenna, Italy, March 20-22,2013. Selected for presentation by OMC 2013 Programme Committee following review of information contained in the abstract submitted by the authors.
9. Baig M. T, Rahman M. K. and Al-Majed A. (2017)//**Application of Nanotechnology in Oil Well Cementing**// SPE-187543-MS prepared for presentation at the SPE Kuwait Oil& Gas Show and Conference held in Kuwait City, Kuwait, 15-18 October 2017.
10. Mezger T.G (2011)//**The Rheology Handbook**// 3rd Revised Edition. Hanover. (ISBN: 3-86630-864-7)
11. American Petroleum Institute (2003)// **Recommended Practice on the Rheology and the Hydraulics of Oil-well Drilling Fluids**// (accessed 8 December 2017)
12. Skjeggestad O. (1989)// **Boreslamteknologi: Teori og praksis//** Alma Mater Forlag. (ISBN: 82-419-0010-4)
13. Belayneh (2017) //**Advanced drilling lecture note**// UiS

14. Ochoa M.V. (2006)// **Analysis of Drilling Fluid Rheology and Tool Joint Effect to Reduce Errors in Hydraulics Calculations//** PhD Dissertation, Texas A&M University
15. Saasen A., Bui B., Maxey J., Ozbayoglu M. E., Miska S. Z., Yu M. and Takach N.E. (2012)// **Viscoelastic Properties of Oil-Based Drilling Fluids//** Annular Transactions of the Nordic Rheology Society Vol.20, 2012.
16. Thomas Sharman (2015)// **Characterization and Performance Study of OBM at Various Oil-Water Ratios**// MSc Thesis UiS
17. Johancsik C.A, Friesen D.B. and Dowson R. // **Torque and Drag in Directional Wells-Prediction and Measurment**// Journal of Petroleum Technology, June 1984.
18. E.E. Maidla and A.K. Wojtanowicz (1987)// **Field Comparison of 2-D and 3-D Methods for the Borehole Friction Evaluation in Directional Wells**// SPE Annual Technical Conference and Exhibition, 27-30 September, Dallas, Texas.
19. Aadnoy B.S., Fazaelizadeh M. and Hereland G. //**A 3D Analytical Model for Wellbore Friction**// Journal of Canadian Petroleum Technology, October 2010.
20. Zamora M., Roy S. and Slater K., M-I SWACO //**Comparing a Basic Set of Drilling Fluid Pressure-Loss Relationships to Flow-Loop and Field Data**// AADE-05-NTCE-27 paper presented at the AADE 2005 National Technical Conference and Exhibition, held at the Wyndam Greenspoint in Houston, Texas, April 5-7, 2005.
21. Sadigov J. (2013) **//Comparisons of Rheology and Hydraulics Prediction of Mud Systems in Concentric and Eccentric Well Geometry//** MSc Thesis, University of Stavanger, Stavanger, Rogaland (June 2013)
22. Sharma M.M., Zhang R., Chenevert M.E. , Ji L., Guo Q. and Friedheim J.(2012) //**A New Family of Nanoparticle Based Drilling Fluids**// SPE 160045 This paper was prepared for presentation at the SPE Annual Technical Conference and Exhibition held in San Antonio, Texas, USA, 8-10 October 2012.
23. Sedaghatzadeh M., Khodadadi A. A. and Birgani M. R. T. (2012)// **An Improvement in Thermal and Rheological Properties of Water-based Drilling Fluids Using Multiwall Carbon Nanotube (MWCNT)//** Iranian Journal of Oil& Gas Science and Technology, Vol. 1 (2012), No.1, pp. 55-65.
24. Li G., Jinghui Z., Huaizheng Z. and Yegui H. (2012)// **Nanotechnology to Improve Sealing Ability of Drilling Fluids for Shale with Micro-cracks During Drilling**// SPE 156997 prepared for presentation at the SPE International Oilfield Nanotechnology Conference held in Noordwijk, The Netherlands, 12-14 June 2012.
25. Baig M. T., Rahman M. K. and Al-Majed A. (2017)// **Application of Nanotechnology in Oil Well Cementing**// SPE-187543-MS prepared for presentation at the SPE Kuwait Oil& Gas Show and Conference held in Kuwait City, Kuwait, 15-18 October 2017.

26. Moradi B., Pourafshary P., Farahani F. J., Mohammadi M. and Emadi M. A. (2015)// **Application of SiO2 Nano Particles to Improve the Performance of Water Alternating Gas EOR Process**// SPE-178040-MS prepared for presentation at the SPE Oil and Gas India Conference and Exhibition held in Mumbai, India, 24-26 November 2015.
27 Al-Homadhi E.S. (2007)// **Improving Local Bentonite Performance for Drilling Fluids Applications**// SPE 110951 prepared for presentation at the 2007 SPE Saudi Arabia Technical Symposium held in Dhahran, Saudi Arabia, 7-8 May 2007.
28 Kutlic A., Bedekovic G and Sobota I. (2012)// **Bentonite Processing Oplemenjivanje Bentonita**// University of Zagreb, Faculty of Mining, Geology and Petroleum Engineering.

29 Kogel J.E., Trivedi N.C., Barker J.M. and Krukowski S. T. (2006)// **Industrial Minerals& Rocks. Commodites, Markets and Uses//** Society of Mining, Metallurgy, and Exploration, Inc. (SME) (ISBN: 13:978-0-87335-233-8)

30 Strand S. (1999)// **Øvinger I Bore-og Brønnvæsker**// Høgskolen i Stavanger.

31 MISwaco Manual //**Drilling Fluids Engineering Manual, Polymer chemistry and Applications**// Chapter 6, 1998.

32 Maria C Siqueira, Gustavo F Coelho, Márcia R de Moura, Joana D Bresolin, Silviane Z Hubinger, José M Marconcini and Luiz H C Mattoso //**Evaluation of antimicrobial activity of silver nanoparticles for carboxymethylcellulose film applications in food packaging**//Journal of nanoscience and nanotechnology, 14(14), undefined (2014-4-25)

33 Caenn R., Darley H.C.H and Gray G.R. (2011) //**Composition and properties of drilling and completion fluids**// USA: Elsevier Inc.(ISBN:978-0-12-383858-2)

34 Rodney S. Ruoff, Dong Qian, Wing Kam Liu //**Mechanical properties of carbon nanotubes: theoretical predictions and experimental measurements**// C. R. Physique 4 (2003) 993–1008.

35 EPRUI Nanoparticles and. Microspheres Co. Ltd

Appendix

Appendix A: Well and drill string parameters

Hole Section Editor

Hole Name: Hole Section — Import Hole Section

Hole Section Depth (MD): 11000,0 ft — Additional Columns

	Section Type	Measured Depth (ft)	Length (ft)	ID (in)	Drift (in)	Effective Hole Diameter (in)	Friction Factor	Linear Capacity (bbl/ft)	Item Description
1	Casing	4012,5	4012,50	12,615	12,459	12,615	0,44	0,1547	13 3/8 in, 54.5 ppf, J-55,
2	Open Hole	11000,0	6987,50	12,615		12,615	0,44	0,1546	
3									

String Editor

String Initialization — String Name: Assembly — String (MD): 11000,0 ft — Specify: Top to Bottom — Import String

Library — Export — Import

	Section Type	Length (ft)	Measured Depth (ft)	OD (in)	ID (in)	Weight (ppf)	Item Description
1	Drill Pipe	10441,00	10441,0	5,000	4,000	28,26	Drill Pipe 5 in, 25.60 ppf, E, 5 1/2 FH, P
2	Heavy Weight	120,00	10561,0	6,625	4,500	70,50	Heavy Weight Drill Pipe Grant Prideco, 6 5/8 in, 70.50 ppf
3	Jar	33,00	10594,0	6,500	2,750	91,79	Hydraulic Jar Dailey Hyd., 6 1/2 in
4	Heavy Weight	305,00	10899,0	5,000	3,000	49,70	Heavy Weight Drill Pipe Grant Prideco, 5 in, 49.70 ppf
5	Sub	5,00	10904,0	6,000	2,400	79,51	Bit Sub 6, 6 x2 1/2 in
6	MWD	85,00	10989,0	8,000	2,500	154,36	MWD Tool 8 , 8 x2 1/2 in
7	Stabilizer	5,00	10994,0	6,250	2,000	93,72	Integral Blade Stabilizer 8 1/2" FG, 6 1/4 x2 in
8	Sub	5,00	10999,0	6,000	2,400	79,51	Bit Sub 6, 6 x2 1/2 in
9	Bit	1,00	11000,0	10,625		166,00	Tri-Cone Bit, 0,589 in²

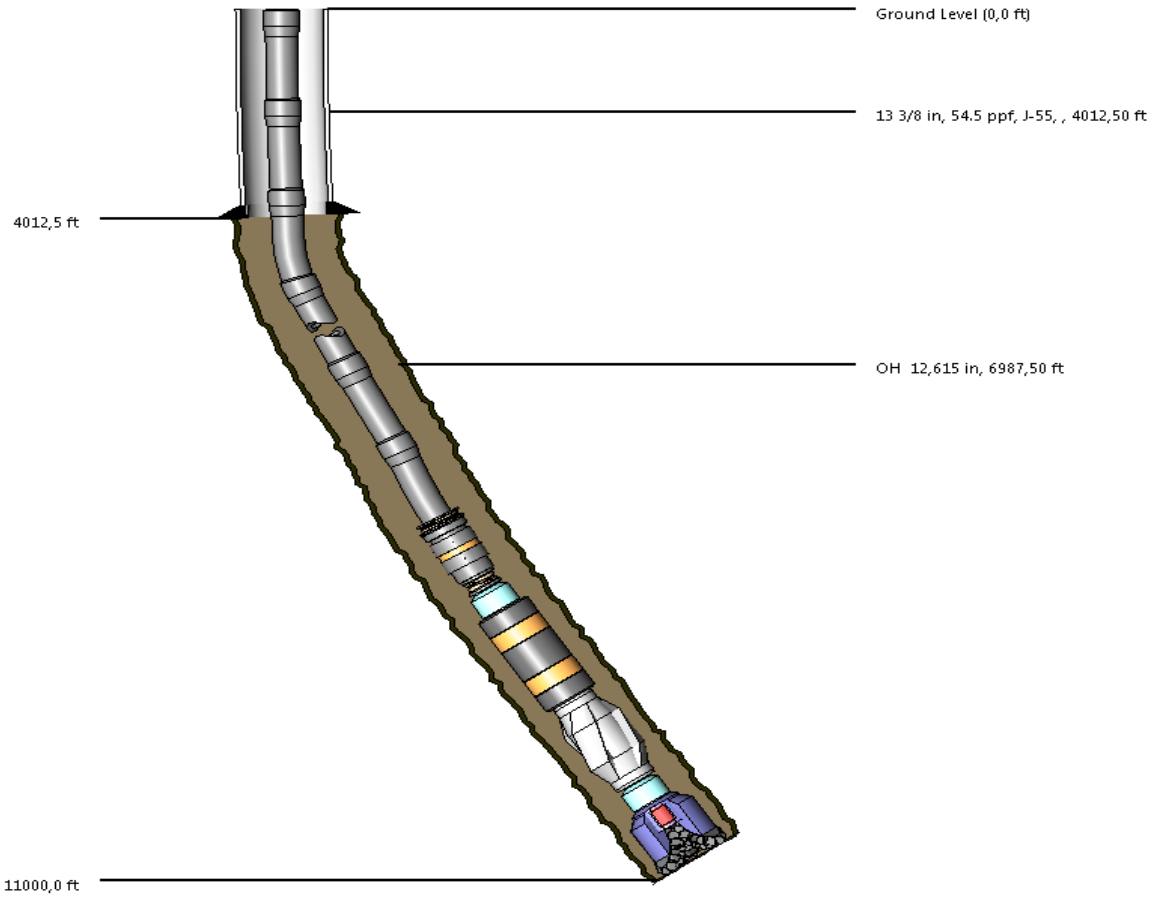

Appendix B: Well path parameters

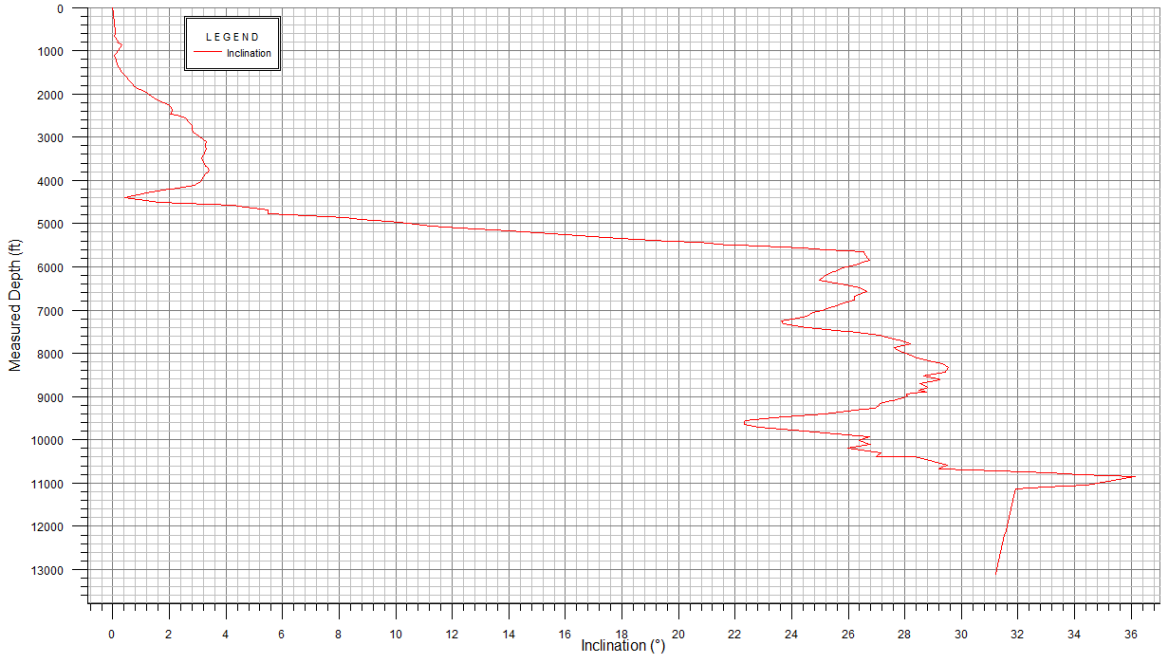

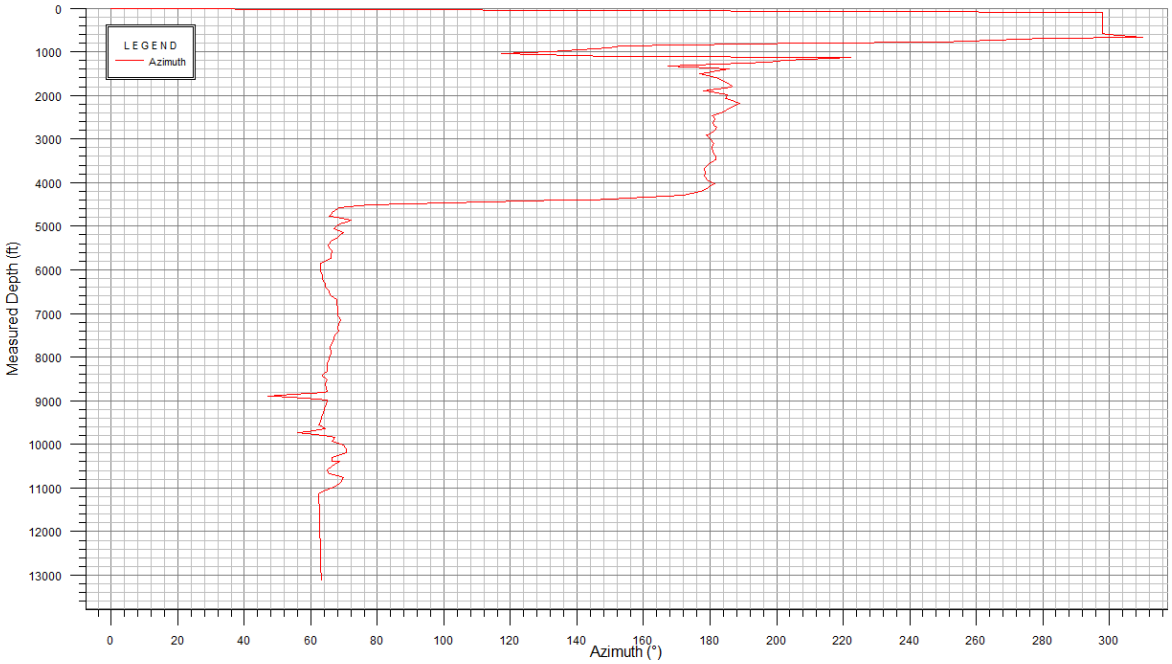

Appendix C: Amplitude Sweep viscoelasticity of drilling fluids

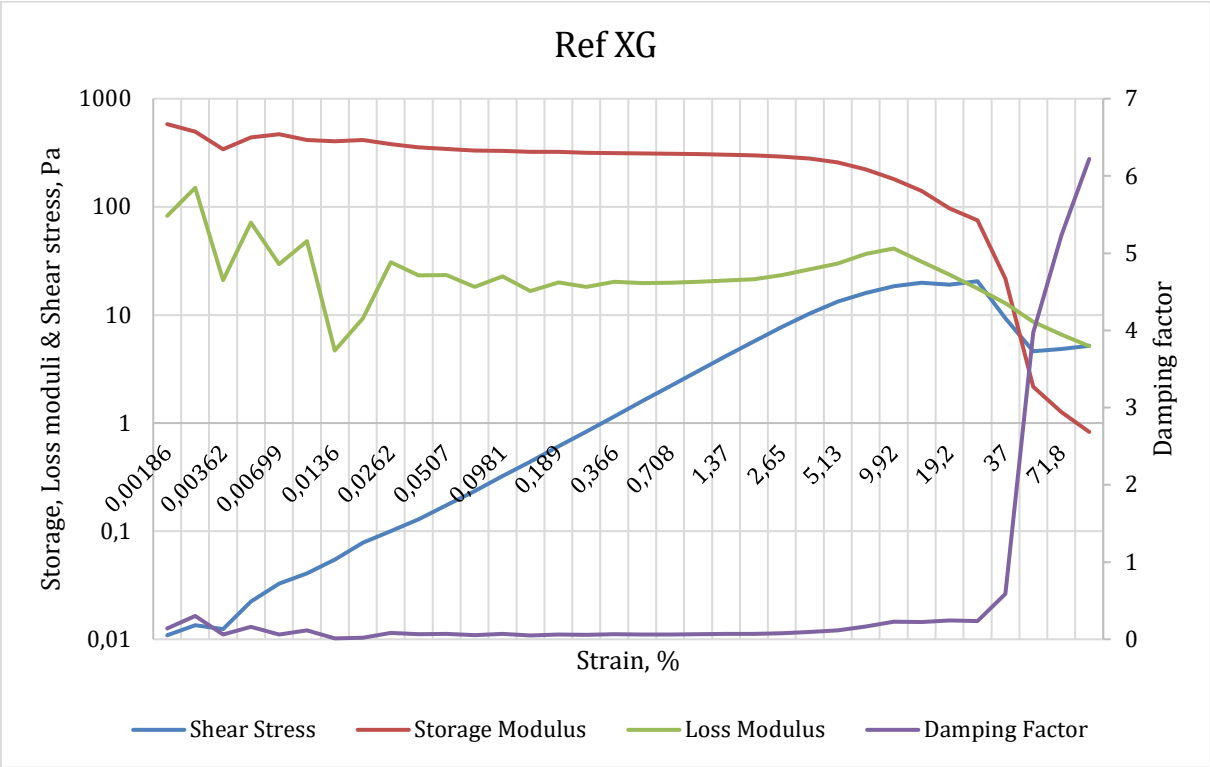

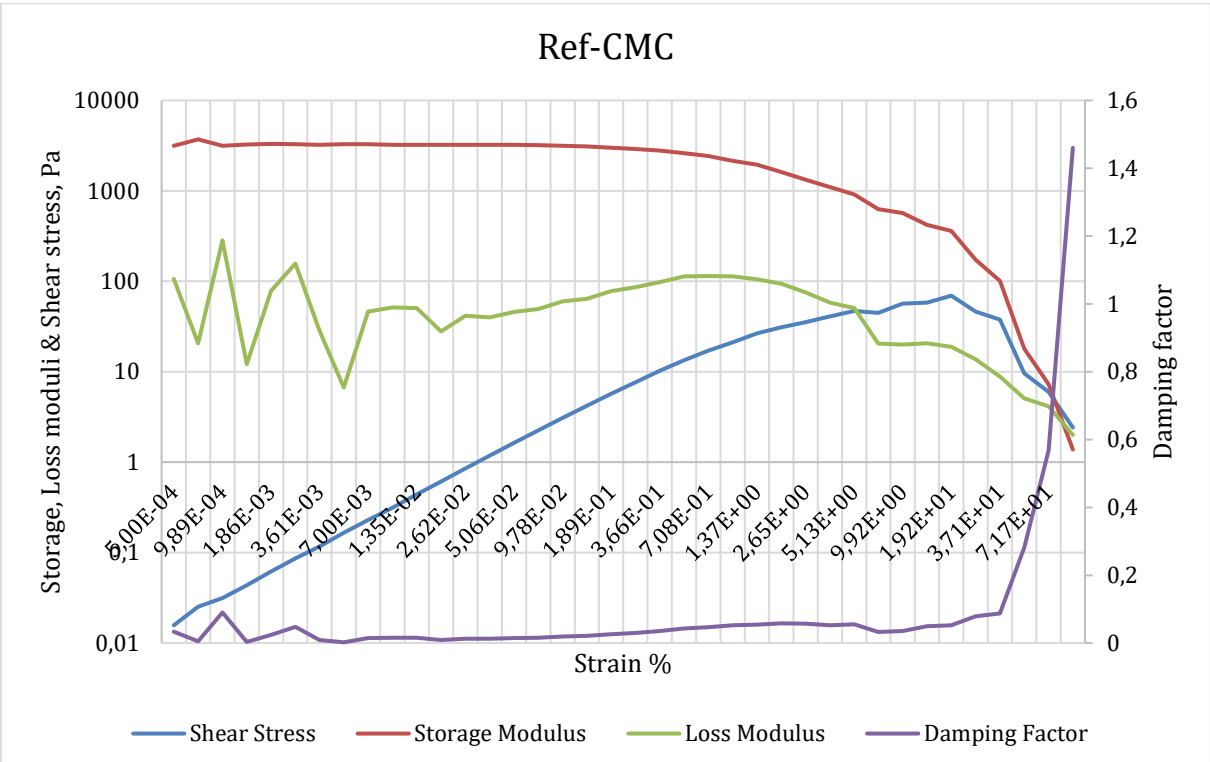

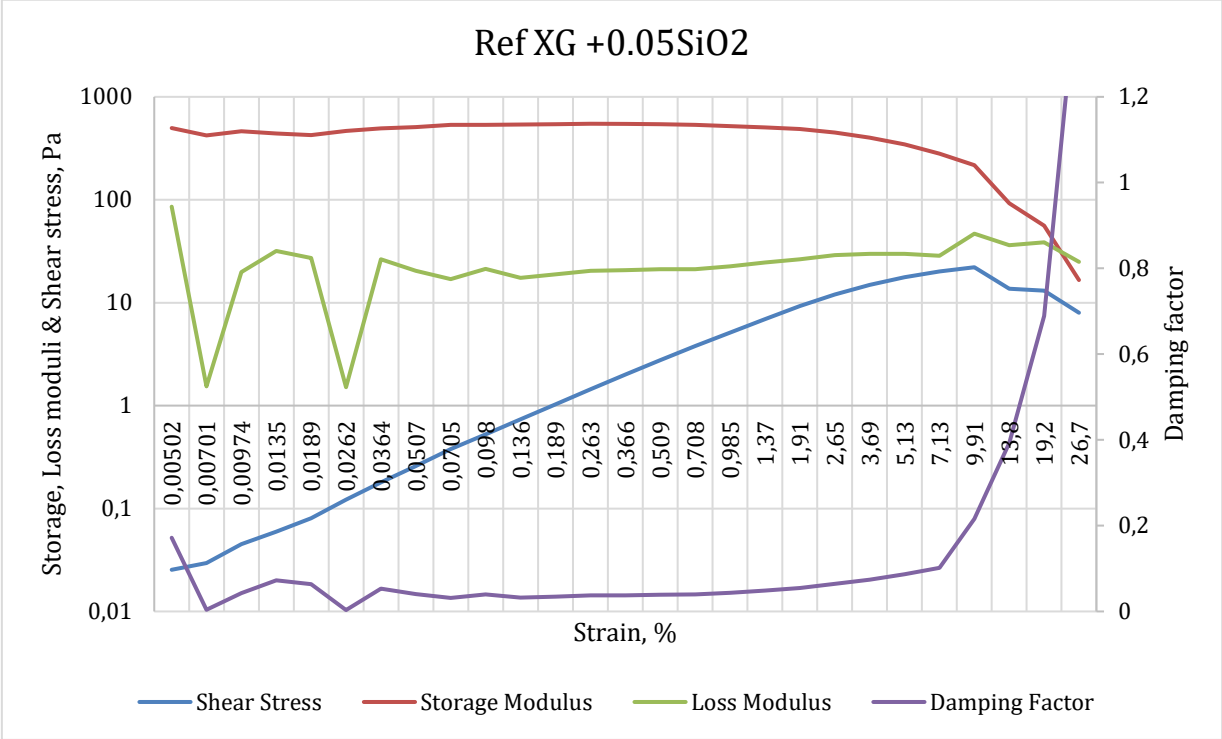
Ref XG +0.05SiO2
Storage, Loss moduli & Shear stress, Pa
Damping factor
Strain, %
1000
100
10
1
0,1
0,01
1,2
1
0,8
0,6
0,4
0,2
0
0,00502
0,00701
0,00974
0,0135
0,0189
0,0262
0,0364
0,0507
0,0705
0,098
0,136
0,189
0,263
0,366
0,509
0,708
0,985
1,37
1,91
2,65
3,69
5,13
7,13
9,91
13,8
19,2
26,7
Shear Stress
Storage Modulus
Loss Modulus
Damping Factor

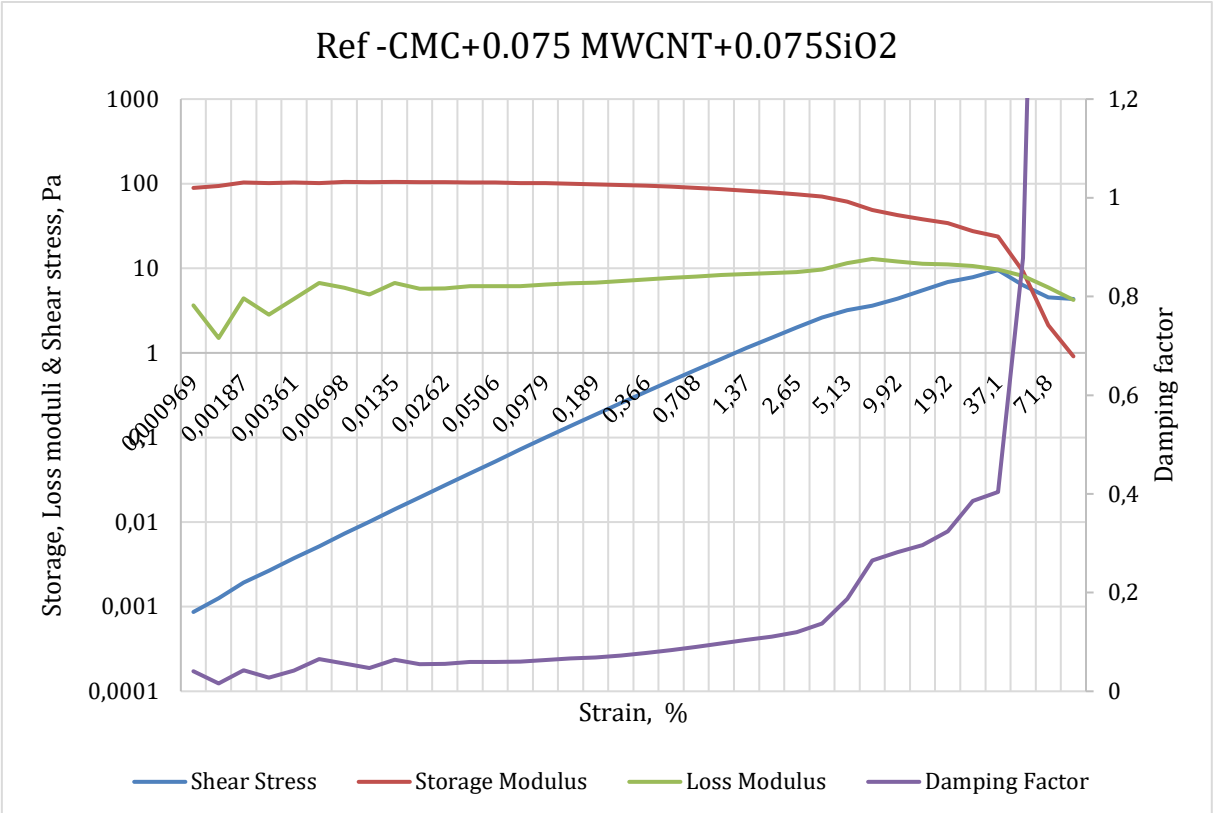
Ref -CMC+0.075 MWCNT+0.075SiO2
Storage, Loss moduli & Shear stress, Pa
Damping factor
Strain, %
1000
100
10
1
0,1
0,01
0,001
0,0001
1,2
1
0,8
0,6
0,4
0,2
0
0,000969
0,00187
0,00361
0,00698
0,0135
0,0262
0,0506
0,0979
0,189
0,366
0,708
1,37
2,65
5,13
9,92
19,2
37,1
71,8
Shear Stress
Storage Modulus
Loss Modulus
Damping Factor

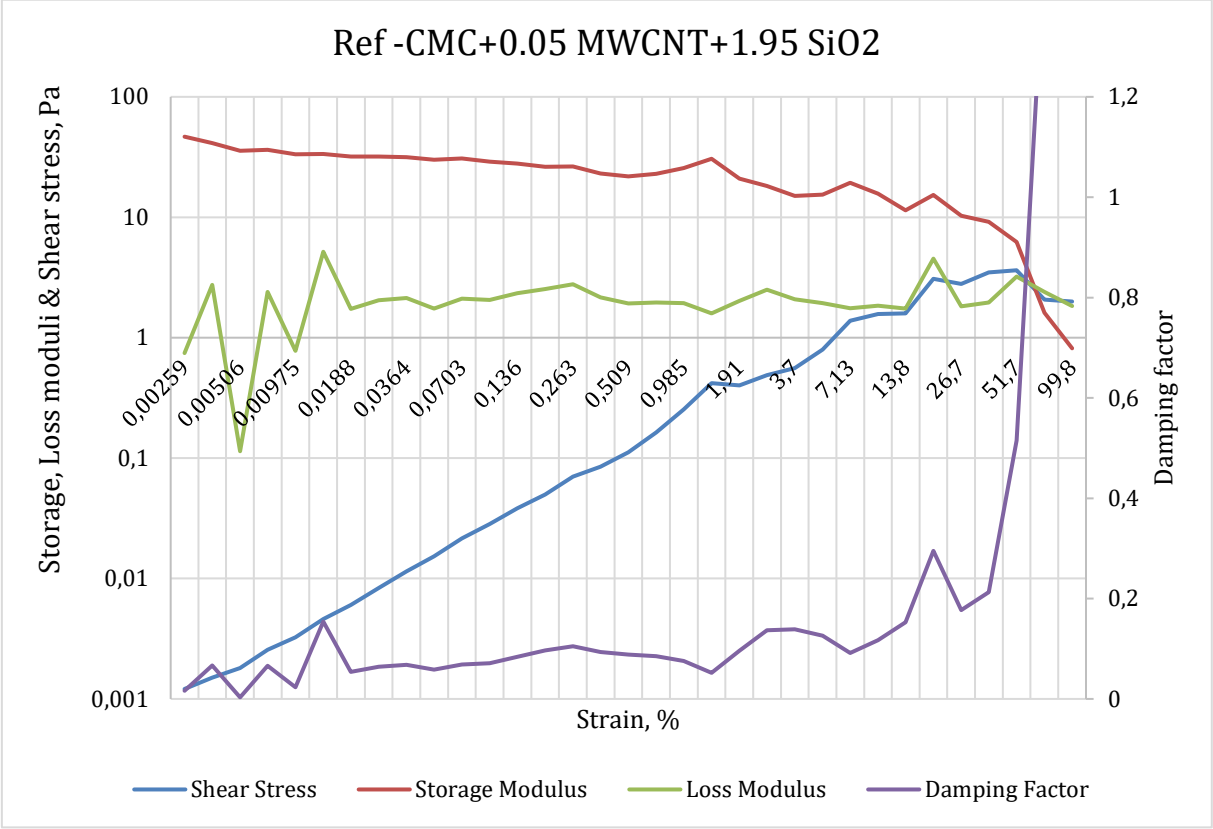
Ref -CMC+0.05 MWCNT+1.95 SiO2
Storage, Loss moduli & Shear stress, Pa
Damping factor
Strain, %
100
10
1
0,1
0,01
0,001
1,2
1
0,8
0,6
0,4
0,2
0
0,00259
0,00506
0,00975
0,0188
0,0364
0,0703
0,136
0,263
0,509
0,985
1,91
3,7
7,13
13,8
26,7
51,7
99,8
Shear Stress
Storage Modulus
Loss Modulus
Damping Factor

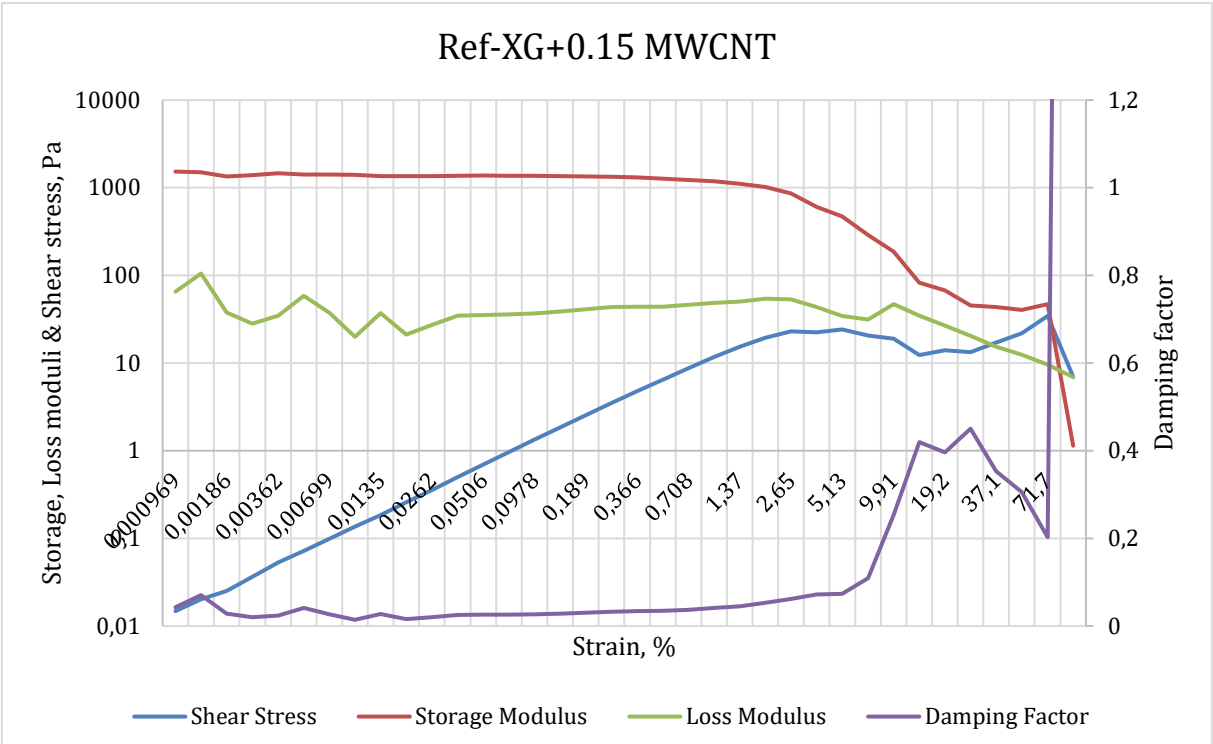
Ref-XG+0.15 MWCNT
Storage, Loss moduli & Shear stress, Pa
Damping factor
Strain, %
10000
1000
100
10
1
0,1
0,01
1,2
1
0,8
0,6
0,4
0,2
0
0,000969
0,00186
0,00362
0,00699
0,0135
0,0262
0,0506
0,0978
0,189
0,366
0,708
1,37
2,65
5,13
9,91
19,2
37,1
71,7
Shear Stress
Storage Modulus
Loss Modulus
Damping Factor

Appendix D: Research paper produced from this MSc work

International Journal of NanoScience and Nanotechnology.
ISSN 0974-3081

http://www.irphouse.com

The Impact of MWCNT on XG Polymer /Salt Treated Laboratory Water Based Drilling Fluid

Afiya Akram
University of Stavanger
Stavanger, Norway

Muhammad Awais Ashfaq Alvi
University of Stavanger
Stavanger, Norway

Mesfin Belayneh
University of Stavanger
Stavanger, Norway

ABSTRACT

In this paper, multi-walled carbon nanotubes (MWCNT) were added in the laboratory water based drilling fluid to study its effect on the properties of the drilling fluid.

The experimental test results show that addition of 0.02 wt. % and 0.38wt. % MWCNT reduced the friction coefficient of drilling fluid by 30 % and 50 %, respectively. This reduction consequently contributes to lower torque and drag. In addition, nanoparticles also improved the rheological properties of the drilling fluid.

1 INTRODUCTION

Nanotechnology has been applied in the field of electronics, biomedince and material science and have shown improved performance. Nanotechnology creates materials with improved properties due to their tunable electronic, physical, chemical, electrical, thermal, mechanical and optical properties. [1].

Several research papers reported the positive impact of nanoparticles in drilling fluids. For instance nanoparticles improves the properties of drilling fluid like rheology (*Vryzas et al, (2016)),* [2] *Parizad and Shahbazi* [3], reduces filtrate loss and mud cake thickness (*Vryzas et al, (2016)* [2], *Parizad and Shahbazi* (2016) [3], Ismail et al (2014) [4], *Zakaria, Husein et al, (2012*) [5]), reducing permeability of the shale (*Sharma et al, (2012)* [6]), increasing lubricity (*Taha et al. (2015*) [7]) and increasing well strength (Charles et al, (2013) [8]).

Multiwalled carbon nanotube (MWCNT) has shown improved rheological properties of drilling fluid *Ismail et al (2014)* [4] and in cement (*Santra et al, (2012)* [9] and *Shah et*

all, (2009) [10]). In the present paper, the performance of 20-40nm MWCNT's were tested to investigate its effect on lubricity and rheological properties of the drilling fluid.

2 EXPERIMENTAL INVESTIGATION

Nanoparticle free reference (or base fluid) laboratory drilling fluid was formulated by mixing bentonite, salt and polymer in water. The impact of nanoparticle on the reference system were studied by adding 0.0095-0.38 wt. % of nanoparticle. The following section presents the description of drilling fluid formulation, testing and characterization.

2.1 MWCNT nanoparticle description

Carbon nanotube (CNT) is a cylindrical molecule that is composed of carbon atoms. In carbon nanotubes, each neighbouring atoms are bonded with strong covalent bond. CNT's are lightweight materials having good electrical, thermal and mechanical properties as well as shows resistance to corrosion. [*Ruoff et al. (2003) 11]*. **Figure 1** shows the SEM image of carbon nanotubes having size in the range of 20-40nm and 2.1gm/cc. EPRUI Nanoparticles and Microspheres Co. Ltd provided the nanotubes which were used in this study. [12].

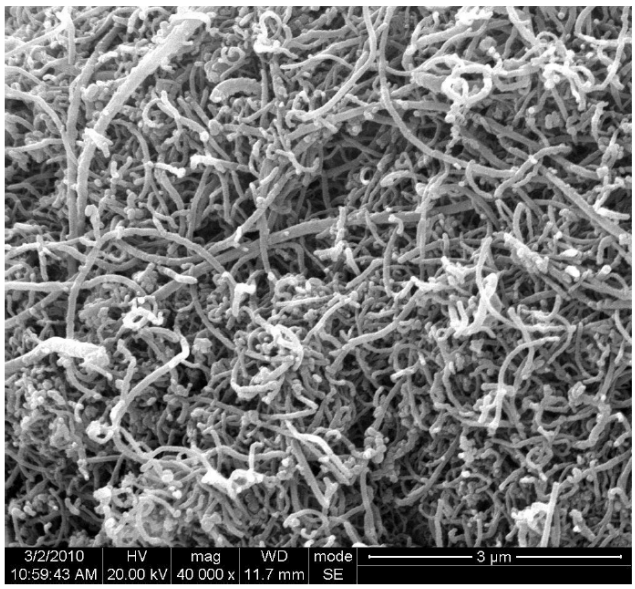

Figure 1: Morphology of MWCNT particles – SEM photograph.

2.2 MWCNT nanoparticle treated drilling fluid formulation

Based on the field case studies performed by Ahmed et al's [13], the concentration of bentonite in the water based drilling fluid is about 5% with respect to the weight. In this paper, the conventional laboratory drilling fluid was formulated by mixing 500ml of fresh water, 2.5g of salt (KCl), 0.5g of xanthan gum (XG) polymer and 25g of bentonite (i.e. 5wt.%). This drilling fluid formulation was termed as reference fluid that is nanoparticle free fluid (Base fluid). Nanoparticle based drilling fluids were prepared by mixing

nanoparticles in the reference drilling fluid formulation. The drilling fluid ingredients were mixed with a high speed Hamilton beach mixer, and were aged for 48 hours in order to swell bentonite. All the tests were carried-out according to API RP 13B-1 [14]. **Table 1** shows the test matrix of drilling fluids treated with MWCNT.

Additives	**Base fluid**	**Base fluid +0.05g MWCNT**	**Base fluid + 0.10g MWCNT**	**Base fluid + 0.15g MWCNT**	**Base fluid + 0.20g MWCNT**	**Base fluid + 2.0g MWCNT**
Water [ml]	500	500	500	500	500	500
XG polymer [g]	0.5	0.5	0.5	0.5	0.5	0.5
KCl [g]	2.5	2.5	2.5	2.5	2.5	2.5
MWCNT [g]	0	0.05	0.1	0.15	0.2	2.0
Bentonite [g]	25	25	25	25	25	25

Table 1: Test matrix of MWCNT nanoparticle in XG/KCL system

2.2.1 Rheological parameters evaluation

Figure 2 displays the Fann© model 35 Viscometer responses of the drilling fluids presented in the Table 1. As can be seen in the figure, all the MWCNT nanoparticles based drilling fluids increases the viscometer responses and shear stress values as compared to the nanoparticles free reference drilling fluid. However, the viscosity response is nonlinear as the concentration varies.

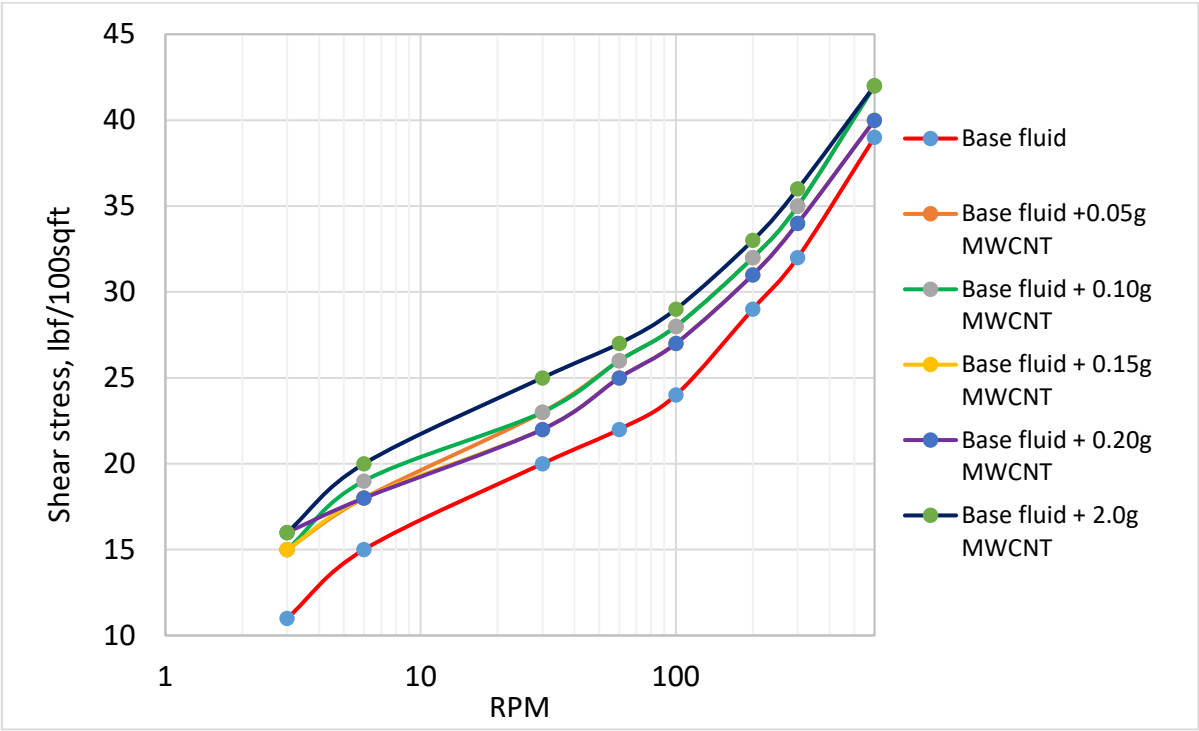

Figure 2: Viscometer measurement of test matrix –Table 1

There are several rheology models documented in the literatures namely, Bingham, Power law, Herschel-Bulkley, and Robertson-Stiff models can be mentioned among others. The shear stress-strain of the measured drilling fluids do not behave as the API Bingham and Power law. However, for the analysis of the impact of MWCNT on the rheological properties, the API models were considered.

Figure 3 shows the Bingham plastic parameters of the drilling fluids. The results indicated that addition of nanoparticles having concentrations in the range of (0.15g, 0.2 & 2 g) the plastic viscosity of drilling fluid is being reduced by about -14%. The lower concentrations in the range of (i.e. 0.05g - 0.2g) and the higher concentration (2 g) of nanoparticles increased the yield strength by 12% & 20%, respectively. Similarly the lower yield strength (LSYS) increased nonlinearly in the range of 71-100%, which is positive with respect to barite/solid sagging control.

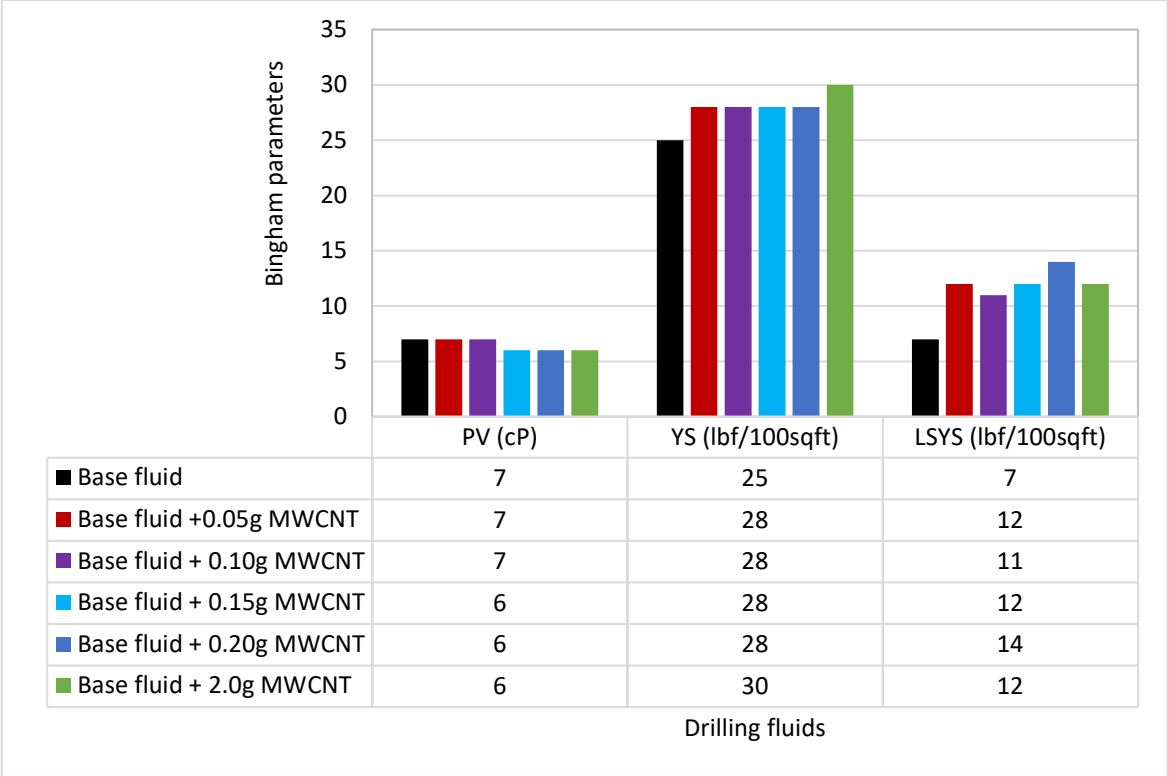

	PV (cP)	YS (lbf/100sqft)	LSYS (lbf/100sqft)
Base fluid	7	25	7
Base fluid +0.05g MWCNT	7	28	12
Base fluid + 0.10g MWCNT	7	28	11
Base fluid + 0.15g MWCNT	6	28	12
Base fluid + 0.20g MWCNT	6	28	14
Base fluid + 2.0g MWCNT	6	30	12

Figure 3: Drilling fluids Bingham parameters

Figure 4 displays Power-law parameters (consistency index (k) and flow index (n)) of the drilling fluids. The results show that nanoparticles increased the k-value but decreased the n- values. However, 0.05 g and 0.1 g MWCNT shows the similar trends. With the increase in the concentration of nanoparticles from 0.15 g and 0.20 g, the k-value and n-values remain almost the same. Impact of the nanoparticles on the Bingham and Power-law parameters is reflected on the hydraulic and hole-cleaning performances of the drilling fluids.

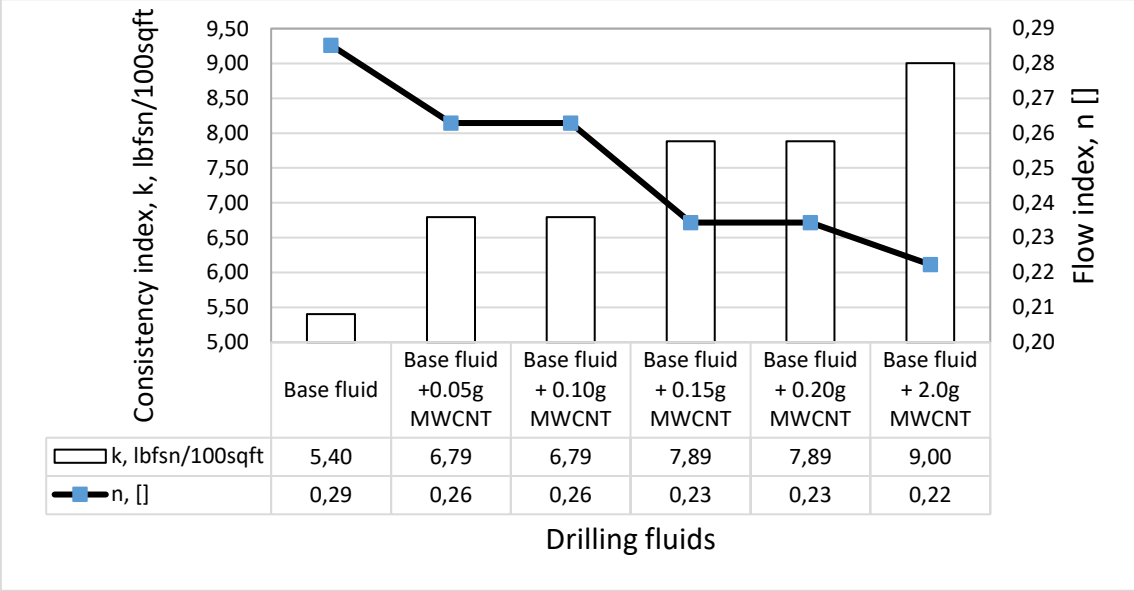

Figure 4: Drilling fluids Power-law parameters

2.2.2 Coefficient of friction evaluation

CSM tribometer [15] was used to measure the lubricity of the drilling fluids. For the measurement, 6 chromium steel ball was used on the plate surface. The experiments were lasted for 10min with the linear speed of 3cm/s. For all tests, a constant normal force of 5N was applied on the tribometer arm. The lubricity of the formulated drilling fluids have been measured at 22^0C. Repeat tests were performed to achieve reproducable results and the average values are reported as shown in the **Figure 5**. As shown, addition of 0.02 wt % and 0.38wt. % MWCNT decreased the coefficient of friction of the base drilling fluid by 30% and 50%, respectively. This has positive impact on torque and drag load reductions.

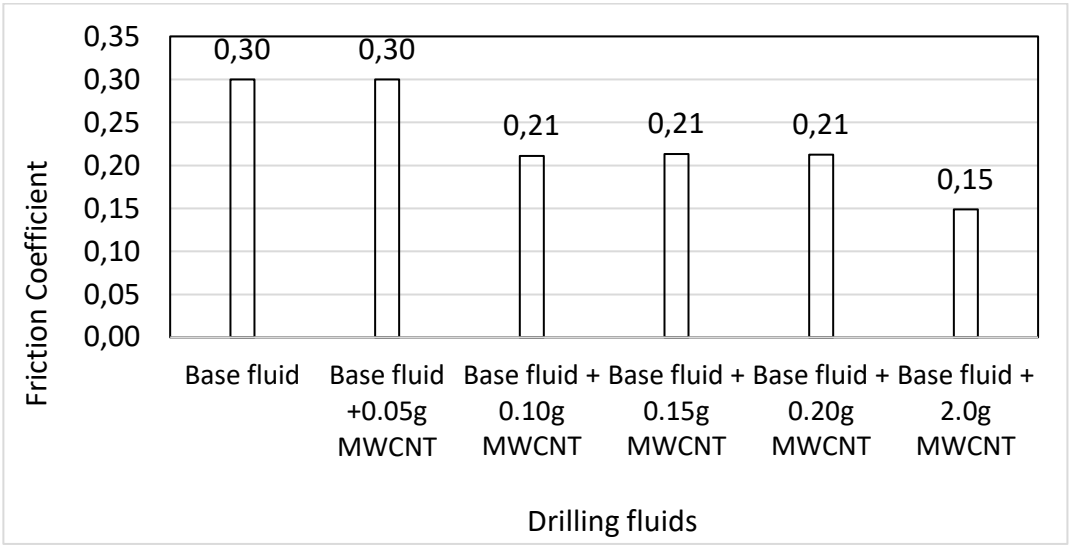

Figure 5: Friction coefficient of MWCNT treated- and reference drilling fluid

4 SUMMARY

In this paper, the effect of MWCNT nanoparticles in laboratory drilling fluid were evaluated. The drilling fluids were characterized at temperature of 22^{o}C. Based on the drilling fluid properties (rheology, lubricity) results, the main observations can be summarized as:

- Addition of 0.020wt. % and 0.38wt. % MWCNT reduced the average coefficient of friction by 30% and 50%, respectively.

- These additives also improve the Bingham and Power-law parameters significantly.

Nanoparticle treated drilling fluids believed to have a potential to reduce drilling related problems and improve drilling fluid performances. For instance, reduction in the friction coefficient can be beneficial to reduce torque and drag.

References

[1] K. Arivalagan1, S. Ravichandran, K. Rangasamy And E.Karthikeyan //**Nanomaterials and its Potential Applications**// International Journal of ChemTech Research CODEN (USA): IJCRGG ISSN: 0974-4290 Vol. 3, No.2, pp 534-538, April-June 2011

[2] Z. Vryzas, V. Zaspalis , L. Nalbantian , O. Mahmoud , , H. A. Nasr-El-Din, V. C. Kelessidis, //**A Comprehensive Approach for the Development of New Magnetite Nanoparticles Giving Smart Drilling Fluids with Superior Properties for HP/HT Applications** //IPTC-18731-MS International Petroleum Technology Conference, 14-16 November, Bangkok, Thailand 2016

[3] A. Parizad, K. Shahbazi, //**Experimental investigation of the effects of sno2 nanoparticles and kcl salt on a water base drilling fluid properties**//The Canadian Journal of Chemical Engineering 94 (10) (2016) 1924-1938.

[4] Ismail, A. R. (2014). //**Improve Performance of Water-based Drilling Fluids//** Sriwijaya International Seminar on Energy-Environmental Science and Technology.

[5] Mohammad F. Zakaria, Maen Husein, Geir Hareland, 2012//**Novel Nanoparticle-Based Drilling Fluid with Improved Characteristics// SPE** 156992-MS, paper presented at the SPE International Oilfield Nanotechnology Conference , 12-14 June 2012, Noordwijk, The Netherlands

[6] Mukul M. Sharma, R. Zhang, M.E. Chenevert, L. Ji, Q. Guo, J. Friedheim, **2012 //A New Family of Nanoparticle Based Drilling Fluids// SPE 160045** This paper was prepared for presentation at the SPE Annual Technical Conference and Exhibition held in San Antonio, Texas, USA, 8-10 October 2012.

[7] N. M. Taha, S. Lee, et al. //**Nano graphene application improving drilling fluids performance//** In International Petroleum Technology Conference. International Petroleum Technology Conference, 2015.

[8] Charles O. Nwaoji, Geir Hareland, Maen Husein, Runar Nygaard, and Mohammad Ferdous Zakaria, 2013//**Wellbore Strengthening-Nano-Particle Drilling Fluid Experimental Design Using Hydraulic Fracture Apparatus// SPE** 163434 SPE /

IADC Drilling Conference and Exhibition, Mar 05 -07, 2013 2013, Amsterdam, The Netherlands
[9] Santra, A. K., et al. (2012). **Influence of Nanomaterials in Oilwell Cement Hydration and Mechanical Propertie**s. SPE International Oilfield Nanotechnology Conference and Exhibition, Society of Petroleum Engineers.
[10] Shah, S. P., Konsta-Gdoutos, M.S., and Metaxa, Z.S. (2009). //A**dvanced Cement Based Nanocomposites**.// Recent Advances in Mechanics Selected Papers from the Symposium on Recent Advances in Mechanics. Academy of Athens, Athens, Greece.
[11] Rodney S. Ruoff, Dong Qian, Wing Kam Liu //**Mechanical properties of carbon nanotubes: theoretical predictions and experimental measurements**// C. R. Physique 4 (2003) 993–1008
[12] EPRUI Nanoparticles and Microspheres Co. Ltd.
[13]Ahmed S. Mohammed, C. Vipulanandan., P.E. and D. Richardson//**Range of Rheological Properties for Bentonite Drilling Muds //** CIGMAT-2013 Conference & Exhibition
[14] API RP 13-B1, R**ecommend Practice for Field Testing Water-Based Drilling Fluids**, third edition. 2003. Washington, DC: API.
[15] CSM Instruments http://www.csm-instruments.com

List of figures

List of tables

Table 5.10: Summary of extended reach with nanoparticle enhanced drilling fluids with XG as a polymer

Table 5.11. Cutting and drilling parameters

List of symbols

A, B and C	Robertson and Stiff model parameters.
d	Outer diameter of the drill string
D	Well diameter
f	Friction factor
G'	Storage Modulus and
G''	Loss modulus
K	Consistency index
n	Flow-behavior index
N	Contact forces
N_{Re}	Reynolds number
PP	Pump pressure
r	Radius of the drill string
T	Torque
W	Weight per unit length
δ	Phase angle
β	Buoyancy factor
γ	Shear rate
θ	Well inclination
φ	Azimuth
ρ_{st}	Static mud density
μ	Coefficient of friction,
μ_p	Plastic viscosity
τ	Shear stress
τ_o	HB-yield stress
τ_y	Unified model yield stress
ΔP	Pressure loss in annulus
ΔPs	Pressure loss at surface equipment
ΔPdp	Pressure loss inside of drill string
ΔPdc	Pressure loss inside of drill collar

ΔP_{adp}	Pressure loss in annulus (drill pipe/well or casing)
ΔP_{adc}	Pressure loss in annulus (drill collar/well)
ΔP_b	Pressure loss across the drill bit

List of abbreviations

API	American Petroleum Institute
BHA	Bottom Hole Assembly
CMC	Carboxymethyl cellulose
ECD	Equivalent Circulation density
EDS	Elemental Dispersive Spectroscopy
EOR	Enhanced Oil Recovery
GPM	Gallon per minute
HPHT	High Pressure High Temperature
LSYS	Lower shear yield stress
LVER	Linear Viscoelastic range
MD	Measured depth
MWCNT	Multiwall Carbon nanotube
OBM	Oil Based Mud
PV	Plastic viscosity
ROP	Rate of Penetration
RPM	Rotation per minute
SEM	Scan Electron Microscope
TVD	True vertical depth
UCA	Ultrasonic cement analyzer
WBM	Water Based Mud
XG	Xanthan Gum
YS	Yield stress